Scattering from a vegetation layer with an irregular vegetation soil boundary

Richard A. Hevenor

OCTOBER 1981

U.S. ARMY CORPS OF ENGINEERS
ENGINEER TOPOGRAPHIC LABORATORIES
FORT BELVOIR, VIRGINIA 22060

E T L

U.S. ARMY ENGINEER TOPOGRAPHIC LABORATORIES
ETL

UNCLASSIFIED

SECURITY CLASSIFICATION OF THIS PAGE *(When Data Entered)*

REPORT DOCUMENTATION PAGE		READ INSTRUCTIONS BEFORE COMPLETING FORM
1. REPORT NUMBER ETL – 0270	2. GOVT ACCESSION NO.	3. RECIPIENT'S CATALOG NUMBER
4. TITLE *(and Subtitle)* SCATTERING FROM A VEGETATION LAYER WITH AN IRREGULAR VEGETATION SOIL BOUNDARY		5. TYPE OF REPORT & PERIOD COVERED Technical Report June 1979 – June 1980 6. PERFORMING ORG. REPORT NUMBER
7. AUTHOR(s) Richard A. Hevenor		8. CONTRACT OR GRANT NUMBER(s)
9. PERFORMING ORGANIZATION NAME AND ADDRESS U.S. Army Engineer Topographic Laboratories Fort Belvoir, Virginia 22060		10. PROGRAM ELEMENT, PROJECT, TASK AREA & WORK UNIT NUMBERS 4A161102B52C
11. CONTROLLING OFFICE NAME AND ADDRESS U.S. Army Engineer Topographic Laboratories Fort Belvoir, Virginia 22060		12. REPORT DATE October 1981 13. NUMBER OF PAGES 113
14. MONITORING AGENCY NAME & ADDRESS*(if different from Controlling Office)*		15. SECURITY CLASS. *(of this report)* Unclassified 15a. DECLASSIFICATION/DOWNGRADING SCHEDULE
16. DISTRIBUTION STATEMENT *(of this Report)* Approved for Public Release; Distribution Unlimited.		
17. DISTRIBUTION STATEMENT *(of the abstract entered in Block 20, if different from Report)*		
18. SUPPLEMENTARY NOTES		
19. KEY WORDS *(Continue on reverse side if necessary and identify by block number)* Electromagnetic Waves Vegetation Scattering		

20. ABSTRACT *(Continue on reverse side if necessary and identify by block number)*

A theoretical model is computed for the backscattering of electromagnetic waves from a layer of vegetation by using a first-order renormalization technique to determine volume scattering. The vegetation soil interface is assumed rough according to the tangent plane approximation and the scattering from this boundary is added incoherently to the volume scattering result. The mean wave in the vegetation is obtained using a bilocal approximation of the Dyson's equation. A free space dyadic Green's function is used, along with a correlation function of the dielectric fluctuationsthat are exponential in form and that also possess different correlation lengths ℓ_x, ℓ_y, and

DD FORM 1 JAN 73 1473 EDITION OF 1 NOV 65 IS OBSOLETE

UNCLASSIFIED

SECURITY CLASSIFICATION OF THIS PAGE *(When Data Entered)*

20. Continued

ℓ_z in the x, y, and z, directions. Effective propagation constants are obtained for both horizontal and vertical polarization. The scattered wave is solved for by using a two-dimensional Fourier transform technique, and the boundary conditions at either end of the vegetation layer are matched. The far field backscatter coefficients are computed for both horizontal and vertical polarizations. The mean and variance of the dielectric fluctuations are calculated with the aid of Peake's model for the dielectric constant of vegetation. The theory is matched to experimental data taken from a corn field. The resulting values for the correlation parameters are then used to monitor the growth pattern of the corn field over a period of time. Comparisons between the theoretical and experimental results over this time period are shown. The theory is also matched to experimental data from spring and fall deciduous trees.

PREFACE

The authority for performing the work described in this report is contained in Project 4A161102B52C, "Research in Geodetic, Cartographic, and Geographic Sciences."

The theory described is the result of in-house work and represents an application of the renormalization technique for studying scattering from certain types of vegetation. A solution for the mean wave is obtained by using the bilocal approximation of the Dyson's equation. A Fourier transform of the dyadic Green's function is used to compute a solution utilizing an anisotropic correlation function for the random dielectric fluctuations. The scattered waves are computed from the mean wave and finally the radar backscatter coefficient is calculated. The influence of a rough surface under the vegetation is considered by using a noncoherent technique.

This task was performed under the supervision of Dr. Frederick Rohde, Team Leader, Center for Theoretical and Applied Physical Sciences; Mr. Melvin Crowell, Jr., Director, Research Institute.

COL Daniel L. Lycan, CE and COL Edward K. Wintz, CE were Commanders and Directors and Mr. Robert P. Macchia was Technical Director of the Engineer Topographic Laboratories during the study period.

CONTENTS

ILLUSTRACTIONS

SCATTERING FROM A VEGETATION LAYER WITH AN IRREGULAR VEGETATION SOIL BOUNDARY

INTRODUCTION

PURPOSE

This research report presents a theory for analyzing the nature of radar wave scattering from certain types of vegetation. The vegetation is simulated by a continuous random medium, and use is made of a first-order renormalization technique to calculate the radar backscatter coefficient. The influence of an irregular vegetation soil interface has also been considered, using a noncoherent approach.

BACKGROUND

In a previous report,[1] a derivation was presented of the radar backscatter coefficient from a half space of random medium using a first-order renormalization solution for the scattered wave and an isotropic correlation function for the random dielectric fluctuations. Recently, Fung solved the problem of scattering from a vegetation layer by using a scalar first-order renormalization approach.[2] In his solution, however, he did not consider the existance of a rough vegetation soil boundary. He did consider an anisotropic correlation function in which the horizontal variation is different from the vertical.

Tsang and Kong solved the problem of volume scattering from a half space random medium that contains lateral and vertical fluctuations.[3] A radiative transfer approach was used to calculate the backscattering cross sections up to second order in approximation. This enabled the cross polarized terms to be obtained.

There are two important practical applications for developing and analyzing various radar scattering theories. The first application is radar image simulation of terrain features. In this problem, the radar system parameters and terrain parameters are known and used to calculate a radar response in the form of a gray tone or density.

---

[1] R.A. Hevenor, *Backscattering of Radar Waves By Vegetated Terrain*, U.S. Army Engineer Topographic Laboratories, Fort Belvoir, VA. ETL-0105, June 1977, AD-A047 669.

[2] A.K. Fung, "Scattering From a Vegetation Layer," *IEEE Transactions on Geoscience Electronics*, Vol. GE-17, No. 1, January 1979.

[3] L. Tsang and J.A. Kong, "Radiative Transfer Theory for Active Remote Sensing of Half Space Random Media," *Radio Science*, Vol. 13, No. 5, September-October 1978.

The scattering theories can be used to compute the radar backscatter coefficient, which in turn is used to calculate gray tone. Using scattering theories in this type of application is straightforward, even though a solution for any one particular scattering problem may be extremely complicated.

The second application is in the field of remote sensing of terrain in which the sensor responses must be used to determine various terrain parameters. Using scattering theories for this application is not straightforward.

However, there are two important uses of scattering theories that bear directly on remote sensing. The first use is a parameter sensitivity study. The theory can be used to analyze the influence of various vegetation, terrain, and radar parameters upon the sensor response. Such parameters as surface roughness, soil moisture, vegetation height, and density could be varied one at a time to determine the influence on the sensor response. This type of analysis should lead to determining what radar parameters are most sensitive to certain terrain parameter changes. This type of analysis assumes the existance of scattering theories that have been developed and compared with existing experimental data.

The second use is to analyze the radar response for two different types of terrain features to see if the two features could be distinguished from each other on an image. Once again, this would assume the existance of scattering theories that have been developed and tested against experimental data. These applications provide the incentive for developing, analyzing, and testing various scattering theories.

In this report, the geometry of the scattering problem to be solved and the basic technique used for the solution will be discussed. In the analysis section, the derivation of the necessary equations will be provided. In the results section, the resulting theory will be compared with existing experimental data, and a study on the sensitivity of the input parameters will be provided.

In this report, the rationalized MKS system of units is used. A line under a symbol will be used to represent a vector quantity. A double line under a symbol will be used to represent a dyadic. A list of the most important symbols is provided at the end of this report.

In figure 1, the scattering geometry of the vegetation problem is shown. A plane wave with a time harmonic of exp (jωt) is incident from free space at an angle θ_i onto a layer of vegetation. The mean thickness of the vegetation is L. The vegetation soil boundary is considered to be randomly rough according to the tangent plane approximation. The vegetation is simulated by a continuous random medium in which $\epsilon(\underline{r})$ and $\sigma(\underline{r})$ represent the three-dimensional random dielectric and conductivity fluctuations, respectively. These fluctuations consist of the sum of an average and a fluctuating component. The standard deviations of the fluctuations are represented by η_1 and η_2. The angle of refraction of the mean wave in the random medium is θ_e.

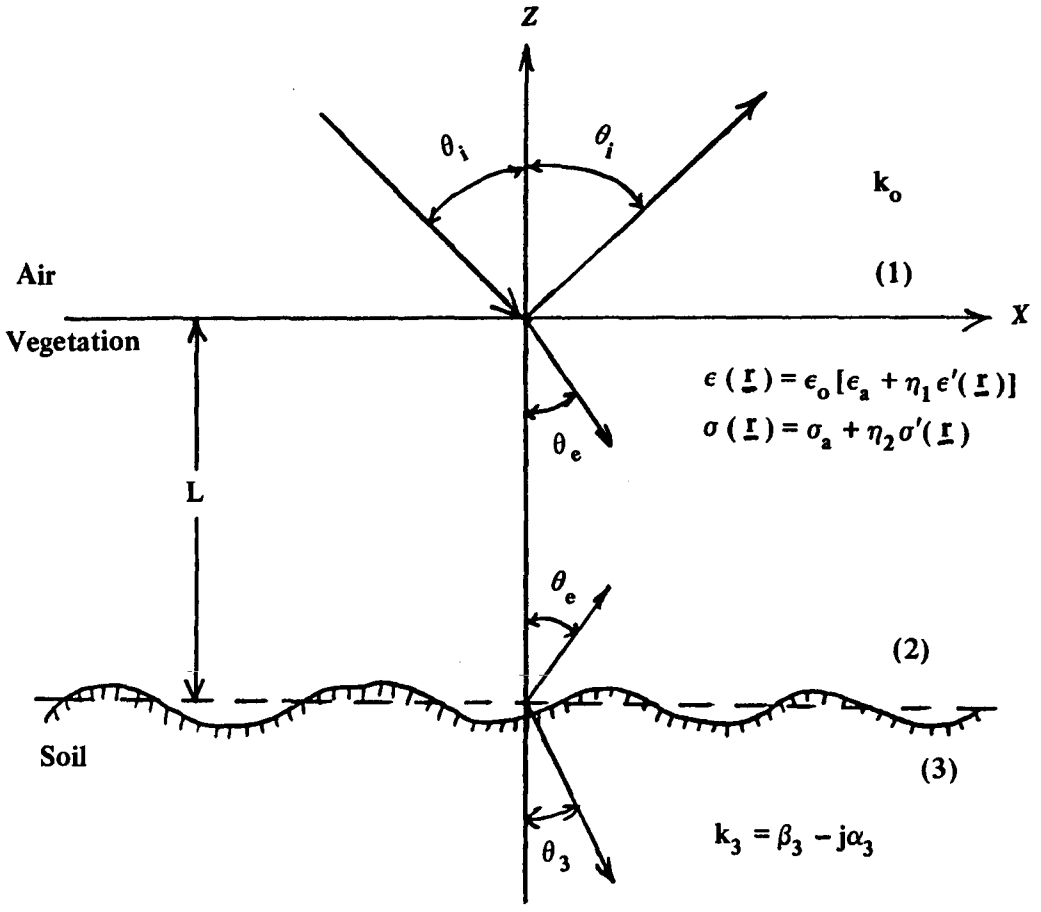

FIGURE 1. Scattering Geometry.

The soil below the vegetation represented by medium 3 is assumed homogeneous with a complex propagation constant k_3. The magnetic permeability for all three media is assumed to be that of free space. The electric field ($\underline{E}_i$) incident onto the vegetation layer can be written as follows:

$$\underline{E}_i = \left\{a_1 \underline{a}_x + a_2 \underline{a}_y + a_3 \underline{a}_z\right\} e^{-jk_o(x\sin\theta_i - z\cos\theta_i)}$$

where $\underline{a}_x$, $\underline{a}_y$, and $\underline{a}_z$ are unit vectors in the x, y, and z directions, respectively. The constants a_1, a_2, and a_3 are arbitrary, allowing for the consideration of both horizontal and vertical polarizations. A first-order renormalization method will be used to calculate the mean and scattered waves in the random medium. A solution will be developed first for the case where the vegetation soil boundary is a plane interface. The irregular boundary will be considered in a noncoherent manner afterwards. The dielectric and conductivity fluctuation terms ($\epsilon'(\underline{r})$ and $\sigma'(\underline{r})$ are considered as being generated by statistically homogeneous random processes. The means and correlation functions of the random processes are defined as follows:

$$\langle \epsilon'(\underline{r}) \rangle = \langle \sigma'(\underline{r}) \rangle = 0$$

$$\langle \epsilon'(\underline{r})\,\epsilon'(\underline{r}') \rangle = \langle \sigma'(\underline{r})\,\sigma'(\underline{r}') \rangle = e^{-|x-x'|/\ell_x}\, e^{-|y-y'|/\ell_y}\, e^{-|z-z'|/\ell_z}$$

where ℓ_x, ℓ_y, and ℓ_z are the correlation distances in the x, y, and z directions, respectively. The correlation functions have been chosen to be anisotropic. This representation, with unequal correlation distances, is believed to be closer to reality than an isotropic correlation function. This is because the size of vegetation scatterers in a horizontal plane is not the same as the size of the scatterers in a vertical plane. The mean wave in the random medium is determined from the bilocal approximation of the Dyson's equation:

$$[\nabla x \nabla x - k_a^2] \langle \underline{E}(\underline{r}) \rangle - \int_{V'} \langle \xi(\underline{r})\,\xi(\underline{r}') \rangle \langle \underline{E}(\underline{r}') \rangle \cdot \underline{\Gamma}(\underline{r}, \underline{r}')\, d\underline{r}' = 0$$

where $\langle \underline{E}(\underline{r}) \rangle$ is the mean wave in the random medium.

$$\xi(\underline{r}) = -j\omega\mu_0\eta_2\sigma'(\underline{r}) + \omega^2\mu_0\epsilon_0\eta_1\epsilon'(\underline{r}).$$

$$k_a^2 = -j\omega\mu_0\sigma_a + \omega^2\mu_0\epsilon_0\epsilon_a.$$

$\underline{\underline{\Gamma}}(\underline{r}, \underline{r}')$ is the dyadic Green's function.

V' is the volume of the random medium.

In the next section, plane wave solutions will be sought to the Dyson equation using an infinite space dyadic Green's function. It should be noted that the mean wave is located in the integrand, making any solution very difficult. Once the mean wave has been calculated and the appropriate boundary conditions have been matched for the mean waves in all three media, then the scattered wave in the vegetation layer can be calculated from the following equation:

$$[\nabla x \nabla x - k_a^2]\,\underline{E}_s(\underline{r}) = \xi(\underline{r}) < \underline{E}(\underline{r}) >$$

where $E_s(r)$ is the scattered wave.

The mean wave acts as a source term for the scattered wave, which will be computed using a Fourier transform technique. This in turn will enable the scattered waves in air to be determined. The necessary boundary conditions will be matched, and the backscatter coefficient will be calculated for horizontal and vertical polarizations. The influence of the rough boundary between the vegetation and the soil will be considered apart from the volume scattering solution, using the tangent plane method. The backscatter coefficient for rough surface scattering will be modified by the attenuation through the vegetation. This result will then be added to the volume scattering solution to obtain a final answer for the backscatter coefficient. An elementary permittivity model will be developed that will relate certain parameters of the random media to the parameters of actual vegetation. A discussion of results section will follow in which the theoretical results are compared with actual experimental data. Also, a parameter sensitivity study will be conducted on the theory to determine the influence of various parameter changes upon the final result.

ANALYSIS

In this section, the necessary mathematical derivations will be provided to enable a scattering model for vegetation to be obtained. First, a solution for the mean wave will be presented and then the scattered wave will be calculated.

MEAN WAVE SOLUTION

The first step in obtaining a solution to the Dyson equation is to write the dyadic Green's function:

$$\underline{\Gamma}(\underline{r},\underline{r}') = \frac{\nabla\nabla'}{k_a^2} - \underline{I}\ G_o(\underline{r},\underline{r}') \tag{1}$$

where $\underline{I}$ is the unit dyadic, and $G_o(\underline{r},\underline{r}')$ is the scalar Green's function that satisfies the following equation:

$$(\nabla^2 + k_a^2)\, G_o(\underline{r},\underline{r}') = \delta(\underline{r}-\underline{r}') \tag{2}$$

The solution for equation (2) is usually expressed in terms of $R = |\underline{r} - \underline{r}'|$ However, this particular form is not useful when working with an anisotropic correlation function that is expressed in rectangular coordinates. We shall therefore seek a solution to (2) that uses rectangular coordinates. Let $G_o(\underline{r},\underline{r}')$ take the following form:

$$G_o(\underline{r},\underline{r}') = \frac{1}{(2\pi)^3}\int \underline{dk}\,\widetilde{G}_o(\underline{k})\, e^{i\underline{k}\cdot(\underline{r}-\underline{r}')} \tag{3}$$

where

$$\underline{k} = k_x\underline{a}_x + k_y\underline{a}_y + k_z\underline{a}_z$$

Substituting (3) into (2) results in a solution for $\widetilde{G}_o(\underline{k})$.

$$\widetilde{G}_o(\underline{k}) = \frac{1}{k_a^2 - k_x^2 - k_y^2 - k_z^2} \tag{4}$$

When (4) is placed in (3) and integration is performed in the complex k_z plane, $G_o(\underline{r},\underline{r}')$ becomes

$$G_o(\underline{r},\underline{r}') = \frac{j}{8\pi^2}\int_{-\infty}^{\infty} dk_x \int_{-\infty}^{\infty} dk_y \cdot \frac{\exp[j\{k_x(x-x')+k_y(y-y')-k_z'|z-z'|\}]}{k_z'} \tag{5}$$

$$k_z' = \sqrt{k_a^2 - k_x^2 - k_y^2}$$

Transforming (5) into polar form results in

$$G_o(\underline{r},\underline{r}') = \frac{j}{8\pi^2}\int_0^{\infty} dk \int_0^{2\pi} d\theta \cdot k\frac{\exp[j\{k(x-x')\cos\theta + k(y-y')\sin\theta - \sqrt{k_a^2-k^2}\,|z-z'|\}]}{\sqrt{k_a^2-k^2}} \tag{6}$$

$$k = \sqrt{k_x^2+k_y^2} \qquad k_x = k\cos\theta \qquad k_y = k\sin\theta$$

When (6) is used in (1), the dyadic Green's function becomes

$$\underline{\underline{\Gamma}}(\underline{r},\underline{r}') = \frac{j}{8\pi^2}\int_0^{\infty} dk \int_0^{2\pi} d\theta \frac{k}{\sqrt{k_a^2-k^2}}\{\underline{C}(k,\theta)\underline{B}(k,\theta)/k_a^2 - \underline{\underline{I}}\} \cdot \exp[j\{k(x-x')\cos\theta + k(y-y')\sin\theta - \sqrt{k_a^2-k^2}\,|z-z'|\}] \tag{7}$$

where

$$\underline{C}(k,\theta) = \underline{a}_x(jk\cos\theta) + \underline{a}_y(jk\sin\theta) + \underline{a}_z f_2(k)$$

$$\underline{B}(k,\theta) = \underline{a}_x(-jk\cos\theta) + \underline{a}_y(-jk\sin\theta) + \underline{a}_z f_1(k)$$

$$f_1(k) = \begin{cases} j\sqrt{k_a^2 - k^2} & \text{when } z > z' \\ -j\sqrt{k_a^2 - k^2} & \text{when } z < z' \end{cases}$$

and

$$f_2(k) = \begin{cases} -j\sqrt{k_a^2 - k^2} & \text{when } z > z' \\ j\sqrt{k_a^2 - k^2} & \text{when } z < z' \end{cases}$$

Plane wave solutions to the Dyson equation take the following form:

$$\langle \underline{E}(\underline{r}) \rangle = \underline{A} e^{-j\underline{k}_e \cdot \underline{r}}$$

The vector $\underline{A}$ can be obtained by matching boundary conditions. The mean wave is seen to propagate with an effective propagation constant $\underline{k}_e$, which must be determined. When the above equation is placed in the Dyson equation along with the dyadic Green's function given by (7), the following equation is obtain when the cross correlation terms between the dielectric and conductivity are ignored:

$$[\nabla x \nabla x - k_o^2 \underline{\underline{\hat{\epsilon}}}] \underline{A} e^{-j\underline{k}_e \cdot \underline{r}} = 0 \tag{8}$$

$$\underline{\underline{\hat{\epsilon}}} = \frac{k_a^2}{k_o^2} \underline{\underline{I}} - \frac{1}{(2\pi)^3} \underline{\underline{M}} \tag{9}$$

$$\underline{\underline{M}} = j\pi(\eta^2\eta_2^2 - k_o^2\eta_1^2) \int \underline{dr'} \int_o^\infty dk \int_o^\pi d\theta$$

$$\cdot d(k) e^{-|x - x'|/\ell_{x_e} - |y - y'|/\ell_{y_e} - |z - z'|/\ell_z}$$

$$\cdot e^{+j\underline{k}_e \cdot (\underline{r} - \underline{r}')} [\underline{\underline{C}}(k, \theta) \underline{\underline{B}}(k, \theta) / k_a^2 - \underline{\underline{I}}] \exp [j \{k(x - x')\cos\theta$$

$$+ k(y - y')\sin\theta - \sqrt{k_a^2 - k^2}\ |z - z'|\}] \tag{10}$$

$$d(k) = k / \sqrt{k_a^2 - k^2}$$

$$\eta = \sqrt{\mu_o / \epsilon_o}$$

The integral in $\underline{r}'$ is allowed to be over all space. For the case where ℓ_z is very small this should be a good approximation except for the points extremely close to either boundary. By carrying out the integration in $\underline{r}'$, one obtains a result for M_{ij} that represents the ij$^{\underline{th}}$ element of the dyadic $\underline{\underline{M}}$.

$$M_{ij} = 4K\ell_x\ell_y\ell_z \int_0^{\infty} dk \int_0^{2\pi} d\theta d(k) \{ g(k) \cdot [F_1(k,\theta)F_{1j}(k,\theta) + k_a^2 \delta_{ij}] + h(k) [F_{2i}(k,\theta)F_{2j}(k,\theta) + k_a^2 \delta_{ij}] \} / \{1 + \ell_x^2(k_{ex} + k\cos\theta)^2] \cdot [1 + \ell_y^2(k_{ey} + k\sin\theta)^2] \} \quad (11)$$

where

$$g(k) = \frac{-1}{1 + j\ell_z(k_{ez} + \sqrt{k_a^2 - k^2})} \qquad h(k) = \frac{1}{j\ell_z(k_{ez} - \sqrt{k_a^2 - k^2}) - 1}$$

$$F_{11}(k,\theta) = jk\cos\theta \qquad F_{12}(k,\theta) = jk\sin\theta \qquad F_{13}(k,\theta) = j\sqrt{k_a^2 - k^2}$$

$$F_{21}(k,\theta) = jk\cos\theta \qquad F_{22}(k,\theta) = jk\sin\theta \qquad F_{23}(k,\theta) = -j\sqrt{k_a^2 - k^2}$$

$$\delta_{ij} = 1 \quad \text{when } i = j$$

$$\delta_{ij} = 0 \quad \text{when } i \neq j$$

$$K = j\pi(\eta^2\eta_2^2 - k_o^2\eta_1^2) / k_a^2$$

The form of the incident wave dictates that $k_{ey} = 0$ and $k_{ex} = k_o \sin\theta_i$. This result makes the following elements of the $\hat{\underline{\epsilon}}$ dielectric tensor become equal to zero:

$$\hat{\epsilon}_{12} = \hat{\epsilon}_{21} = \hat{\epsilon}_{23} = \hat{\epsilon}_{32} = 0$$

The above result is easily shown by considering a transformation of (11) back to rectangular coordinates and recognizing that the integrand is even in k_y. Carrying out the indicated differentiation in equation (8) and writing the result in matrix form produces

$$\begin{bmatrix} k_{ez}^2 - k_o^2\hat{\epsilon}_{11} & 0 & -k_{ez}k_o\sin\theta_i - k_o^2\hat{\epsilon}_{13} \\ 0 & k_{ez}^2 + k_o^2\sin\theta_i - k_o^2\hat{\epsilon}_{22} & 0 \\ k_{ez}k_o\sin\theta_i - k_o^2\hat{\epsilon}_{13} & 0 & k_o^2\sin^2\theta_i - k_o^2\hat{\epsilon}_{33} \end{bmatrix} \begin{bmatrix} A_x e^{-j\underline{k}_e \cdot \underline{r}} \\ A_y e^{-j\underline{k}_e \cdot \underline{r}} \\ A_z e^{-j\underline{k}_e \cdot \underline{r}} \end{bmatrix} = 0 \qquad (12)$$

In forming the above matrix, use has been made of the fact that $k_{ey} = 0$ and $k_{ex} = k_o \sin\theta_i$. Now, only solutions for k_{ez} are needed. Two solutions can be developed for k_{ez}, one for a horizontally polarized wave and one for a vertically polarized wave. For a horizontally polarized wave, one has $A_x = A_z = 0$ and $A_y \neq 0$. The following equation can be used to determine k_{ez} for this case:

$$\left\{k_{ez}^2 + k_o^2\sin^2\theta_i - k_o^2\hat{\epsilon}_{22}\right\} A_y e^{-j\underline{k}_e \cdot \underline{r}} = 0 \qquad (13)$$

Since the term outside the brackets is not zero, this means that the quantity inside the brackets must be zero.

$$k_{ez} = \pm k_o \sqrt{\sin^2\theta_i - \hat{\epsilon}_{22}} \qquad (14)$$

The above result is not an explicit solution for k_{ez} since this quantity also appears in the integral of M_{22}. A first approximation for k_{ez} can be obtained by letting $\eta_1 = \eta_2 = 0$. This represents the case where there are no random fluctuations at all.

$$k_{ez}^{(0)} = -\sqrt{k_a^2 - k_o^2\sin^2\theta_i}$$

The above value can be used to compute M_{22}, which in turn can be used to calculate a new value of k_{ez} that will be called k_h. The minus sign on the square root is chosen over the plus sign to consider waves propagating in the minus z direction.

$$k_h = -k_o\sqrt{\sin^2\theta_i - \hat{\epsilon}_{22}} \tag{15}$$

When computing k_h in (15), the expression for $k_{ez}^{(o)}$ is used to calculate M_{22}. It is interesting to see that even when k_a is real, k_h still comes out complex so that the mean wave decays as it propagates into the medium. This decay has been explained as resulting from multiple scattering. It is not clear, however, how much multiple scattering is being considered. For a vertical polarized wave, $A_x \neq 0$, $A_y = 0$, and $A_z \neq 0$. This leads to the following determinant:

$$\begin{vmatrix} k_{ez}^2 - k_o^2\hat{\epsilon}_{11} & -k_{ez}k_o\sin\theta_i - k_o^2\hat{\epsilon}_{13} \\ -k_o k_{ez}\sin\theta_i - k_o^2\hat{\epsilon}_{13} & k_o^2(\sin^2\theta_i - \hat{\epsilon}_{33}) \end{vmatrix} = 0$$

The above determinant provides another solution for k_{ez}.

$$k_{ez} = k_o\left\{\frac{-\hat{\epsilon}_{13}\sin\theta_i \pm\sqrt{\hat{\epsilon}_{13}^2\sin^2\theta_i - \hat{\epsilon}_{33}(\hat{\epsilon}_{11}\sin^2\theta_i - \hat{\epsilon}_{11}\hat{\epsilon}_{33} + \hat{\epsilon}_{13}^2)}}{\epsilon_{33}}\right\} \tag{16}$$

Once again a first approximation for k_{ez} can be obtained for the case where the random dielectric and conductivity fluctuations disppear ($\eta_1 = \eta_2 = 0$).

$$k_{ez}^{(0)} = -\sqrt{k_a^2 - k_o^2\sin^2\theta_i}$$

This value for k_{ez} can be used to calculate the elements of the dielectric tensor. These elements are used in (16) to compute a new value for k_{ez}, which will be called k_v.

$$k_v = -k_o\left\{\frac{\hat{\epsilon}_{13}\sin\theta_i + \sqrt{\hat{\epsilon}_{13}^2\sin^2\theta_i - \hat{\epsilon}_{33}(\hat{\epsilon}_{11}\sin^2\theta_i - \hat{\epsilon}_{11}\hat{\epsilon}_{33} + \hat{\epsilon}_{13}^2)}}{\hat{\epsilon}_{33}}\right\}$$

The sign associated with the square root has been chosen as minus in order to consider waves propagating in the minus z direction. The effective propagation constant for the mean wave has been determined, and now the amplitude must be calculated by matching appropriate boundary conditions. The total mean electric field in air can be written as:

$$\underline{E}_1(r) = \left\{ [a_1 \underline{a}_x + a_2 \underline{a}_y + a_3 \underline{a}_z]\, e^{jk_o z \cos\theta_i} + [R_1 \underline{a}_x + R_2 \underline{a}_y + R_3 \underline{a}_z]\, e^{-jk_o z \cos\theta_i} \right\} e^{-jk_o x \sin\theta_i}$$

$$z \geq 0 \qquad (17)$$

The first bracketed term in (17) is the incident wave, and the second bracketed term is the reflected wave. The unknowns in (17) are represented by R_1, R_2, and R_3. However, it will not be necessary to obtain an explicit solution for them since they are not needed in determining the scattered waves. The total mean electric field in the vegetation ($E_2(r)$) can be written in the following form, using previous results:

$$\underline{E}_2(r) = \left\{ T_2 \underline{a}_y e^{p_1 z} e^{jq_1 z} + (T_1 \underline{a}_x + T_3 \underline{a}_z) e^{p_2 z} e^{jq_2 z} + V_2 \underline{a}_y e^{-p_2 z} e^{-jq_2 z} + (V_1 \underline{a}_x + V_3 \underline{a}_x) e^{-p_2 z} e^{-jq_2 z} \right\} e^{-jk_o x \sin\theta_i}$$

$$-L \leq z \leq 0 \qquad (18)$$

where

$$p_1 + jq_1 = -jk_h$$

$$p_1 = \mathrm{Im}(k_h) \qquad q_1 = -\mathrm{Re}(k_h)$$

also

$$p_2 + jq_2 = -jk_v$$

$$p_2 = \mathrm{Im}(k_v) \qquad q_2 = -\mathrm{Re}(k_v)$$

In (18), both upward and downward waves have been considered. The unknowns are represented by the amplitudes T_1, T_2, T_3, V_1, V_2, and V_3. An explicit solution for each of these is required in terms of propagation constants, medium characteristics, and layer thickness. The explicit solution is needed to compute the scattered waves. An expression for the mean wave in the homogeneous soil medium can be written as

$$\underline{E}_3(\underline{r}) = [W_1\underline{a}_x + W_2\underline{a}_y + W_3\underline{a}_z]e^{-jk_0 x\sin\theta_i}e^{jk_3 z\cos\theta_3}$$

$$z \leqslant -L \qquad (19)$$

In the soil, the mean wave propagates in the minus z direction and the constants W_1, W_2, and W_3 are the unknown amplitudes. Once again, no explicit solution will be required for these amplitudes since they are not needed to compute the scattered waves. To compute the six amplitudes of the mean wave in the vegetation, the following boundary conditions are used:

$$E_{1x} = E_{2x} \text{ at } z = 0$$

$$E_{1y} = E_{2y} \text{ at } z = 0$$

$$\frac{\partial E_{1z}}{\partial y} - \frac{\partial E_{1y}}{\partial z} = \frac{\partial E_{2z}}{\partial y} - \frac{\partial E_{2y}}{\partial z} \text{ at } z = 0$$

$$\frac{\partial E_{1x}}{\partial z} - \frac{\partial E_{1z}}{\partial x} = \frac{\partial E_{2x}}{\partial z} - \frac{\partial E_{2z}}{\partial x} \text{ at } z = 0$$

$$E_{2x} = E_{3x} \text{ at } z = -L$$

$$E_{2y} = E_{3y} \text{ at } z = -L$$

$$\frac{\partial E_{2z}}{\partial y} - \frac{\partial E_{2y}}{\partial z} = \frac{\partial E_{3z}}{\partial y} - \frac{\partial E_{3y}}{\partial z} \text{ at } z = -L$$

$$\frac{\partial E_{2x}}{\partial z} - \frac{\partial E_{2z}}{\partial x} = \frac{\partial E_{3x}}{\partial z} - \frac{\partial E_{3z}}{\partial x} \quad \text{at } z = -L$$

$$D_{1z} = D_{2z} \text{ at } z = 0$$

$$D_{2z} = D_{3z} \text{ at } z = -L$$

$$\underline{D}_1 = \epsilon_o \underline{E}_1$$

$$\underline{D}_2 = \epsilon_v E_{2x} \underline{a}_x + \epsilon_h E_{2y} \underline{a}_y + \epsilon_v E_{2z} \underline{a}_z$$

where

$$\epsilon_h = \frac{q_1^2 - p_1^2}{\omega^2 \mu_o} \text{ evaluated at } \theta_i = 0°$$

$$\epsilon_v = \frac{q_2^2 - p_2^2}{\omega^2 \mu_o} \text{ evaluated at } \theta_i = 0°$$

$$\underline{D}_3 = \epsilon_3 \underline{E}_3$$

where ϵ_3 is the dielectric constant of the soil. Two divergence conditions will also be used, along with the above boundary conditions.

$$\nabla \cdot \underline{E}_1 = 0 \quad \text{and} \quad \nabla \cdot \underline{E}_3 = 0$$

When the equations for the mean fields given by (17) through (19) are placed in the boundary conditions, the result is 12 equations and 12 unknowns. Explicit solutions are only required for the six amplitudes associated with the mean wave in the random medium. Solving for these six values yields the following results:

$$T_2 = \frac{2jk_o a_{12} a_2 \cos\theta_i}{a_{21} a_{12} - a_{11} a_{22}} \tag{20}$$

$$V_2 = \frac{-2jk_o a_2 a_{11} \cos\theta_i}{a_{21}a_{12} - a_{11}a_{22}} \tag{21}$$

$$T_1 = \frac{jk_o b_{12}\left\{2a_1\cos\theta_i + \sin\theta_i(1-\epsilon_o/\epsilon_v)[a_3 + a_1\tan\theta_i]\right\}}{b_{21}b_{12} - b_{11}b_{22}} \tag{22}$$

$$V_1 = \frac{-jk_o b_{11}\left\{2a_1\cos\theta_i + \sin\theta_i(1-\epsilon_o/\epsilon_v)[a_3 + a_1\tan\theta_i]\right\}}{b_{21}b_{12} - b_{11}b_{22}} \tag{23}$$

$$T_3 = \frac{1}{\epsilon_v\left[e^{-p_2 L}e^{-jq_2 L} - e^{p_2 L}e^{jq_2 L}\right]} \left\{\frac{\epsilon_3 k_o \sin\theta_i}{k_3\cos\theta_3}\right.$$

$$\cdot\left[T_1 e^{-p_2 L}e^{-jq_2 L} + V_1 e^{p_2 L}e^{jq_2 L}\right] - \epsilon_o e^{p_2 L}e^{jq_2 L}$$

$$\left.\cdot\left[a_3 - \tan\theta_i\,(T_1 + V_1 - a_1)\right]\right\} \tag{24}$$

$$V_3 = \epsilon_o/\epsilon_v\,[a_3 - \tan\theta_i\,(T_1 + V_1 - a_1)] - T_3 \tag{25}$$

The parameters used in the above equations are defined below:

$$a_{11} = (jk_3\cos\theta_3 - p_1 - jq_1)e^{-p_1 L}e^{-jq_1 L}$$

$$a_{12} = (jk_3\cos\theta_3 + p_1 + jq_1)e^{p_1 L}e^{jq_1 L}$$

$$a_{21} = jk_o\cos\theta_i + p_1 + jq_1$$

$$a_{22} = jk_o\cos\theta_i - p_1 - jq_1$$

$$b_{11} = e^{-p_2 L}e^{-jq_2 L}(p_2 + jq_2 - \alpha)$$

$$b_{12} = -e^{p_2 L}e^{jq_2 L}(p_2 + jq_2 + \alpha)$$

$$b_{21} = p_2 + jq_2 + jk_o[\cos\theta_i + \sin\theta_i \tan\theta_i(1-\epsilon_o/\epsilon_v)]$$

$$b_{22} = -\{p_2 + jq_2 - jk_o[\cos\theta_i + \sin\theta_i \tan\theta_i(1-\epsilon_o/\epsilon_v)]\}$$

where

$$\alpha = j\{k_3\cos\theta_3 + k_o^2\sin^2\theta_i(1-\epsilon_3/\epsilon_v)/(k_3\cos\theta_3)\}$$

Now that the mean waves have been fully determined, the scattered waves can be calculated. The scattered waves in the upper medium (air) will then be used to compute the backscatter coeffieient.

SCATTERED WAVE SOLUTION

In the random medium, the scattered or incoherent field is calculated from the following equation:

$$[\nabla x \nabla x - k_a^2]\underline{E}_s^{(2)}(\underline{r}) = \xi(\underline{r}) < \underline{E}(\underline{r}) > \qquad (26)$$

For our problem, the mean wave $< \underline{E}(\underline{r}) >$ is given by $\underline{E}_2(\underline{r})$ as shown in (18). A superscript 2 is used with $\underline{E}_s^{(2)}(\underline{r})$ to indicate clearly the scattered field in the random medium. A solution for this scattered field can be obtained by using a two-dimensional Fourier transform.

$$\underline{E}_s^{(2)}(\underline{r}) = \frac{1}{(2\pi)^2}\int \underline{dk}_t \underline{G}_s(\underline{k}_t, z)e^{j\underline{k}_t \cdot \underline{r}_t} \qquad (27)$$

where

$$\underline{k}_t = k_x\underline{a}_x + k_y\underline{a}_y \qquad \underline{r}_t = x\underline{a}_x + y\underline{a}_y$$

$$\underline{G}_s(\underline{k}_t, z) = G_{sx}(\underline{k}_t, z)\underline{a}_x + G_{sy}(\underline{k}_t, z)\underline{a}_y + G_{sz}(\underline{k}_t, z)\underline{a}_z$$

When the complete expression for the mean wave in the random medium as given by (18) is placed in (26), a term of the form $\xi(r)\exp(-jk_o x\sin\theta_i)$ on the right side results. This term will be written as a two-dimensional Fourier transform.

$$S(\underline{k}_t, z) = \int \underline{dr}_t \xi(\underline{r}) e^{-jk_o x \sin\theta_i} e^{-j\underline{k}_t \cdot \underline{r}_t}$$

$$\xi(\underline{r}) e^{-jk_o x \sin\theta_i} = \frac{1}{(2\pi)^2} \int \underline{dk}_t S(\underline{k}_t, z) e^{j\underline{k}_t \cdot \underline{r}_t} \tag{28}$$

When (27) and (28) are placed in (26) and the result is put in matrix form,

$$\begin{bmatrix} (k_y^2 - k_a^2 - D_z^2) & -k_x k_y & jk_x D_z \\ -k_x k_y & (k_x^2 - k_a^2 - D_z^2) & jk_y D_z \\ jk_x D_z & jk_y D_z & (k_x^2 + k_y^2 - k_a^2) \end{bmatrix} \begin{bmatrix} G_{sx} \\ G_{sy} \\ G_{sz} \end{bmatrix} = \begin{bmatrix} f_x(z) \\ f_y(z) \\ f_z(z) \end{bmatrix} \tag{29}$$

where D_z represents the differential operator d/dz. The quantities on the right side of (29) are defined below:

$$f_x(z) = S(\underline{k}_t, z)[T_1 e^{p_2 z} e^{jq_2 z} + V_1 e^{-p_2 z} e^{-jq_2 z}]$$

$$f_y(z) = S(\underline{k}_t, z)[T_2 e^{p_1 z} e^{jq_1 z} + V_2 e^{-p_1 z} e^{-jp_1 z}]$$

$$f_z(z) = S(\underline{k}_t, z)[T_3 e^{p_2 z} e^{jq_2 z} + V_3 e^{-p_2 z} e^{-jq_2 z}]$$

Solutions for the quantities G_{sx}, G_{sy}, and G_{sz} can be obtained by solving the three differential equations in (29) using the method of variation of parameters.

$$G_{sx}(\underline{k}_t, z) = A_1 e^{-jk'_z z} + A_2 e^{jk'_z z} + \frac{1}{2jk'_z k_a^2} \left[\int_{-L}^{z} f(z) e^{jk'_z z} dz\right] \cdot e^{-jk'_z z} - \frac{1}{2jk'_z k_a^2} \left[\int_{L}^{z} f(z) e^{-jk'_z z} dz\right] e^{jk'_z z} \tag{30}$$

$$G_{sy}(\underline{k}_t, z) = B_1 e^{-jk'_z z} + B_2 e^{jk'_z z} - \frac{1}{2jk_z k_a^2} \left[\int_{-L}^{z} h(z) e^{jk'_z z} dz \right]$$

$$\cdot e^{-jk'_z z} + \frac{1}{2jk_z k_a^2} \left[\int_{-L}^{z} h(z) e^{-jk'_z z} dz \right] e^{jk'_z z} \qquad (31)$$

$$G_{sz}(\underline{k}_t, z) = \frac{(k_x A_1 + k_y B_1)}{k'_z} e^{jk'_z z} - \frac{(k_x A_2 + k_y B_2)}{k'_z}$$

$$\cdot e^{jk'_z z} + \frac{e^{-jk'_z z}}{2jk'^2_z k_a^2} \int_{-L}^{z} \left[k_x f(z) - k_y h(z) \right] e^{jk'_z z} dz$$

$$+ \frac{e^{jk'_z z}}{2jk'^2_z k_a^2} \int_{-L}^{z} \left[k_x f(z) - k_y h(z) \right] e^{-jk'_z z} dz - \frac{f_z(z)}{k'^2_z} \qquad (32)$$

$$k'_z = \sqrt{k_a^2 - k_x^2 - k_y^2}$$

$$f(z) = f_x(z)[k_a^2 - k_x^2] - k_y k_x f_y(z) + jk_x D_z f_z(z)$$

$$h(z) = \frac{k_y(k_a^2 - k_y^2)}{k_x} f_x(z) - (k_a^2 - k_y^2) f_y(z) - jk_y D_z f_z(z)$$

$$+ \frac{k_y}{k_x} (k_x^2 + k_y^2 - k_a^2) f_x(z)$$

The quantities A_1, A_2, B_1, and B_2 are not functions of z and at present, are unknown. Although the solutions for G_{sx}, G_{sy}, and G_{sz} are rather formidable in appearance, it will be found after some mathematical manipulations that a solution will emerge. The three components of the scattered electric field in the upper medium ($z > 0$) can be written in the following form:

$$E_{sx}^{(1)}(r) = \frac{1}{(2\pi)^2} \int \underline{dk}_t A_x(\underline{k}_t) e^{j(k_x x + k_y y - k_{1z} z)} \tag{33}$$

$$E_{sy}^{(1)}(\underline{r}) = \frac{1}{(2\pi)^2} \int \underline{dk}_t A_y(\underline{k}_t) e^{j(k_x x + k_y y - k_{1z} z)} \tag{34}$$

$$E_{sz}^{(1)}(\underline{r}) = \frac{1}{(2\pi)^2} \int \underline{dk}_t A_z(\underline{k}_t) e^{j(k_x x + k_y y - k_{1z} z)} \tag{35}$$

where

$$k_{1z} = \sqrt{k_o^2 - k_x^2 - k_y^2}$$

The parameter k_{1z} was obtained by taking any one of the field components given above and putting it into the free space scalar wave equation. The superscript 1 is used to refer to the field in the upper medium, which is air. Therefore, $E_{sx}^{(1)}(\underline{r})$ would indicate the x component of the scattered electric field in air. The components of the scattered electric field in the soil $(z < -L)$ can be written as follows:

$$E_{sx}^{(3)}(\underline{r}) = \frac{1}{(2\pi)^2} \int \underline{dk}_t C_x(\underline{k}_t) e^{j(k_x x + k_y y + k_{3z} z)} \tag{36}$$

$$E_{sy}^{(3)}(\underline{r}) = \frac{1}{(2\pi)^2} \int \underline{dk}_t C_y(\underline{k}_t) e^{j(k_x x + k_y y + k_{3z} z)} \tag{37}$$

$$E_{sz}^{(3)}(\underline{r}) = \frac{1}{(2\pi)^2} \int \underline{dk}_t C_z(\underline{k}_t) e^{j(k_x x + k_y y + k_{3z} z)} \tag{38}$$

where

$$k_{3z} = \sqrt{k_3^2 - k_x^2 - k_y^2}$$

The superscript 3 refers to the computation of the scattered fields in the soil. The expression for k_{3z} is obtained by putting any one of the field components into the

scalar wave equation, which has a propagation constant k_3. The unknowns associated with the scattered waves are represented by A_x, A_y, A_z, A_1, A_2, B_1, B_2, C_x, C_y, and C_z. The only unknowns for which an explicit solution is needed are A_x, A_y, and A_z. Since the only interest is in computing the backscattered far field in air, complete solutions for the scattered fields in the other mediums are not needed. The boundary conditions that the scattered waves must satisfy are provided below:

$$E_{sx}^{(1)} = E_{sx}^{(2)} \text{ at } z = 0$$

$$E_{sy}^{(1)} = E_{sy}^{(2)} \text{ at } z = 0$$

$$\frac{\partial E_{sz}^{(1)}}{\partial y} - \frac{\partial E_{sy}^{(1)}}{\partial z} = \frac{\partial E_{sz}^{(2)}}{\partial y} - \frac{\partial E_{sy}^{(2)}}{\partial z} \text{ at } z = 0$$

$$\frac{\partial E_{sx}^{(1)}}{\partial z} - \frac{\partial E_{sz}^{(1)}}{\partial x} = \frac{\partial E_{sx}^{(2)}}{\partial z} - \frac{\partial E_{sz}^{(2)}}{\partial x} \text{ at } z = 0$$

$$E_{sx}^{(2)} = E_{sx}^{(3)} \text{ at } z = -L$$

$$E_{sy}^{(2)} = E_{sy}^{(3)} \text{ at } z = -L$$

$$\frac{\partial E_{sz}^{(2)}}{\partial y} - \frac{\partial E_{sy}^{(2)}}{\partial z} = \frac{\partial E_{sz}^{(3)}}{\partial y} - \frac{\partial E_{sy}^{(3)}}{\partial z} \text{ at } z = -L$$

$$\frac{\partial E_{sx}^{(2)}}{\partial z} - \frac{\partial E_{sz}^{(2)}}{\partial x} = \frac{\partial E_{sx}^{(3)}}{\partial z} - \frac{\partial E_{sz}^{(3)}}{\partial x} \text{ at } z = -L$$

The boundary conditions given above, along with the divergence equations in the two homogeneous media allow ten independent equations to be formulated.

$$k_x A_x + k_y A_y = k_{1z} A_z \tag{39}$$

$$k_x C_x + k_y C_y = -k_{3z} C_z \tag{40}$$

$$A_x = A_1 + A_2 + \frac{1}{2jk_z' k_a^2} \int_{-L}^{o} f(z)[e^{jk_z' z} - e^{-jk_z' z}]\,dz \tag{41}$$

$$A_y = B_1 + B_2 + \frac{1}{2jk_z' k_a^2} \int_{-L}^{o} h(z)[e^{-jk_z' z} - e^{jk_z' z}]\,dz \tag{42}$$

$$C_x = e^{jk_{3z}L}\left\{A_1 e^{jk_z' L} + A_2 e^{-jk_z' L}\right\} \tag{43}$$

$$C_y = e^{jk_{3z}L}\left\{B_1 e^{jk_z' L} + B_2 e^{-jk_z' L}\right\} \tag{44}$$

$$jk_y A_z + jk_{1z} A_y = jk_y G_{sz}(k_t, o) - \left.\frac{\partial G_{sy}}{\partial z}\right|_{z=0} \tag{45}$$

$$k_{1z} A_x + k_x A_z = j \left.\frac{\partial G_{sx}}{\partial z}\right|_{z=0} + k_x G_{sz}(k_t, o) \tag{46}$$

$$jk_y G_{sz}(k_t, -L) - \left.\frac{\partial G_{sy}}{\partial z}\right|_{z=-L} = jk_y C_z e^{-jk_{3z}L} - jk_{3z} C_y e^{jk_{3z}L} \tag{47}$$

$$\left.\frac{\partial G_x}{\partial z}\right|_{z=-L} - jk_x G_{sx}(k_t, -L) = jk_{3z} C_x e^{-jk_{3z}L} - jk_x C_z e^{-jk_{3z}L} \tag{48}$$

A solution for A_x, A_y, and A_z using the above equations would be quite difficult for arbitrary values of k_x and k_y. However, since we are only interested in the backscattered far field in air, a basic expression for the far field can be obtained by using the Stratton-Chu integral as modified by Silver.[4] When equations (33) through (35) are evaluated on the surface ($z = 0$) and placed into the Stratton-Chu integral, the following equation for the scattered far field ($\underline{E}_{sf}$) will result:

---

[4] S. Silver, *Microwave Antenna Theory and Design*, McGraw Hill, New York, 1947.

$$\underline{E}_{sf} = \frac{2\cos\theta_i\,(jk_o)e^{-jk_oR}}{4\pi R}\;\underline{a}_x A_x(k_o\sin\theta_i,\,0) + \underline{a}_y A_y(k_o\sin\theta_i,\,0)$$

$$+\,\underline{a}_z A_z(k_o\sin\theta_i,\,0) \tag{49}$$

Where R is the distance from the origin of the coordinate system to the field point where $\underline{E}_{sf}$ is required. It can now be seen that solutions for A_x, A_y, and A_z are only needed for values of $k_x = k_o\sin\theta_i$ and $k_y = 0$. When the appropriate expressions for the derivatives are substituted into equations (45) through (48) and we let $k_y = 0$, the 10 equations (39) through (48) become.

$$k_x A_x = k_{1z} A_z \tag{50}$$

$$k_x C_x = k_{3z} C_z \tag{51}$$

$$A_x = A_1 + A_2 + \frac{I_1}{2jk_z' k_a^2} \tag{52}$$

$$A_y = B_1 + B_2 + \frac{I_2}{2jk_z' k_a^2} \tag{53}$$

$$C_x = e^{jk_{3z}L}\left[A_1 e^{jk_z'L} + A_2 e^{-jk_z'L}\right] \tag{54}$$

$$C_y = e^{jk_{3z}L}\left[B_1 e^{jk_z'L} + B_2 e^{-jk_z'L}\right] \tag{55}$$

$$jk_{1z}A_y = jk_z'B_1 - jk_z'B_2 - \frac{I_3}{2k_a^2} \tag{56}$$

$$k_{1z}A_x + k_x A_z = k_z'A_1 - k_z'A_2 + \frac{1}{2jk_a^2}(1 + k_x^2/k_z'^2)I_4$$

$$+\,\frac{k_x^2}{k_z'}(A_1 - A_2) - \frac{k_x f_z(0)}{k_z'^2} \tag{57}$$

$$-k_z' B_1 e^{jk_z' L} + k_z' B_2 e^{-jk_z' L} = k_{3z} C_y e^{-jk_{3z} L} \tag{58}$$

$$A_2(k_z'^3 + k_x^2 k_z') e^{-jk_z' L} - A_1(k_z'^3 + k_x^2 k_z') e^{jk_z' L} + k_x f_z(-L)$$

$$= k_z'^2 e^{-jk_{3z} L}(k_{3z} C_x - k_x C_z) \tag{59}$$

The quantities I_1, I_2, I_3, and I_4 used in the above equations are integrals in z and are defined below:

$$I_1 = \int_{-L}^{o} f(z) \left[e^{jk_z' z} - e^{-jk_z' z} \right] dz$$

$$I_2 = \int_{-L}^{o} h(z) \left[e^{-jk_z' z} - e^{jk_z' z} \right] dz$$

$$I_3 = \int_{-L}^{o} h(z) \left[e^{jk_z' z} + e^{-jk_z' z} \right] dz$$

$$I_4 = \int_{-L}^{o} f(z) \left[e^{jk_z' z} + e^{-jk_z' z} \right] dz$$

The functions f(z), h(z) and k_z' can be evaluated at $k_y = 0$, before integration takes place. When all the above equations are used to solve for A_x, A_y, and A_z, the following results are derived:

$$A_x(k_x, o) = b_1 f_z(-L) + b_2 f_z(o) + \int_{-L}^{o} f(z) \left\{ b_5 e^{jk_z' z} + b_6 e^{-jk_z' z} \right\} dz \tag{60}$$

$$A_y(k_x, o) = \frac{-1}{jk_a^2 \; k_{1z}(1+\tilde{a}_1) + k_z'(1-\tilde{a}_1)} \int_{-L}^{o} h(z)$$

$$\cdot \left\{ \tilde{a}_1 e^{-jk_z'z} + e^{jk_z'z} \right\} dz \qquad (61)$$

$$A_z(k_x, o) = k_x \left\{ b_1 f_z(-L) + b_2 f_z(o) + \int_{-L}^{o} f(z) \right.$$

$$\left. \cdot \left[b_5 e^{jk_z'z} + b_6 e^{-jk_z'z} \right] dz \right\} / \; k_{1z} \qquad (62)$$

In the above three equations, k_x is to be evaluated at $k_o \sin\theta_i$. The new quantities introduced into the above equations are defined below:

$$\tilde{a}_1 = (k_z' - k_{3z}) e^{-2jk_z'L} / (k_z' + k_{3z})$$

$$\tilde{a}_2 = \frac{\left[k_{3z}(k_z'^3 + k_x^2 k_z') - k_z'^2(k_{3z}^2 + k_x^2) \right] e^{-2jk_z'L}}{\left[k_{3z}(k_z'^3 + k_x^2 k_z') + k_z'^2(k_{3z}^2 + k_x^2) \right]}$$

$$\tilde{a}_3 = \frac{k_{3z} k_x e^{-jk_z'L}}{\left[k_{3z}(k_z'^3 + k_x^2 k_z') + k_z'^2(k_{3z}^2 + k_x^2) \right]}$$

$$\tilde{a}_4 = k_z'^2(k_{1z}^2 + k_x^2)$$

$$\tilde{a}_5 = k_{1z}(k_z'^3 + k_z' k_x^2)\,(1 - \tilde{a}_2)$$

$$\tilde{a}_6 = k_{1z}(k_z'^3 + k_z' k_x^2)\tilde{a}_3$$

$$\tilde{a}_7 = k_{1z}(k_z'^2 + k_x^2) / (2jk_a^2)$$

$$\tilde{a}_8 = \tilde{a}_5 + \tilde{a}_4 (\tilde{a}_2 + 1)$$

$$b_1 = 2k_{1z}(k_z^3 + k_z' k_x^2)\tilde{a}_3 / \tilde{a}_8$$

$$b_2 = -k_{1z} k_x (1 + \tilde{a}_2) / \tilde{a}_8$$

$$b_3 = \tilde{a}_7 (1 + \tilde{a}_2) / \tilde{a}_8$$

$$b_4 = \tilde{a}_5 / (2j\tilde{a}_8 k_z' k_a^2)$$

$$b_5 = b_3 + b_4$$

$$b_6 = b_3 - b_4$$

If the receiver in the far field is sensitive to a unit polarization vector $\underline{e}_r$, then the received field (E_R) will be

$$E_R = \underline{e}_r \cdot \underline{E}_{sf}$$

where $\underline{e}_r$ in general has three components ($\underline{e}_r = \underline{a}_x e_{rx} + \underline{a}_y e_{ry} + \underline{a}_z e_{rz}$). The next step in calculating the backscatter coefficient is to determine the statistical average of $E_R E_R^*$, using (49).

$$\begin{aligned} \langle E_R E_R^* \rangle = \frac{4k_o^2 \cos^2\theta_i}{16\pi^2 R^2} \Big\{ & e_{rx} e_{rx}^* \langle A_x A_x^* \rangle + 2\mathrm{Re}[e_{rx} e_{ry} \\ & \cdot \langle A_x A_y^* \rangle] + 2\mathrm{Re}[e_{rx} e_{rz}^* \langle A_x A_z^* \rangle] + e_{ry}^2 \\ & \cdot \langle A_y A_y^* \rangle + 2\mathrm{Re}[e_{ry} e_{rz}^* \langle A_y A_z^* \rangle] + e_{rz} e_{rz}^* \\ & \cdot \langle A_z A_z^* \rangle \Big\} \end{aligned} \tag{63}$$

The brackets $<-----> $ around $E_R E_R^*$ are used to indicate the calculation of the statistical average. The possibility of e_{rx} and e_{rz} being complex is anticipated, with e_{ry} always being real. What is required now is the computation of each of the six terms inside the brackets of (63). The determination of $<A_y A_y^*>$ will be considered first:

$$<A_y A_y^*> = k_a^2 k_a^{*2} M_o M_o^* \int_{-L}^{o} dz \int_{-L}^{o} dz \int_{-\infty}^{\infty} dx$$

$$\cdot \int_{-\infty}^{\infty} dx' \int_{-\infty}^{\infty} dy \int_{-\infty}^{\infty} dy' <\xi(\underline{r})\xi^*(\underline{r}')>$$

$$\cdot \hat{f}(z, z') \exp[-2jk_o(x - x')\sin\theta_i] \qquad (64)$$

where

$$<\xi(\underline{r})\xi^*(\underline{r}')> = (\omega^2\mu_o^2\eta_2^2 + k_o^4\eta_1^2)e^{-|x-x'|/\ell_x} e^{-|y-y'|/\ell_y} e^{-|z-z'|/\ell_z}$$

$$\hat{f}(z, z') = \tilde{a}_1\tilde{a}_1^* T_2 T_2^* e^{D_1 z} e^{D_1^* z'} + \tilde{a}_1 T_2 a_1^* V_2^* e^{D_1 z} e^{D_2^* z'}$$

$$+ \tilde{a}_1 T_2 T_2^* e^{D_1 z} e^{-D_2^* z'} + \tilde{a}_1 T_2 V_2^* e^{D_1 z} e^{-D_1^* z'}$$

$$+ \tilde{a}_1 V_2 \tilde{a}_1^* T_2^* e^{D_2 z} e^{D_1^* z'} + \tilde{a}_1\tilde{a}_1^* V_2 V_2^* e^{D_2 z} e^{D_2^* z'}$$

$$+ \tilde{a}_1 V_2 T_2^* e^{D_2 z} e^{-D_2^* z'} + \tilde{a}_1 V_2 V_2^* e^{D_2 z} e^{-D_1^* z'}$$

$$+ \tilde{a}_1^* T_2 T_2^* e^{-D_2 z} e^{D_1^* z'} + \tilde{a}_1^* T_2 V_2^* e^{-D_2 z} e^{D_2^* z'}$$

$$+ T_2 T_2^* e^{-D_2 z} e^{-D_2^* z'} + T_2 V_2^* e^{-D_2 z} e^{-D_1^* z'}$$

$$+ V_2 \tilde{a}_1^* T_2^* e^{-D_1 z} e^{D_1^* z'} + \tilde{a}_1^* V_2 V_2^* e^{-D_1 z} e^{D_2^* z'}$$

$$+ V_2 T_2^* e^{-D_1 z} e^{-D_2^* z'} + V_2 V_2^* e^{-D_1 z} e^{-D_1^* z'}$$

where

$$D_1 = p_1 + j(q_1 - k'_z) \quad \text{and} \quad D_2 = -(p_1 + jq_1 + jk'_z)$$

$$M_o = \frac{-1}{jk_a^2 \; k_{1z}(1 + a_1) + k'_z(1 - a_1)}$$

The form of $\hat{f}(z, z')$ given above appears to be very complicated. However, each of the 16 terms in $\hat{f}(z, z')$ consist of simple exponentials in z and z' and therefore can be integrated easily. It should be remember when computing D_1 and D_2 that p_1 and q_1 are real, but k'_z will be complex. Making the substitution that $u = x - x'$ and $v = y - y'$ and transforming the x and y integrals into integrals in u and v produces

$$\langle A_y A_y^* \rangle = (\omega^2 \mu_o^2 \eta_2^2 + k_o^4 \eta_1^2) k_a^2 k_a^{*2} M_o M_o^* \int_{-L}^{o} dz$$

$$\int_{-L}^{o} dz' \int_{-\infty}^{\infty} du \int_{-\infty}^{\infty} dv \int_{-\infty}^{\infty} dx' \int_{-\infty}^{\infty} dy'$$

$$f(z, z') \; e^{-2jk_o u \sin\theta_i} \; e^{-|u|/\ell_x} e^{-|v|/\ell_y} e^{-|z - z'|/\ell_z} \tag{65}$$

The integrals in x' and y' appear somewhat meaningless. These integrals actually represent the illuminated area in the xy plane, since it is physically unrealistic to have backscattered energy from a portion of the surface that is not illuminated. Considering the integrals in x' and y' to form the illuminated area (A_I) and carrying out the integrations in u and v will yield the following result:

$$\langle A_y A_y^* \rangle = \frac{4\ell_x \ell_y A_I (\omega^2 \mu_o^2 \eta_2^2 + k_o^4 \eta_1^2) k_a^2 k_a^{*2} M_o M_o^*}{(1 + 4k_o^2 \ell_x^2 \sin^2\theta_i)}$$

$$\int_{-L}^{o} dz \int_{-L}^{o} dz' \; \hat{f}(z, z') e^{-|z - z'|/\ell_z} \tag{66}$$

Consider now a typical term of $\hat{f}(z, z')$ which is of the form $Ae^{az}e^{bz'}$ where A,a, and b are not functions of z or z', and make a transformation of variables from z and z' to $n_z = z - z'$ and $z'' = z'$. Then, the results of carrying out the integration for this one term becomes

$$\int_{-L}^{0} dz \int_{-L}^{0} dz'\, Ae^{az}\, e^{bz'} e^{-|z - z'|/\ell_z} =$$

$$\frac{A\ell_z}{(a+b)} \left\{ \frac{1 - \ell_z b + \ell_z(a+b)e^{-L(a + 1/\ell_z)} - (1 + \ell_z a)e^{-L(a+b)}}{(1 + \ell_z a)\ (1 - \ell_z b)} \right.$$

$$\left. + \frac{1 - \ell_z a + \ell_z(a+b)e^{-L(1/\ell_z + b)} - e^{-L(a+b)}\ (1 + b\ell_z)}{(1 + \ell_z b)\ (1 - \ell_z a)} \right\}$$

When the answer for the integration in z and z' given above is used for each of the 16 terms in $\hat{f}(z, z')$, then the final result for $< A_y A_y^* >$ can be written.

$$< A_y A_y^* > = \frac{4\ell_x \ell_y \ell_z A_I(\omega^2 \mu_o^2 \eta_2^2 + k_o^4 \eta_1^2) k_a^2 k_a^{*2} M_o M_o^*}{(1 + 4k_o^2 \ell_x^2 \sin^2\theta_i)}$$

$$\cdot \sum_{n=1}^{16} \frac{A_n}{(c_n + d_n)} \left\{ \frac{1 - \ell_z d_n + \ell_z(c_n + d_n)e^{-L(c_n + 1/\ell_z)} - (1 + \ell_z c_n)e^{-L(c_n + d_n)}}{(1 + \ell_z c_n)\ (1 - \ell_z d_n)} \right. \tag{67}$$

$$\left. + \frac{1 - \ell_z c_n + \ell_z(c_n + d_n)e^{-L(d_n + 1/\ell_z)} - e^{-L(c_n + d_n)}\ (1 + d_n \ell_z)}{(1 + \ell_z d_n)\ (1 - \ell_z c_n)} \right\}$$

The values for the A_n's, the c_n's, and d_n's are provided in appendix A and simply come from the expression for $\hat{f}(z, z')$. Using the methodology for computing $< A_y A_y^* >$, one can caluclate all the remaining terms in (63). All of these other terms are given in appendix A. An expression for the radar backscatter coefficient (σ_v^o) can be written in terms of $< E_R E_R^* >$

$$\sigma_v^\circ = \frac{4\pi R^2}{A_I} \frac{< E_R E_R^* >}{\underline{E}_i \cdot \underline{E}_i^*} \tag{68}$$

The subscript v on σ_v° is used to indicate a volume scattering result from a plane layer of random media. No consideration for rough surface scattering is given in σ_v°. Using (63) and the expression for the incident wave given previously, one can write a final result for σ_v°:

$$\sigma_v^\circ = \frac{k_o^2 \cos^2\theta_i}{\pi(a_1 a_1^* + a_2 a_2^* + a_3 a_3^*)} \cdot \Big\{ e_{rx} e_{rx}^* \alpha_{xx} + 2\mathrm{Re}\,[e_{rx} e_{ry} \alpha_{y}] + 2\mathrm{Re}\,[e_{rx} e_{rz}^* \alpha_{xz}] + e_{ry}^2 \alpha_{yy} + 2k_o \sin\theta_i \cdot \mathrm{Re}\,[e_{ry} e_{rz} \alpha_{xy} / k_{1z}] + e_{rz} e_{rz}^* \alpha_{zz} \Big\} \tag{69}$$

where

$$\alpha_{xx} = < A_x A_x^* > / A_I$$

$$\alpha_{xy} = < A_x A_y^* > / A_I$$

$$\alpha_{xz} = < A_x A_z^* > / A_I$$

$$\alpha_{yy} = < A_y A_y^* > / A_I$$

$$\alpha_{zz} = < A_z A_z^* > / A_I$$

Consider now the form of σ_v° for horizontal and vertical polarizations. The following parameters are used to describe a wave that is transmitted with horizontal polarization and horizontal polarization is received.

$$a_1 = 0 \qquad e_{rx} = 0$$

$$a_2 = 1 \qquad e_{ry} = 1$$

$$a_3 = 0 \qquad e_{rz} = 0$$

For these parameters, the backscatter coefficient can be given the additional subscripts of HH to indicate horizontal polarization transmit, and horizontal polarization receive.

$$\sigma^{\circ}_{HHv} = k_o^2 \, \alpha_{yy} \cos^2\theta_i / \pi \qquad ((70)$$

The case of vertical polarization transmit, vertical polarization receive can be characterized as follows:

$$a_1 = \cos\theta_i \qquad e_{rx} = \cos\theta_i$$

$$a_2 = 0 \qquad e_{ry} = 0$$

$$a_3 = \sin\theta_i \qquad e_{rz} = \sin\theta_i$$

The backscatter coefficient associated with these parameters can be given the additional subscripts VV.

$$\sigma^{\circ}_{VVv} = \frac{k_o^2 \cos^2\theta_i}{\pi} \left\{ \alpha_{xx} \cos^2\theta_i + 2\mathrm{Re}\,[\alpha_{xz} \cos\theta_i \sin\theta_i] + \alpha_{zz} \sin^2\theta_i \right\} \qquad (71)$$

If a result is computed for the cross-polarized backscatter coefficient (HV or VH), the term will disappear. The reason for this is that the particular elements of the dyadic M, which would yield cross-polarized terms in the mean wave, are all zero. Next, let's consider the influence of an irregular vegetation-soil boundary.

MODIFYING THE VOLUME SCATTERING RESULTS TO INCORPORATE THE INFLUENCE OF AN IRREGULAR VEGETATION – SOIL BOUNDARY

In this section, we will consider what must be done to equations (70) and (71) to include the influence of a rough ground surface. It is expected that the influence of the rough surface would be greater when the angle of incidence is small. Also, as the vegetation height or density gets larger, less scattering is expected from the ground surface below. In what follows, the horizontal and vertical polarizations will be considered separately.

Consider a horizontally polarized wave incident from free space onto a layer of vegetation that has an average thickness L. The interface between the vegetation and soil will be considered as randomly rough in such a way that the tangent plane approximation is applicable. The radar backscatter coefficient (σ°_{HH}) will be considered as the sum of a term resulting from surface scattering and a term resulting from volume scattering.

$$\sigma^{\circ}_{HH} = \sigma^{\circ}_{HHS} \exp\left[-4\alpha_{e1} L \sec\psi_{e1}\right] + \sigma^{\circ}_{HHv} \tag{72}$$

In equation (72), σ°_{HHS} represents the backscatter coefficient for a randomly rough surface with a guassian distribution of surface heights. The subscript s indicates surface scattering. The quantity σ°_{HHS} is multiplied by a decaying exponential in which α_{e1} is the imaginary part of the effective propagation constant and ψ_{e1} is the true angle of refraction for the mean wave in the vegetation. The second subscript 1 on α_{e1} and ψ_{e1} is used to indicate horizontal polarization since these parameters will have different values for vertical polarization. The effective propagation constant (k_{e1}) can be obtained from k_h.

$$k_{e1}^2 = k_{ez}^2 + k_{ex}^2 = k_h^2 + k_o^2 \sin^2\theta_i$$

If we now let $k_{e1} = \beta_{e1} - j\alpha_{e1}$ and in place of k_h we put $jp_1 - q_1$, then we can solve for β_{e1} and α_{e1}.

$$\beta_{e1} = \rho_{e1}^{1/2} \cos(\phi_{e1}/2)$$

$$\alpha_{e1} = \rho_{e1}^{1/2} \sin(\phi_{e1}/2)$$

Where ρ_{e1} and ϕ_{e1} are defined below:

$$\rho_{e1} = \left\{ 4p_1^2 q_1^2 + (q_1^2 + k_o^2 \sin^2\theta_i - p_1^2)^2 \right\}^{1/2}$$

$$\phi_{e1} = \tan^{-1} \left\{ \frac{2p_1 q_1}{q_1^2 + k_o^2 \sin^2\theta_i - p_1^2} \right\}$$

The planes of constant phase for the mean wave in the random medium are used to calculate an expression for $\sec\psi_{e1}$.

$$\sec \psi_{e1} = \frac{\sqrt{k_o^2 \sin^2\theta_i + \rho_1^2(\beta_{e1}\cos\gamma_1 - \alpha_{e1}\sin\gamma_1)}}{\rho_1 (\beta_{e1}\cos\gamma_1 - \alpha_{e1}\sin\gamma_1)}$$

Where ρ_1 and γ_1 are given below:

$$\rho_1 = \left\{ 4a_1^2 b_1^2 \sin^4\theta_i + [1 - (a_1^2 - b_1^2)\sin^2\theta_i]^2 \right\}^{1/4}$$

$$\gamma_1 = \tfrac{1}{2} \tan^{-1} \left[\frac{2a_1 b_1 \sin^2\theta_i}{1 - (a_1^2 - b_1^2)\sin^2\theta_i} \right]$$

$$a_1 = \frac{k_o \beta_{e1}}{\beta_{e1}^2 + \alpha_{e1}^2} \qquad b_1 = \frac{k_o \alpha_{e1}}{\beta_{e1}^2 + \alpha_{e1}^2}$$

Many derived expressions are available for the backscatter coefficient from a randomly rough surface using the tangent plane method. The following equation will be used:[5]

$$\sigma^\circ_{HHS} = \frac{R_o^2}{4m_s^2 \cos^4\psi_{e1}} \left\{ 1 - \sin^2\psi_{e1} [2(1 - g_o \cos^2\psi_{e1}) - \sin^2\psi_{e1}(1 + g_o^2)] \right\} \exp[-\tan^2\psi_{e1}/(4m_s^2)] \qquad (73)$$

[5] R. A. Hevenor, *Backscattering of Electromagnetic Waves From a Surface Composed of Two Types of Surface Roughness*, U.S. Army Engineer Topographic Laboratories, Fort Belvoir, Virginia. ETL-TR-71-4, October 1971, AD-737 675.

The quantity R_o in (73) represents the Fresnel reflection coefficient and can be computed as follows:

$$R_o = \frac{\beta_{e1} \cos \psi_{e1} - \sqrt{\beta_3^2 - \beta_{e1}^2 \sin^2 \psi_{e1}}}{\beta_{e1} \cos \psi_{e1} + \sqrt{\beta_3^2 - \beta_{e1}^2 \sin^2 \psi_{e1}}}$$

In calculating R_o, we have neglected the effect of the imaginary parts of the propagation constants. The term m_s represents the ratio of the standard deviation of the surface fluctuations to the correlation distance. The quantity g_o is defined by the following expression:

$$g_o = 1 - \frac{2\beta_{e1} \cos \psi_{e1}}{\sqrt{\beta_3^2 - \beta_{e1}^2 \sin^2 \psi_{e1}}}$$

A final equation can now be written for σ^o_{HH} that considers both the volume-scattering and surface-scattering effects.

$$\sigma^o_{HH} = \frac{R_o^2}{4m_s^2 \cos^4 \psi_{e1}} \left\{ 1 - \sin^2 \psi_{e1} \left[2(1 - g_o \cos^2 \psi_{e1}) - \sin^2 \psi_{e1} (1 + g_o^2) \right] \right\} \exp\left[-\tan^2 \psi_{e1}/(4m_s^2)\right] \cdot \exp[-4\alpha_{e1} L \sec \psi_{e1}] + k_o^2 \alpha_{yy} \cos^2 \theta_i / \pi \quad (74)$$

In the same manner, a complete solution for vertical polarization can be obtained:

$$\sigma^o_{VV} = \frac{r_o^2}{4m_s^2 \cos^4 \psi_{e2}} \left\{ 1 + \frac{r'_o \sin^2 \psi_{e2} \cos \psi_{e2}}{\gamma_o^2} \left[2r_o \sin \psi_{e2} + r'_o \cos \psi_{e2} \right] + \frac{2r'_o}{r_o} \sin \psi_{e2} \cos^3 \psi_{e2} \right\}$$

$$\cdot \exp\left[-\tan^2 \psi_{e2}/(4m_s^2)\right] \exp\left[-4\,\alpha_{e2}\, L \sec \psi_{e2}\right]$$

$$+ \frac{k_o^2 \cos^2\theta_i}{\pi} \left\{ \alpha_{xx} \cos^2\theta_i + 2\mathrm{Re}\left[\cos\theta_i \sin\theta_i\, \alpha_{xz}\right] + \alpha_{zz} \sin^2\theta_i \right\} \tag{75}$$

The new quantities introduced into the above equation are defined below:

$$\beta_{e2} = \rho_{e2}^{1/2} \cos(\phi_{e2}/2)$$

$$\alpha_{e2} = \rho_{e2}^{1/2} \sin(\phi_{e2}/2)$$

The quantities ρ_{e2} and ϕ_{e2} are given as follows:

$$\rho_{e2} = \left\{ 4p_2^2 q_2^2 + (q_2^2 + k_o^2 \sin^2\theta_i - p_2^2)^2 \right\}^{1/2}$$

$$\phi_{e2} = \tan^{-1}\left\{ \frac{2p_2 q_2}{q_2^2 + k_o^2 \sin^2\theta_i - p_2^2} \right\}$$

$$\sec \psi_{e2} = \frac{\sqrt{k_o^2 \sin^2\theta_i + \rho_2^2 (\beta_{e2}^2 \cos\gamma_2 - \alpha_{e2} \sin\gamma_2)^2}}{\rho_2 (\beta_{e2} \cos\gamma_2 - \alpha_{e2} \sin\gamma_2)}$$

$$\rho_2 = \left\{ 4a_2^2 b_2^2 \sin^4\theta_i + [1 - (a_2^2 - b_2^2)\sin^2\theta_i]^2 \right\}^{1/4}$$

$$\gamma_2 = \tfrac{1}{2} \tan^{-1}\left[\frac{2a_2 b_2 \sin^2\theta_i}{1 - (a_2^2 - b_2^2)\sin^2\theta_i} \right]$$

where a_2 and b_2 are

$$a_2 = \frac{k_o \beta_{e2}}{\beta_{e2}^2 + \alpha_{e2}^2} \qquad b_2 = \frac{k_o \alpha_{e2}}{\beta_{e2}^2 + \alpha_{e2}^2}$$

$$r_2 = \frac{\beta_3^2 \cos\psi_{e2} - \beta_{e2}\sqrt{\beta_3^2 - \beta_{e2}^2 \sin^2\psi_{e2}}}{\beta_3^2 \cos\psi_{e2} + \beta_{e2}\sqrt{\beta_3^2 - \beta_{e2}^2 \sin^2\psi_{e2}}}$$

$$r_o' = \frac{2\beta_3^2 \beta_{e2} \sin\psi_{e2} (\beta_3^2 - \beta_{e2}^2)}{\sqrt{\beta_3^2 - \beta_{e2}^2 \sin^2\psi_{e2}} \left\{\beta_e^2 \cos\psi_{e2} + \beta_{e2}\sqrt{\beta_3^2 - \beta_{e2}^2 \sin^2\psi_{e2}}\right\}}$$

Equations (74) and (75) are the final results for the radar backscatter coeffieient for horizontal and vertical polarizations. Before the results of computing equations (74) and (75) are shown, an elementary vegetation permittivity model must be developed that relates some of the model input parameters to the complex dielectric constants of vegetation and water.

DEVELOPMENT OF A VEGETATION PERMITTIVITY MODEL

To determine the influence of various vegetation parameters (such as moisture content) upon the calculation of the backscatter coefficient, one must relate some of the permittivity parameters in the scattering model to the physical parameters of the vegetation. Peake and Oliver's model[6] will be used to calculate the relative complex dielectric constant of vegetation ($\hat{\epsilon}_v$):

$$\epsilon_v = (F/2)\mathrm{Re}[\hat{\epsilon}_w] + j(F/3)\mathrm{Im}[\hat{\epsilon}_w]$$

[6]W.H. Peake and T.L. Oliver, *The Response of Terrestrial Surfaces at Microwave Frequencies,* Technical Report AFAL-TR-70-301, The Ohio State University, Electroscience Laboratory, AD-884 106.

where F is the fraction of water by weight in the vegetation; Re[$\hat{\epsilon}_w$] and Im[$\hat{\epsilon}_w$] are the real and imaginary parts of the relative complex dielectric constant of water ($\hat{\epsilon}_w$), which can be written as

$$\hat{\epsilon}_w = 5 + \frac{75}{1 + j(1.85/\lambda)}$$

where λ is the wavelength in centimeters. For particular values of λ and F, we can now compute $\hat{\epsilon}_v$. With a knowledge of $\hat{\epsilon}_v$, one can estimate the average relative complex dielectric constant ($\hat{\epsilon}_a$) by using the following

$$\hat{\epsilon}_a = (V_v \hat{\epsilon}_v + \epsilon_A V_A)/V_T$$

$$\epsilon_a = \mathrm{Re}[\hat{\epsilon}_a] \qquad \sigma_a = -\omega\epsilon_o \left(\frac{V_v}{V_T}\right) \mathrm{Im}(\hat{\epsilon}_v)$$

where V_V is the volume occupied by the vegetation; V_A is the volume occupied by air; V_T is the total volume equal to $V_V + V_A$; ϵ_A is the relative dielectric constant of air, assumed equal to 1. The variances η_1^2 and η_2^2 can be computed by using the following formulas:

$$\eta_1^2 = \frac{V_v (\epsilon_v' - \epsilon_a)^2 + V_A (\epsilon_A - \epsilon_a)^2}{V_T}$$

$$\eta_2^2 = \frac{V_v (\sigma_v - \sigma_a)^2 + V_A \sigma_a^2}{V_T}$$

where

$$\sigma_v = -\omega\epsilon_o F \, \mathrm{Im}[\epsilon_w]/3 \quad \text{and} \quad \epsilon_v' = \mathrm{Re}[\hat{\epsilon}_v]$$

The symbol R_V shall be used to designate the volume ratio V_V / V_T.

The developed model for the radar backscatter coefficient is now complete and calculations can be made. In the next section, computed results will be shown, and the theory will be compared with some existing experimental data.

DISCUSSION OF RESULTS

In this section, some numerical calculations will be shown for the theory derived in the previous section, and a study will be presented of the influence of the various input parameters on the backscatter coefficient. Two computer programs were developed for solving equations (74) and (75). One program solves for equation (74) and the second solves for (75). The solutions to the half-space and plane layer problems are also generated for comparison. A listing of the computer program for solving equation (74) is given in appendix B. The 10 input parameters to the programs are

1. Fraction of water by weight in the vegetation (F)
2. Volume of vegetation divided by the total volume (R_V)
3. Correlation distance in the x direction (ℓ_x)
4. Correlation distance in the y direction (ℓ_y)
5. Correlation distance in the z direction (ℓ_z)
6. Mean thickness of the vegetation layer (L)
7. Relative dielectric constant of the soil below the vegetation (ϵ_g)
8. Conductivity of the soil below the vegetation (σ_3)
9. Frequency (f)
10. Ratio of the standard deviation of the rough surface fluctuations to the correlation distance of the fluctuations (m_s).

The output of the computer programs is the backscatter coefficient in decibels as a function of incidence angle. The backscatter coefficient in decibels is related to the backscatter coefficient as follows:

$$\sigma^\circ \text{ (in decibels)} = 10 \log_{10} \sigma^\circ$$

The backscatter coefficient on the right side of the above equation is computed by (74) or (75). The following discussion centers on figures 2 through 30, which show the results of computing equations (74) and (75). Figures 2 and 3 come from Ulaby and Bush and provide pertinent ground truth data associated with the experimental measurements. Figure 4 comes from Cihlar and Ulaby[7] and provides a relationship between soil moisture and relative complex dielectric constant. Figures 5 through 15 provide a comparison of the developed theory with experimental data taken from a cornfield by Ulaby and Bush.[8]

---

[7]F.T. Ulaby and T.F. Bush, *Corn Growth as Monitores by Radar,* The University of Kansas Center for Research, Inc. RSL Technical Report 117-57, November 1975.

[8]F.T. Ulaby and J. Cihlar, *Dielectric Properties of Soils as a Function of Moisture Content,* The University of Kansas Center for Research, Inc., RSL Technical Report 177-47, November 1974.

FIGURE 2. Corn Ground Truth, 1974.

	Soil Moisture (g/cm^3)			% Plant Moisture	Normalized Plant Water Content (g/m)	Plant Height (m)
Date	N	M	F			
May 20	.19	.19	.24	89.5	77	0.30
May 24	.28	.26	.26	86.5	167	0.40
May 30	.12	.10	.12	87.1	252	0.58
June 5	.10	.13	.10	88.5	262	0.88
June 13	.34	.34	.34	89.9	552	1.25
June 20	.30	.31	.32	89.9	442	1.90
June 26	.06	.09	.08	83.9	383	2.30
July 1	.05	.05	.07	82.4	425	2.60
July 8	.21	.27	.30	84.7	440	2.60
July 11	.17	.15	.15	81.5	490	2.60
July 16	.04	.07	.06	81.5	374	2.60
July 22	.04	.04	.04	73.4	482	2.60
August 5	.06	.07	.07	62.4	236	2.60
Autust 15	.26	.27	.26	52.9	99	2.70
September 5	.31	.30	.29	47.5	151	2.70
September 19	.12	.12	.10	16.5	58	0.23
July 30*	.26	.26	.26	74.8	413	2.60

* = irrigated corn field N = near range sample M = medium range sample F = far range sample

SOURCE : F.T. Ulaby and T.F. Bush, *Corn Growth as Monitored by Radar,* The University of Kansas Center for Research, Inc. RSL Technical Report 117–57, November 1975.

Figure 2. Corn Ground Truth, 1974.

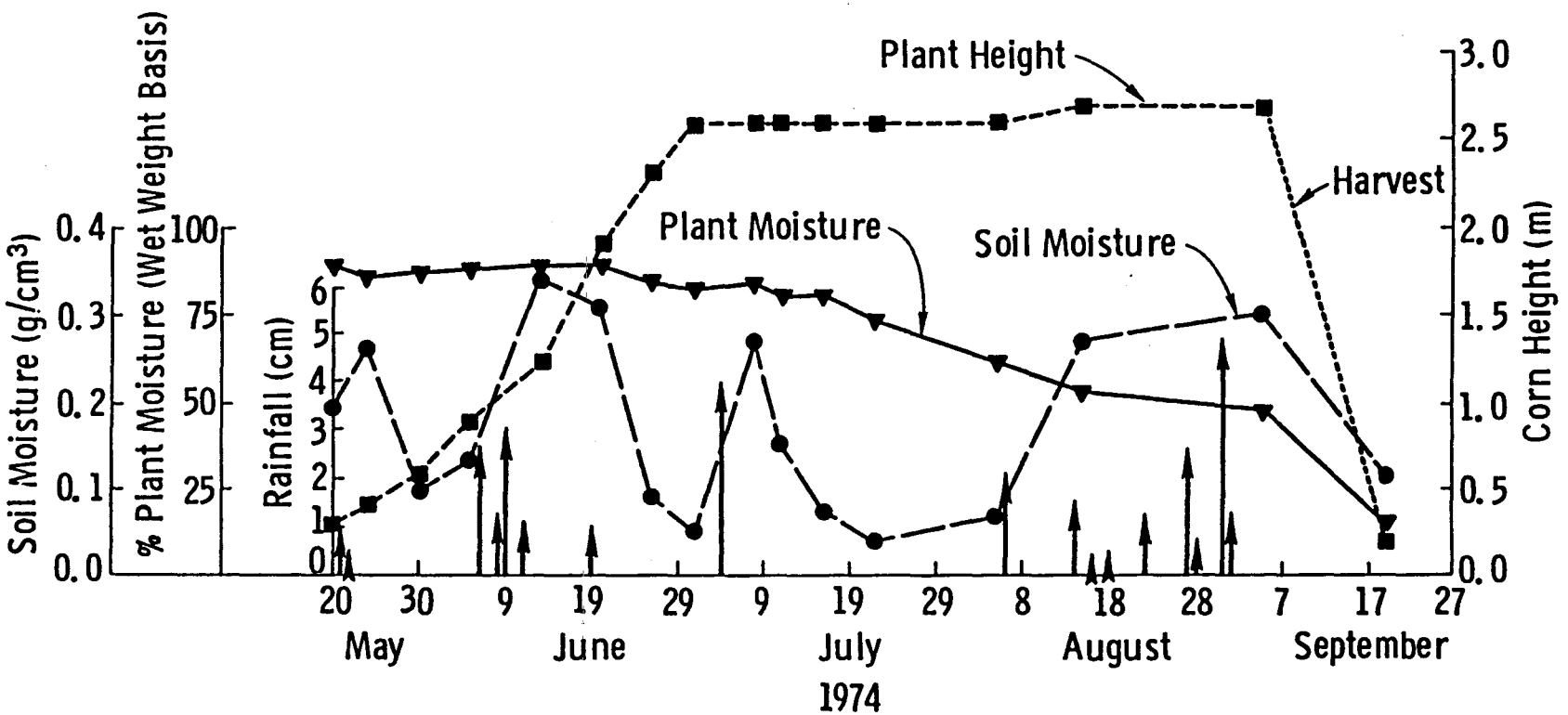

SOURCE : F.T. Ulaby and T.F. Bush, *Corn Growth as Monitored by Radar,* The University of Kansas Center for Research, Inc. RSL Technical Report 117–57, November 1975.

Figure 3. Data Record of Soil Moisture, Plant Moisture, Plant Height, and Precipitation as Measured During the Observation Period.

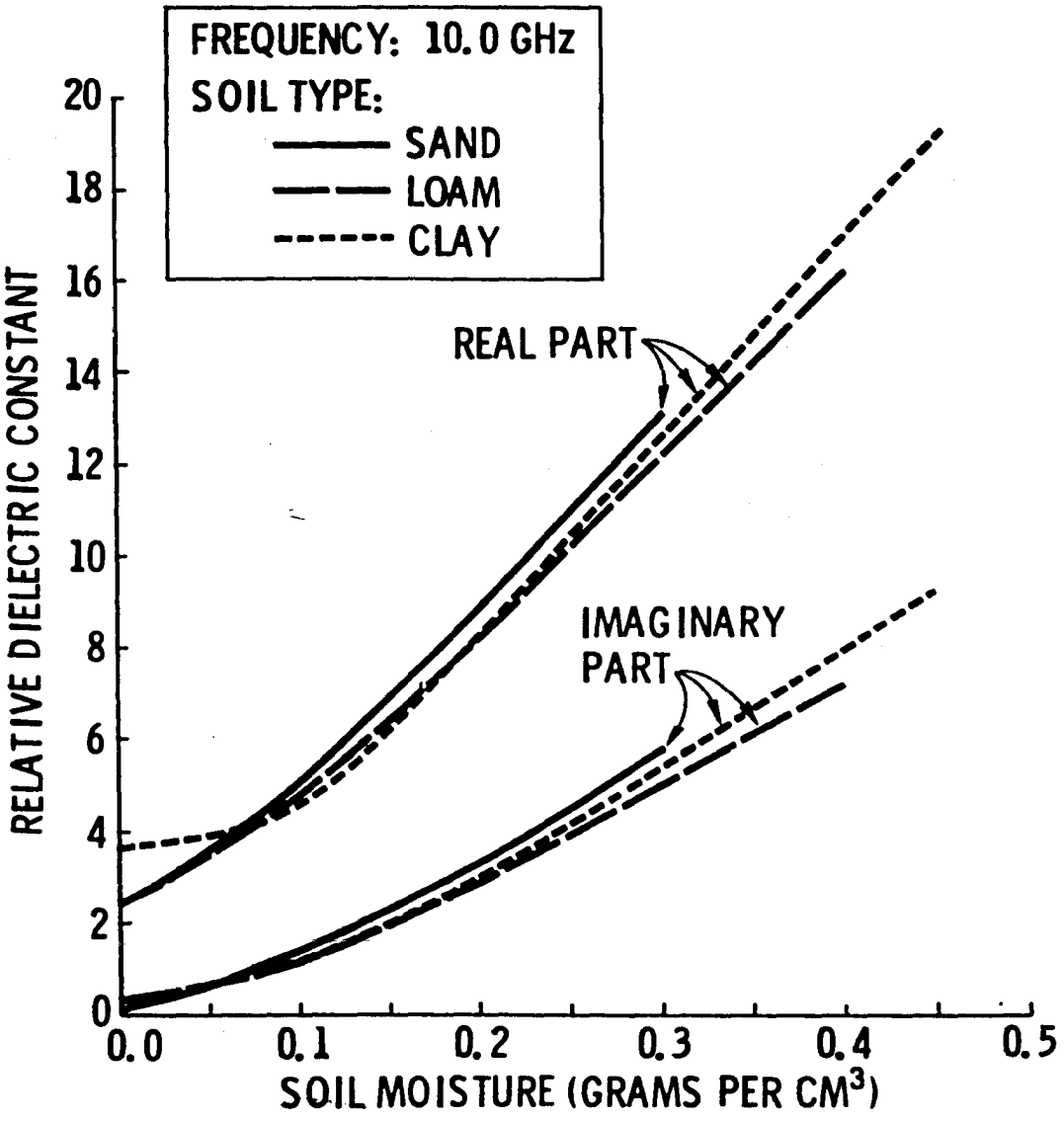

Source : F.T. Ulaby and J. Cihlar, *Dielectric Properties of Soils as a Function of Moisture Content,* The University of Kansas Center for Research, Inc., RSL Technical Report 177–47, November 1974.

Figure 4. Representative Dielectric Constant Values as a Function of Volumetric Water Content.

The soil moisture is obtained from figure 2 for a particular set of measurements performed on a given date. This soil moisture is used along with the curves of figure 4 to determine the relative dielectric constant and the conductivity of the soil. Throughout all comparisons of theory with experiment, it has been assumed that the soil type is a loam. In comparing theory with experiment, remember that certain input parameters to the theoretical model were not known and had to be estimated; whereas, other input parameters were known from the ground truth data collected during the experiment. The unknown input parameters are R_V, ℓ_x, ℓ_y, ℓ_z and m_s.

In figure 5, the theory is matched to the experimental data for corn that is at a height of 30 centimeters. The large rise that occurs in σ° as θ_i goes from 10° to 0° is indicative of a rough surface effect. In this case, the rough surface is quasi-specular since m_s is given such a small value. It can be seen that to match the theory with the experimental data, it was necessary to let ℓ_x be different from ℓ_y and to let ℓ_z be much smaller than ℓ_x or ℓ_y. The fact that ℓ_x is different from ℓ_y shows an anisotropic effect in the horizontal plane, which probably arises from the corn being planted in rows.

Figure 6 matches the theory to experimental data for corn that is 2.3 meters high. It can be seen that a good match is obtained for ℓ_x equal to ℓ_y, indicating that the anistropic effect in the horizontal plane has essentially disappeared for 8.6 GHz. The values of the parameters used for R_V, ℓ_x, ℓ_y, ℓ_z, and m_s in figure 6 are also used in figures 7 through 10 to determine whether the model could provide a correct prediction of σ° for different values of F, soil moisture, and vegetation height.

Figures 7 through 9 show an excellent agreement between theory and experiment. Figure 10 shows an excellent agreement between theory and experiment for angles of incidence equal to and greater than 30°. For angles of incidence less than 30°, the agreement is poor. A possible reason for this poor agreement may be due to the rainfall that came prior to the August 15th measurements. The rainfall could have disturbed the soil surface in both a physical and an electrical manner such that its scattering behavior is no longer predictable from prior values.

Figures 11 and 12 show an attempt to match the theory to the experimental data for frequencies of 11 GHz and 13 GHz. It can be seen that to obtain a good match, the values of ℓ_x and ℓ_y must be altered from the values used at 8.6 GHz. This seems to indicate that as the frequency goes higher, the vegetation medium becomes more complicated and the anisotropic behavior becomes more pronounced.

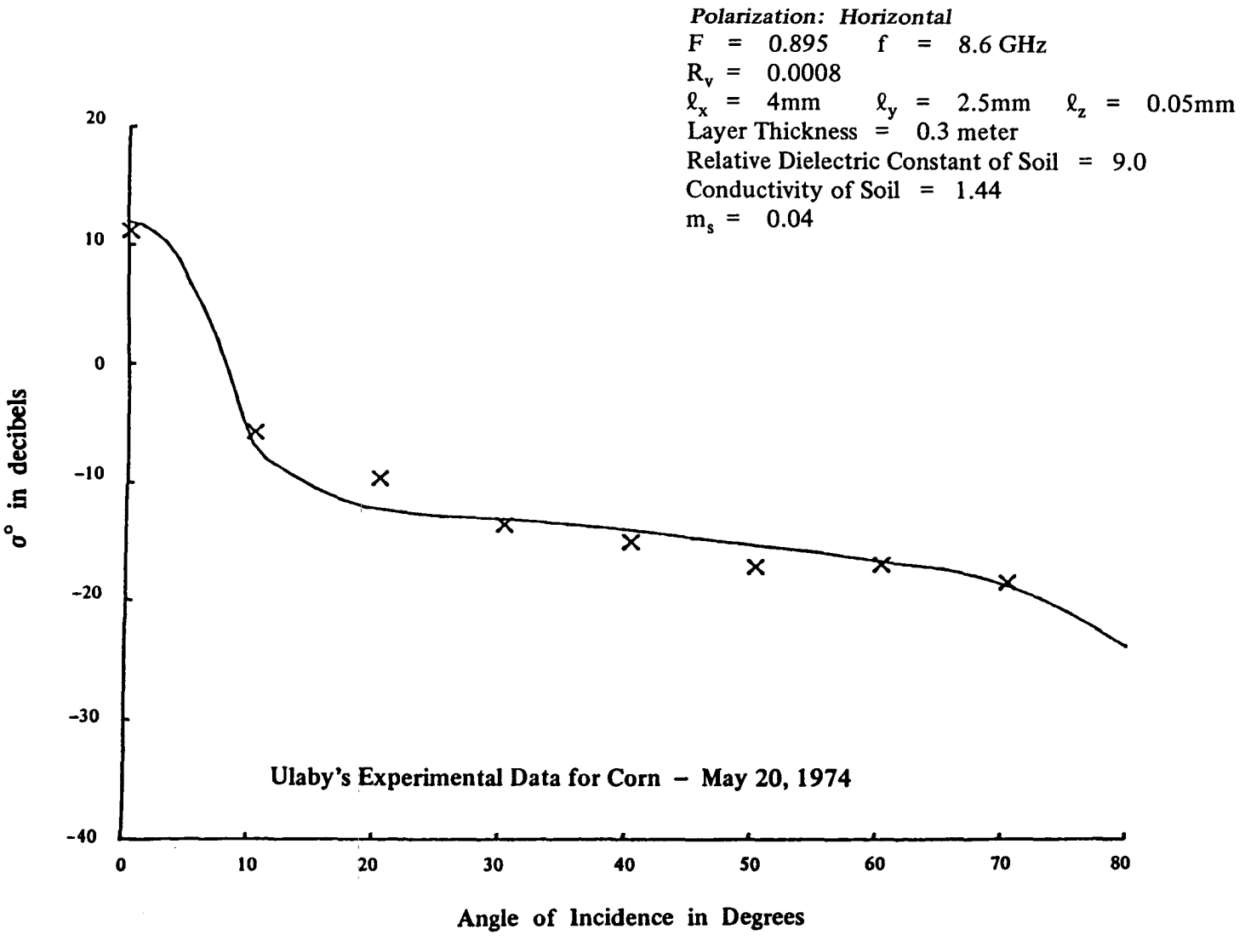

Figure 5. Comparison of Theory with Experimental Data.

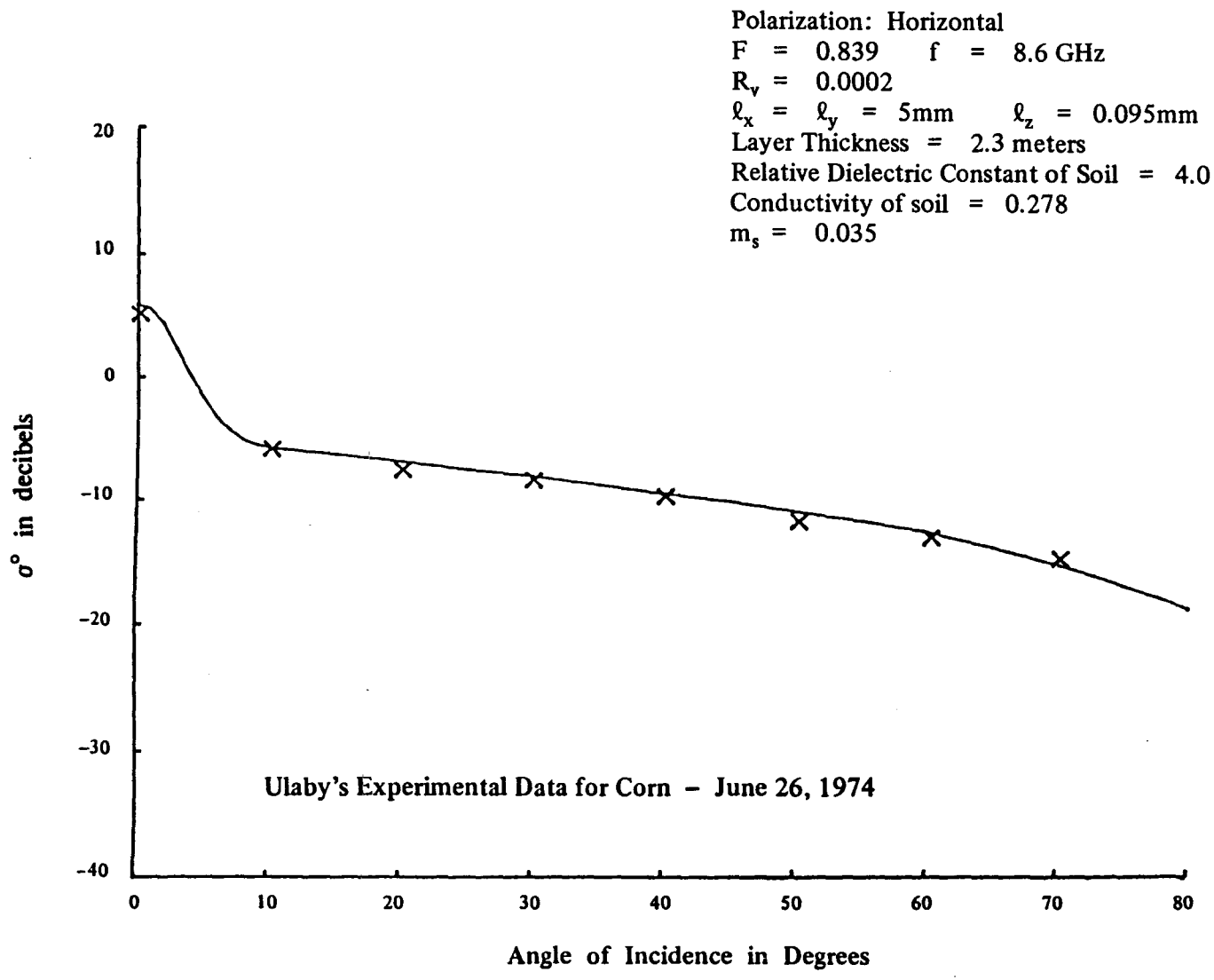

Figure 6. Comparison of Theory with Experimental Data.

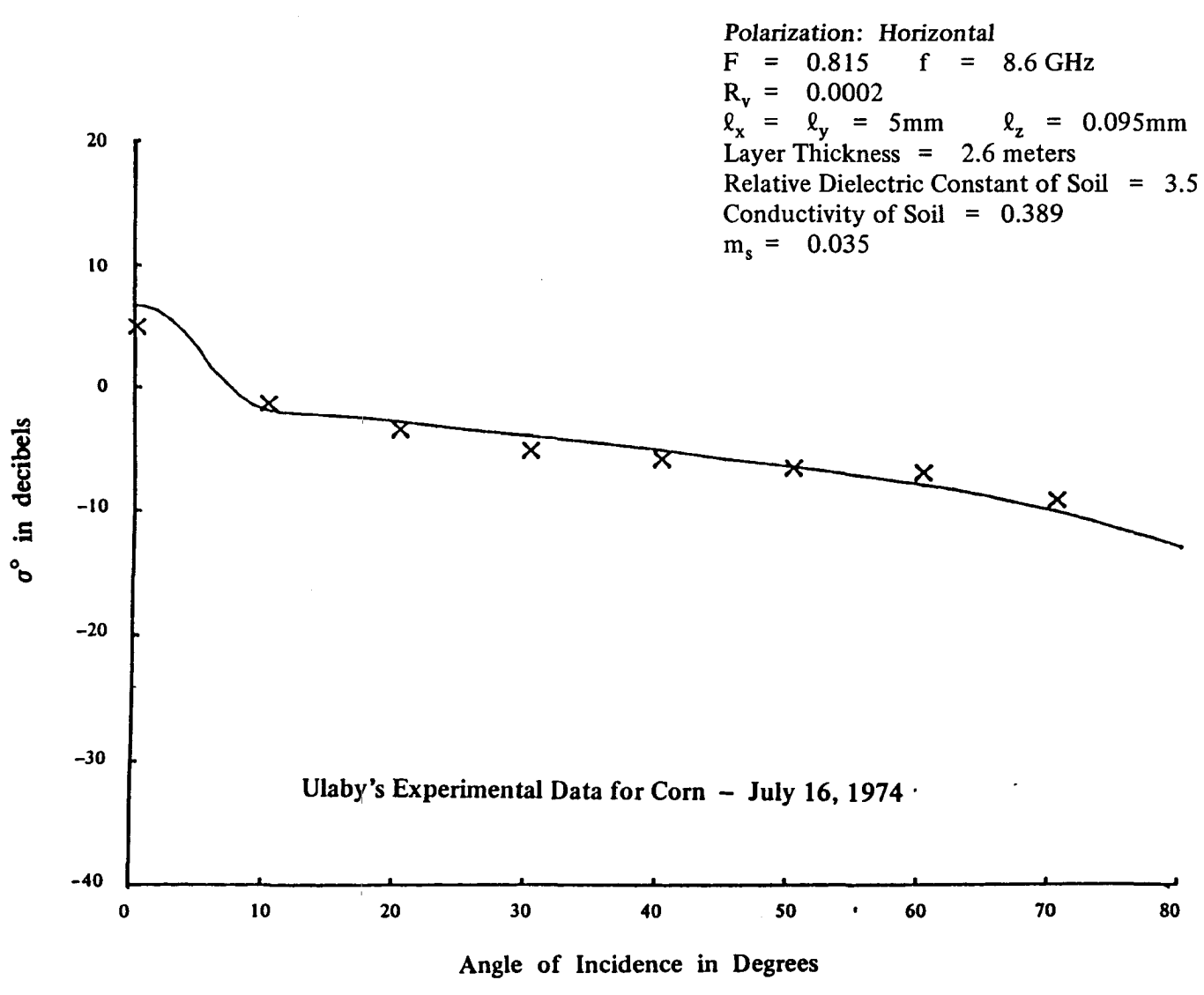

Figure 7. Comparison of Theory with Experimental Data.

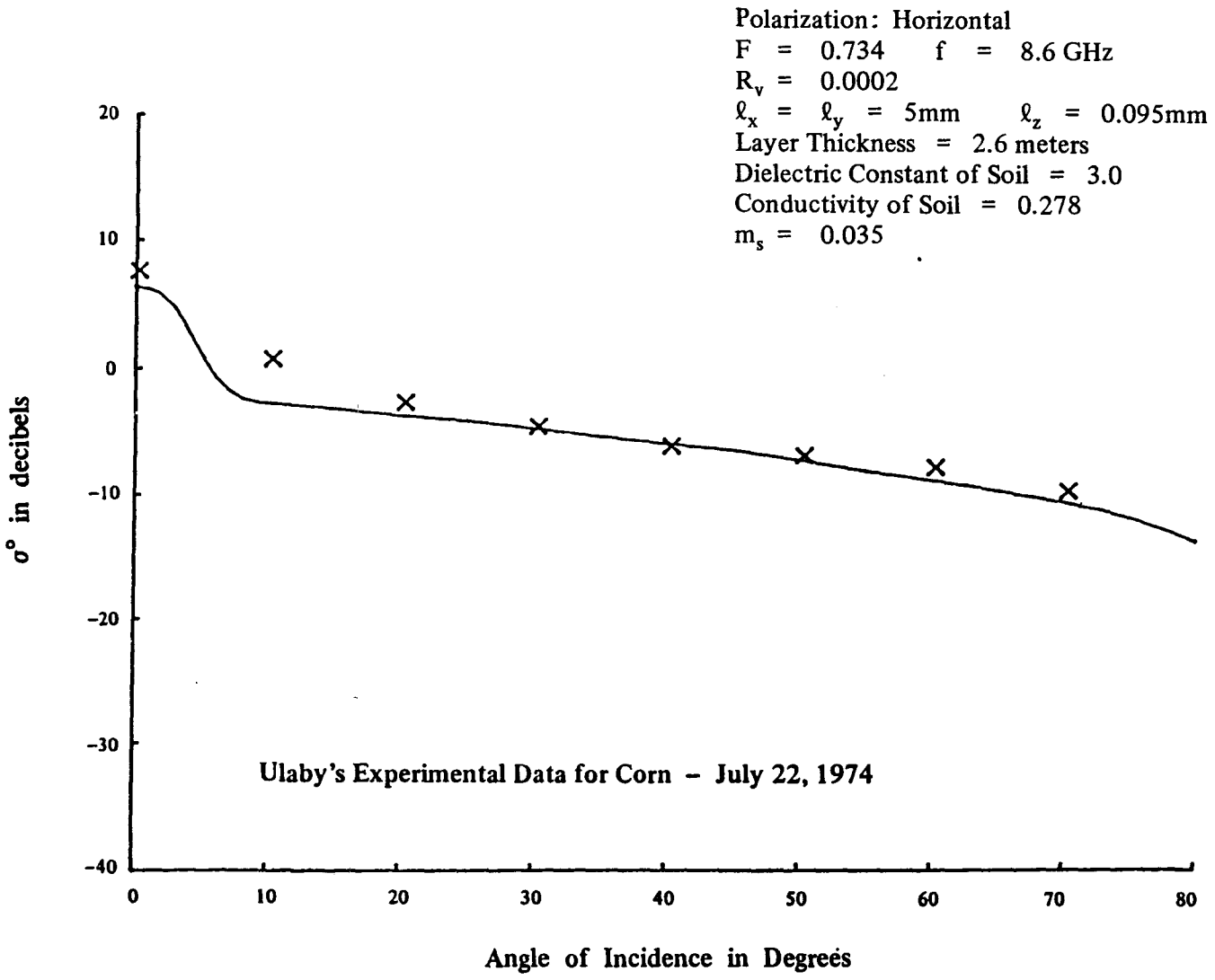

Figure 8. Comparison of Theory with Experimental Data.

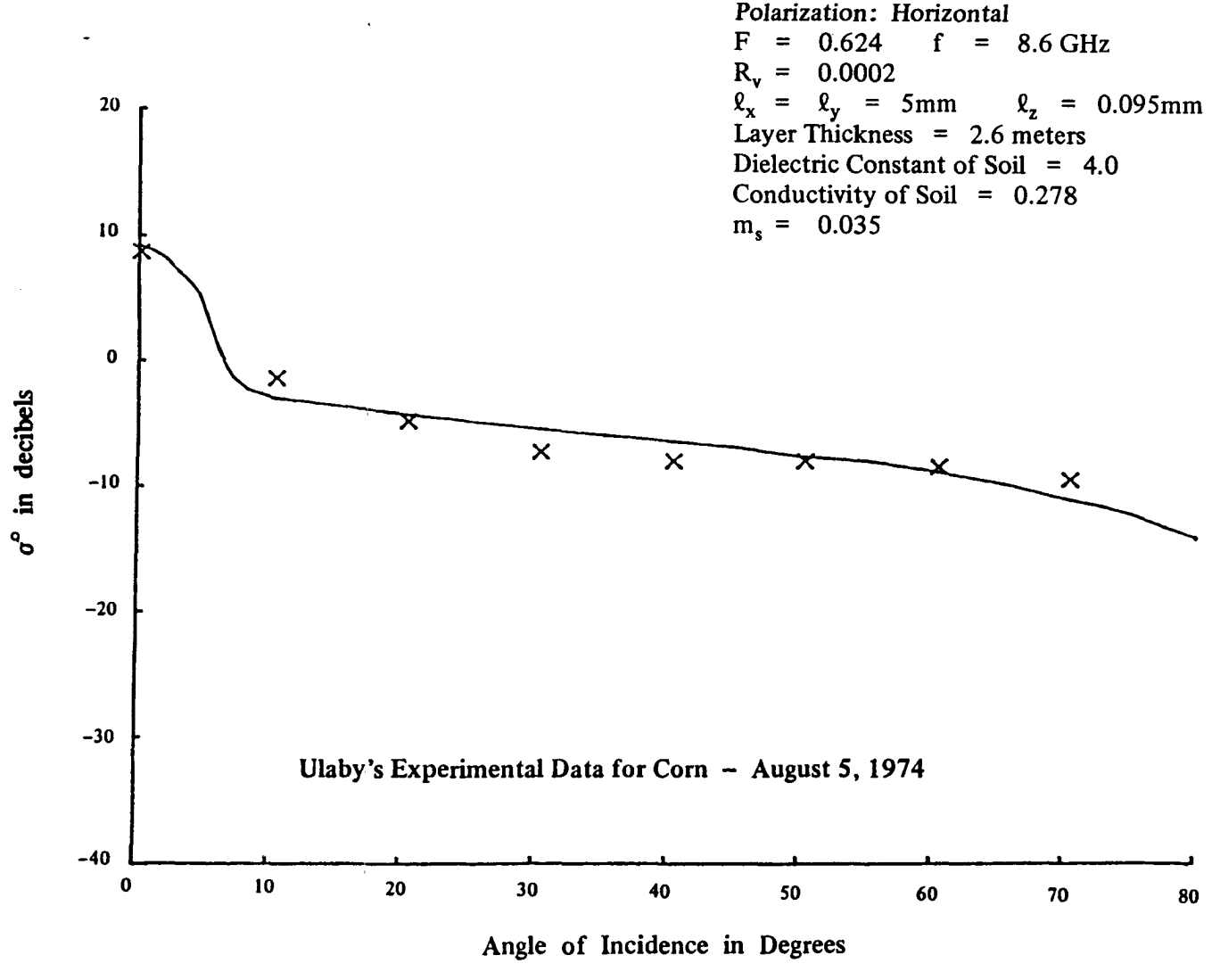

Figure 9. Comparison of Theory with Experimental Data.

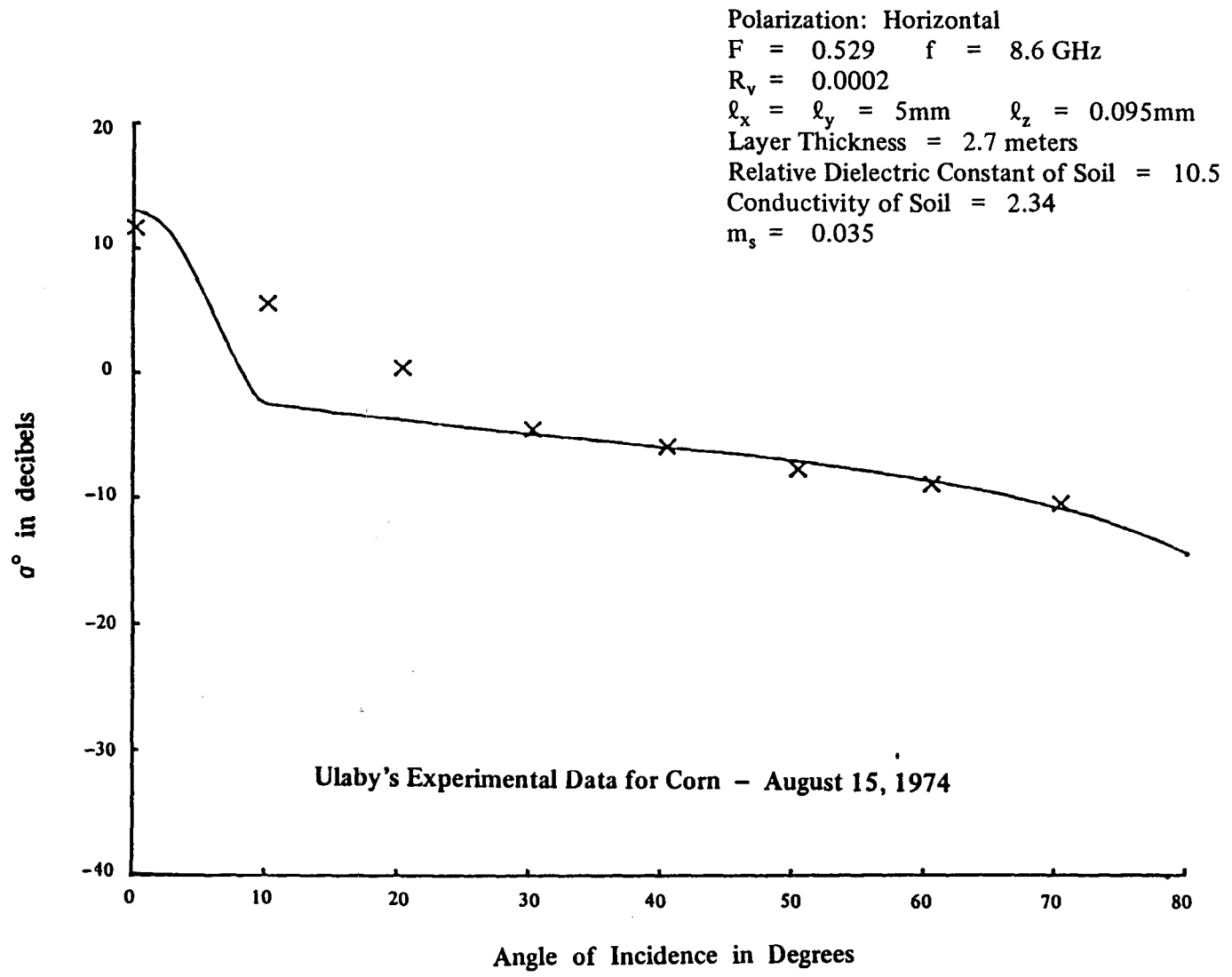

Figure 10. Comparison of Theory with Experimental Data.

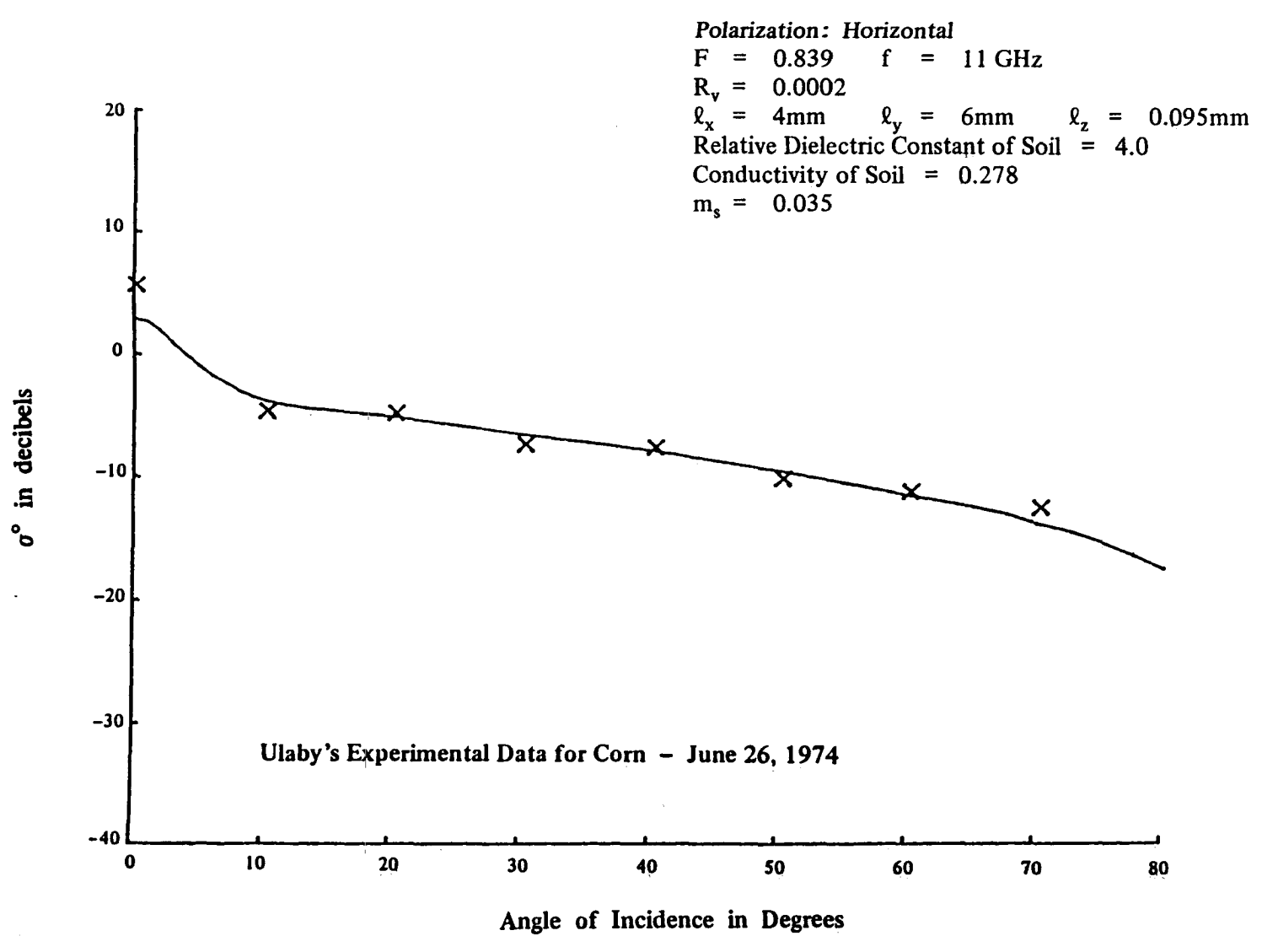

Figure 11. Comparison of Theory with Experimental Data.

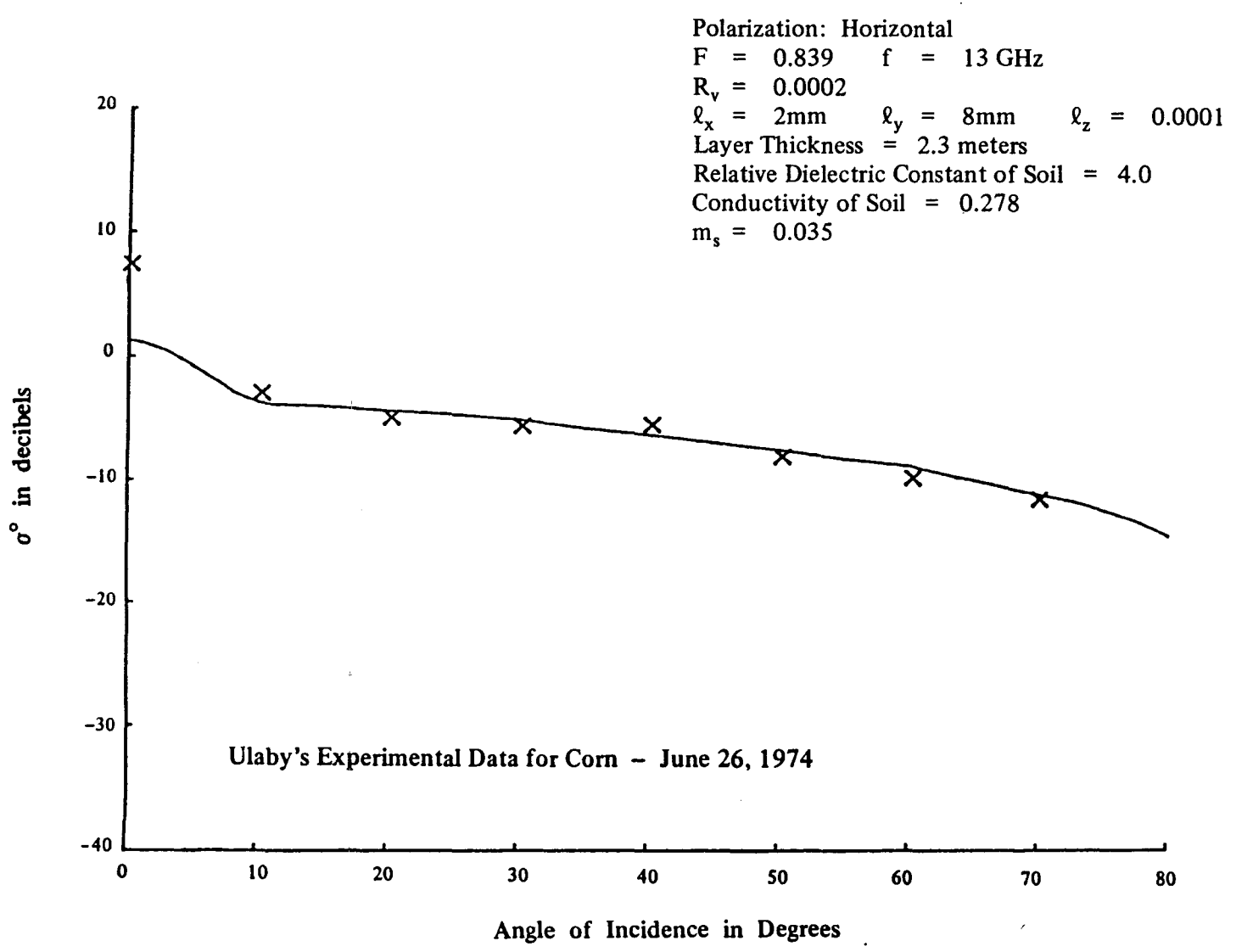

Figure 12. Comparison of Theory with Experimental Data.

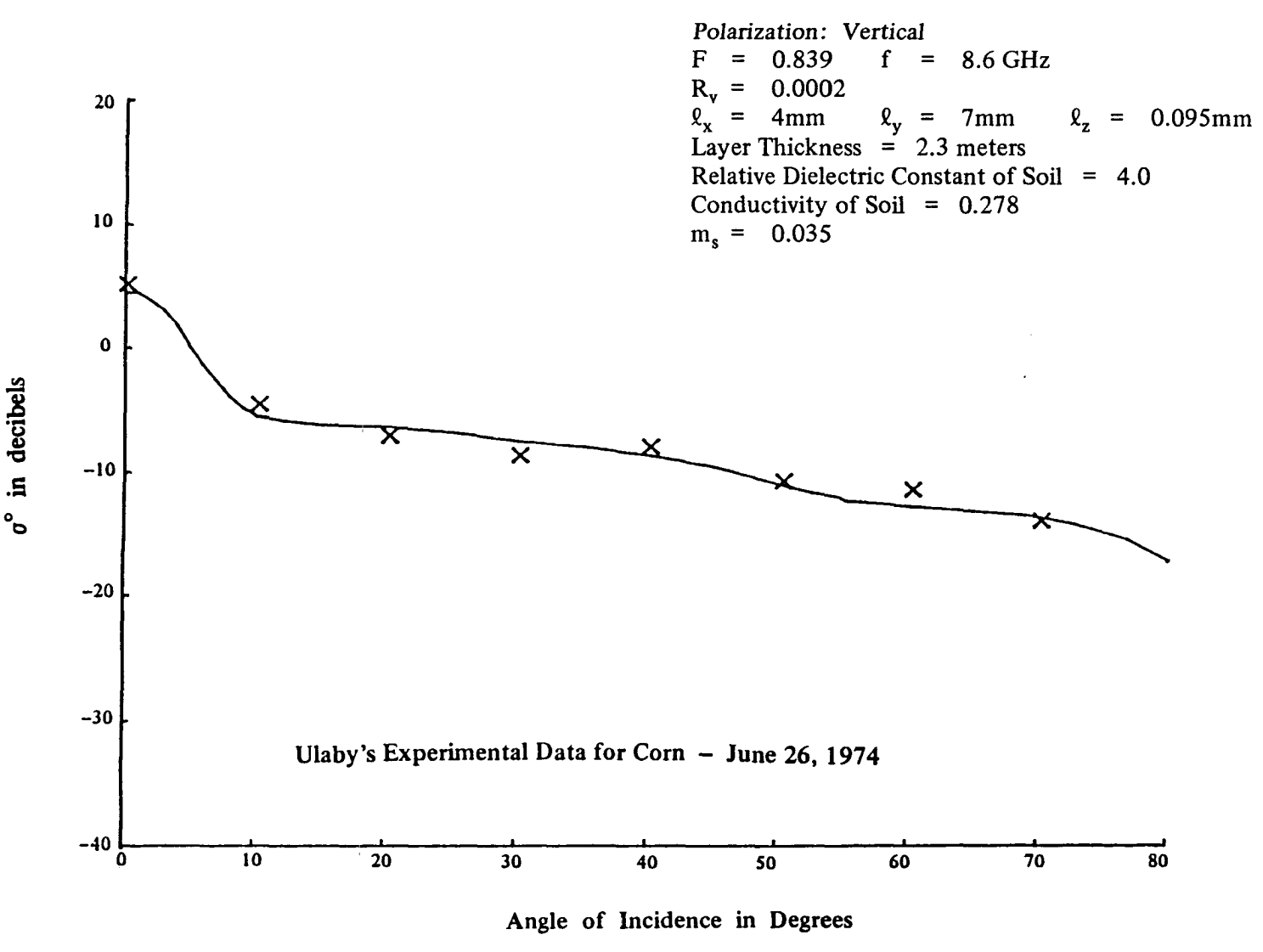

Figure 13. Comparison of Theory with Experimental Data.

In figures 13 through 15 a match is shown of the theory with experimental data for vertical polarization. For all three curves, ℓ_x must be made unequal to ℓ_y to obtain a good match. In figure 16, the variations are shown in the experimental measurements of σ°, which can occur throughout the spring and summer for alfalfa. Large variations in the backscatter coefficient occur prior to and after harvesting.

Figure 17 presents a study of sensor-look direction with respect to vegetation planted in rows. The two parameters $\sigma^\circ_\perp$ and $\sigma^\circ_\parallel$ represent the backscatter coefficient when the look direction is perpendicular and parallel to the rows, respectively. We see that when θ_i equals zero degrees, $\sigma^\circ_\perp$ and $\sigma^\circ_\parallel$ are equal. However, for θ_i greater than zero degrees, $\sigma^\circ_\perp$ is greater than $\sigma^\circ_\parallel$. The theoretical results agree only partically with the experimental results given in figure 18, which comes from Batlivala and Ulaby.[9]

Figure 19 provides a study of backscatter coefficient versus layer thickness for two angles of incidence. For the θ_i equal to zero curve, the solution for σ° with a rough layer differs from the half-space solution by approximately 16dB (decibels) for a layer thickness of 0.5 meters. As the layer thickness is increased, the solution for σ° at θ_i equal to zero, approaches the half-space solution. The θ_i equal to 20° curve also approaches the half-space solution when the layer thickness is increased. In this case, σ° differs from the half-space solution by only about 3.5dB when the layer thickness is 0.5 meters.

Figure 20 presents a study of the skin depth of the mean wave versus incidence angle for three different frequencies. For a horizontally polarized wave, the skin depth is taken to be the reciprocal of p_1, which was derived earlier as part of the solution to the Dyson's equation. It should be remembered that the mean wave decays for two reasons, absorption and scattering. For a frequency of 8.6 GHz, the skin depth goes from approximately 5 meters at θ_i equal to 0° down to 1 meter at θ_i equal to 80°. When the frequency is increased, the overall level of the curve is lowered considerably, but it does not drop off as fast with increasing incidence angle.

In figure 21, the solutions are compared for the half space, the plane layer, and the layer with a rough surface. For angles of incidence between 0° and 30°, the rough interface at the vegetation soil boundary can have a dramatic effect on σ°. In this case, it is clearly not sufficient to use a plane layer model.

---

[9] P.P. Batlivala and F.T. Ulaby, *The Effect of Look Direction on the Radar Return From a Row Crop*, National Aeronautics and Space Administration, Lyndon B. Johnson Space Center, Houston, Texas, RSL Technical Report 264–3, May 1975.

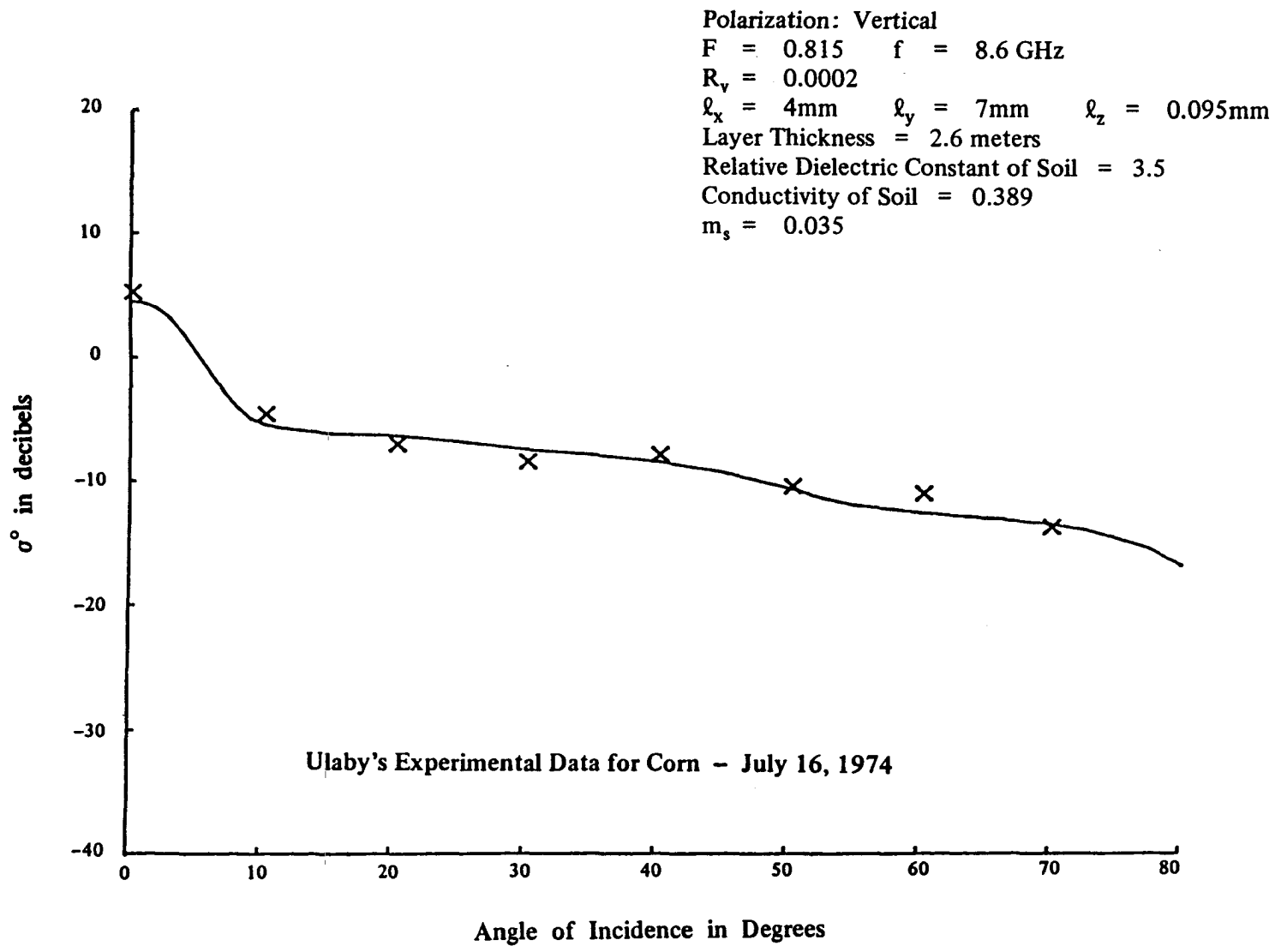

Figure 14. Comparison of Theory with Experimental Data.

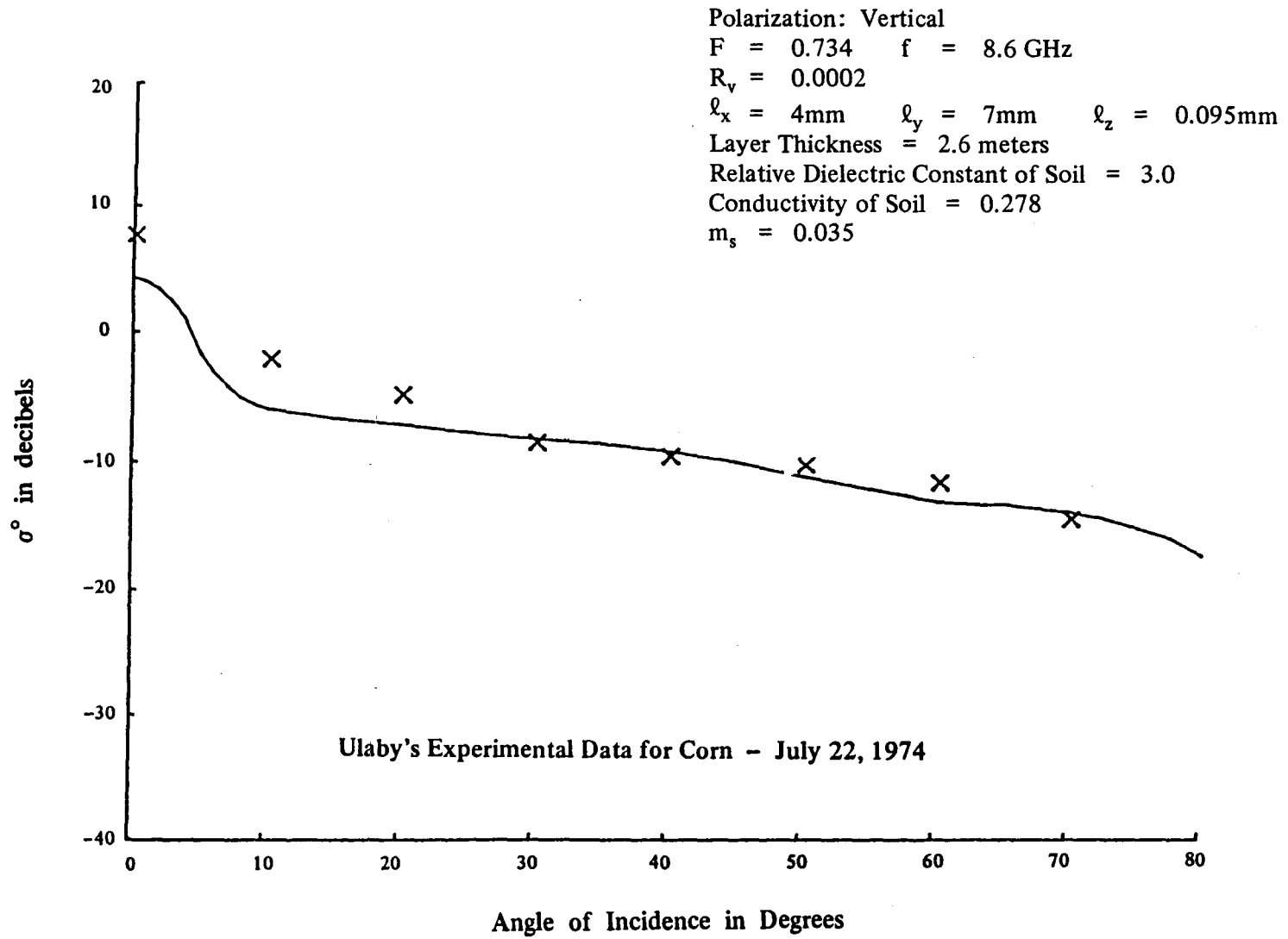

Figure 15. Comparison of Theory with Experimental Data.

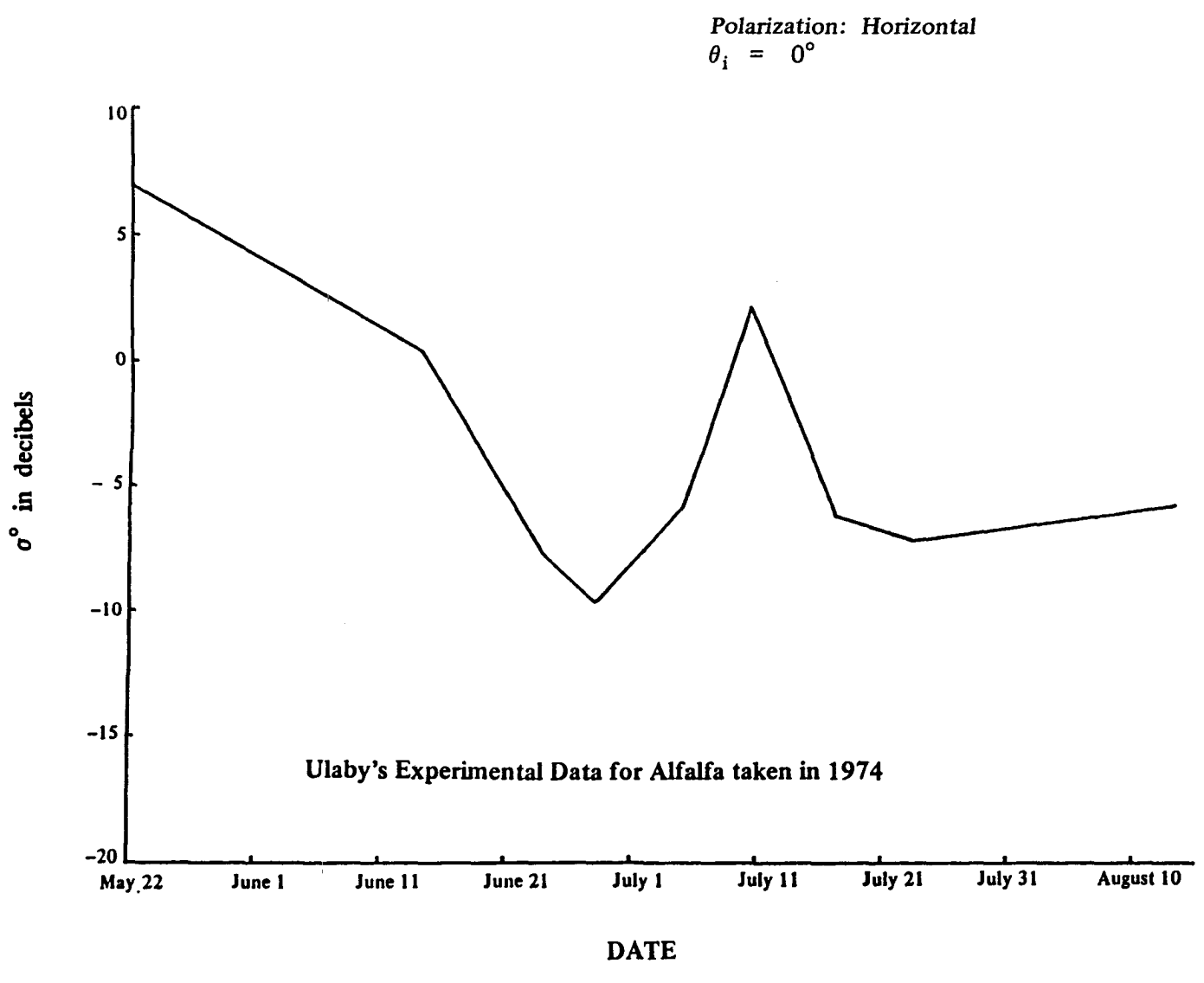

Figure 16. Study of the Experimental Variations of the σ° for Alfalfa.

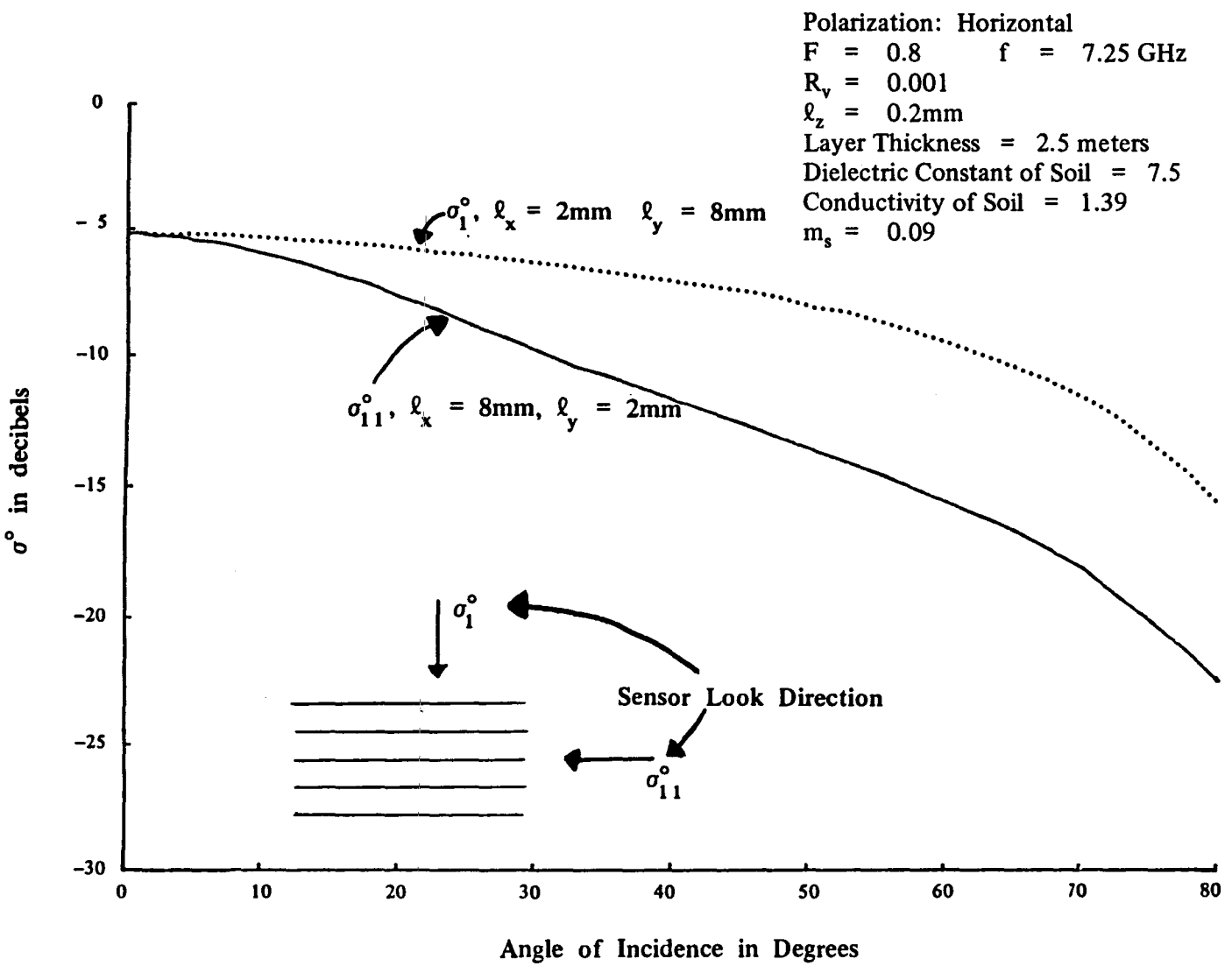

Figure 17. Study of the Sensor Look Direction.

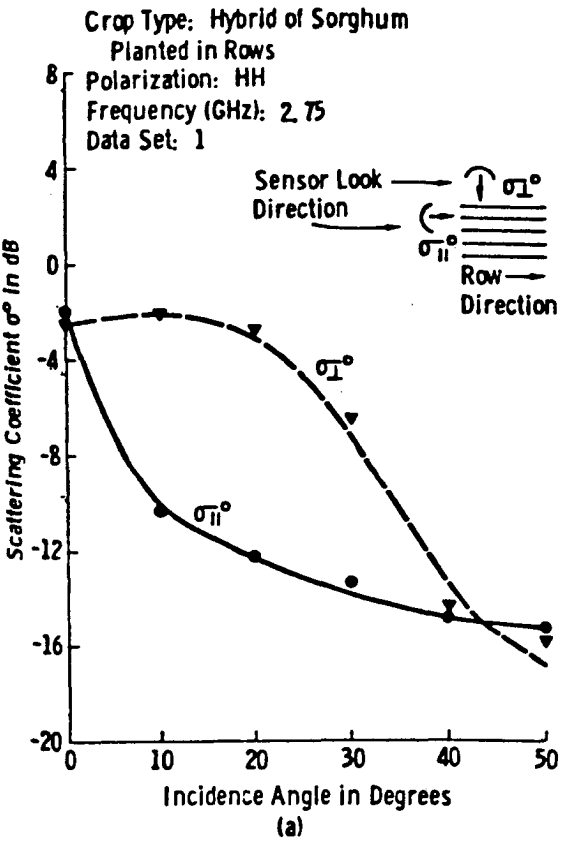

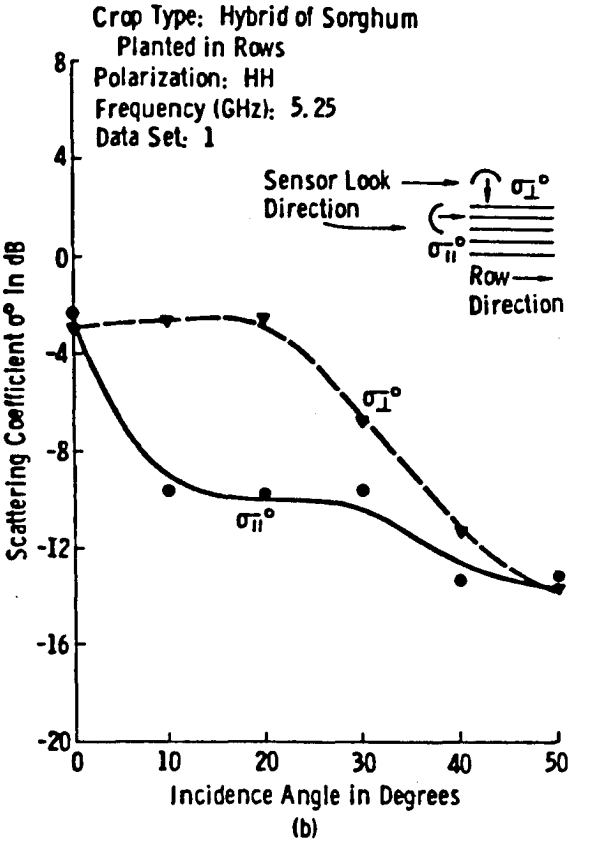

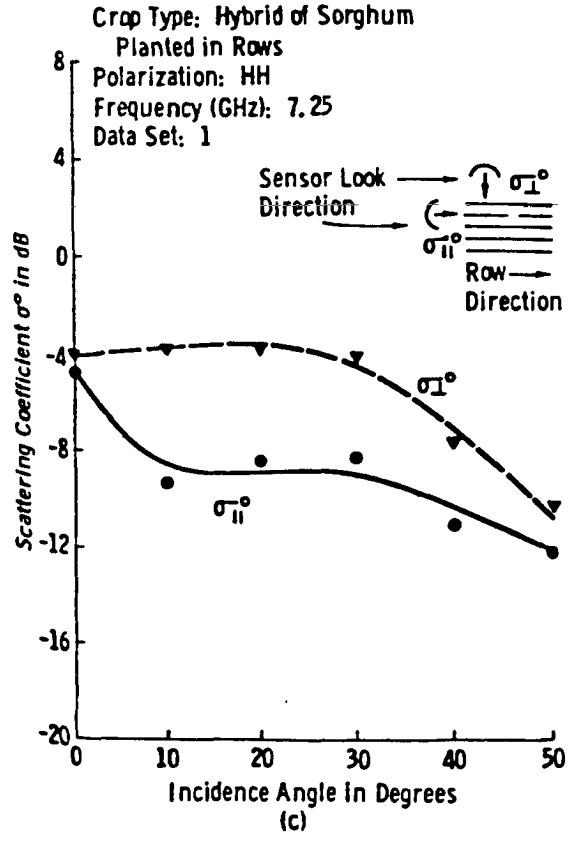

SOURCE : P.P. Batlivala and F.T. Ulaby, *The Effect of Look Direction on the Radar Return From a Row Crop,* National Aeronautics and Space Administration, Lyndon B. Johnson Space Center, Houston, Texas RSL Technical Report 264–3, May 1975.

Figure 18. Scattering Coefficient σ° as a Function of Incidence Angle at (a) 2.75GHz, (b) 5.25GHz, and (c) 7.25GHz. Data set $\neq 1$, July 16, 1974.

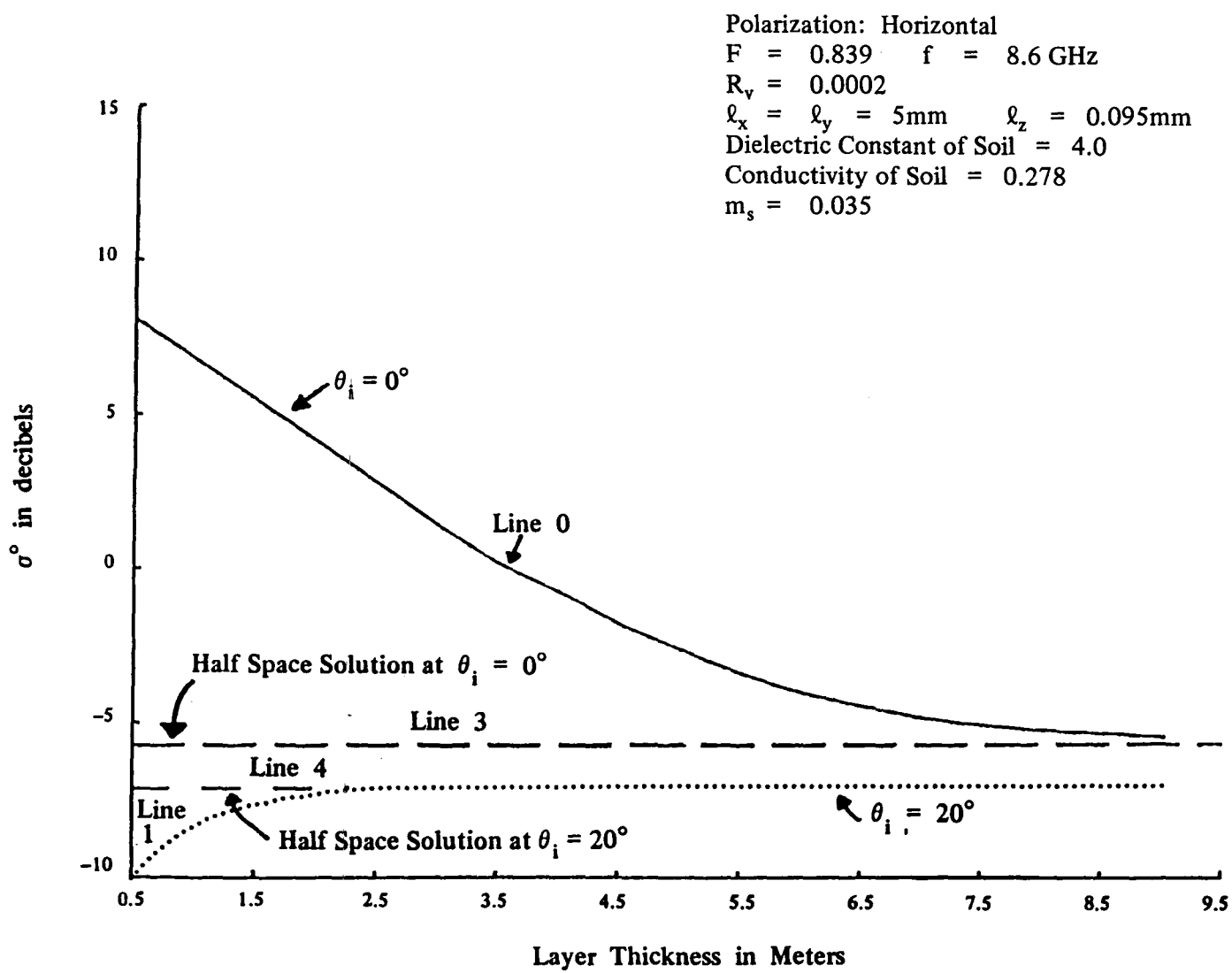

Figure 19. Study of the Variation of σ° with Layer Thickness.

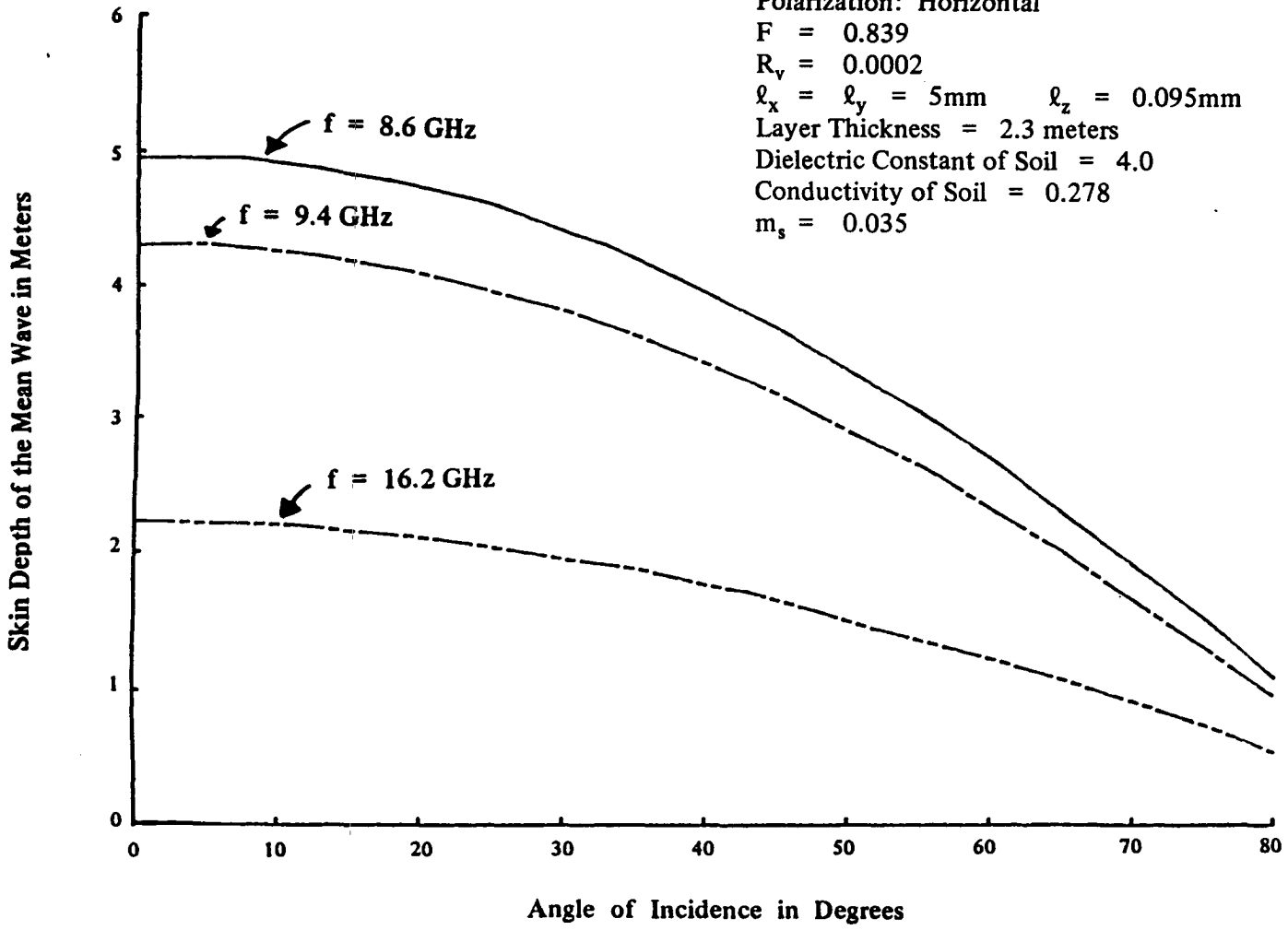

Figure 20. Study of the Skin Depth of the Mean Wave Versus Incidence Angle.

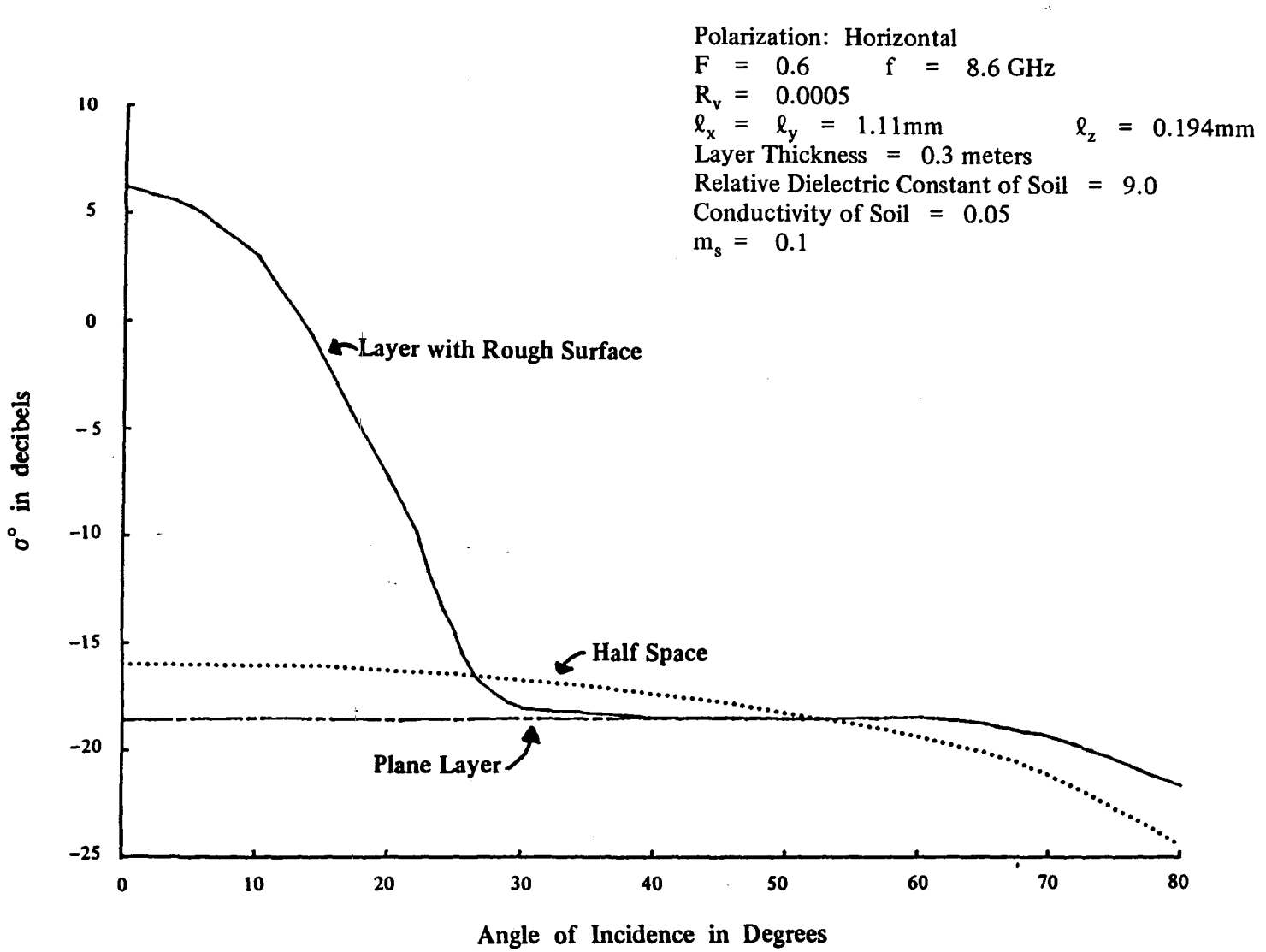

Figure 21. Comparison of Half Space, Plane Layer and Layer with Rough Surface Solutions.

In figures 22 through 30, a sensitivity-of-parameters study is presented. In this study, the input parameters are varied individually to determine the overall effect on the scattering coefficient. In figure 22, a study is provided of σ° variations with F (the vegetation moisture content). When θ_i is greater than 20°, the larger values of F produce higher levels of σ°. The shape of the σ° versus θ_i curve does not change much, but the overall level is significantly different. At approximately $\theta_i = 10^\circ$, a crossover of the curves exists such that the curve with the highest moisture content now yields the lowest value of σ°. The reason for the crossover is that two entirely different mechanisms are responsible for scattering. For θ_i greater than 20°, the volume-scattering mechanism dominates so that higher moisture in the vegetation results in larger backscatter values. However, for angles of incidence θ_i less than 10° when the mechanism for scattering is dominated by the rough surface under the vegetation, the higher moisture values result in lower σ° values. This is because the higher moisture values provide more attenuation of the mean wave, which means that less is available for scattering from the rough surface.

Figure 23 presents a study of σ° variations with the parameter R_V. The smaller value of R_V yields a larger σ° value for small angles of incidence. This is again because rough surface scattering dominates for small angles, and smaller values of R_V mean that more energy gets down to the surface. A crossover occurs at approximately $\theta_i = 15^\circ$ where the volume scattering result begins to dominate. Another crossover occurs between $\theta_i = 40^\circ$ and $\theta_i = 50^\circ$ such that for angles larger than 50°, σ° falls off faster for the larger value of R_V. The reason for this second crossover is possibly because that for the larger value of R_V, the lower interface between the vegetation and soil no longer provides a contribution for backscattering.

Figure 24 presents a study of σ° variations with L (the mean thickness of the vegetation layer). For small angles of incidence, the smaller value of L yields larger values of σ°. The rough surface below the vegetation is dominating the return and the smaller value of L provides a lower attenuation, thus making more energy available for scattering from the surface. A crossover point occurs around $\theta_i = 12^\circ$, which indicates that volume scattering is now beginning to dominate and so the thicker layer will yield a larger value of σ°. Another crossover point occurs at approximately $\theta_i = 67^\circ$. This crossover point possibly indicates that for L = 2 meters, the lower interface is having no influence, but for L = 0.5 meters, the lower interface still provides a contribution.

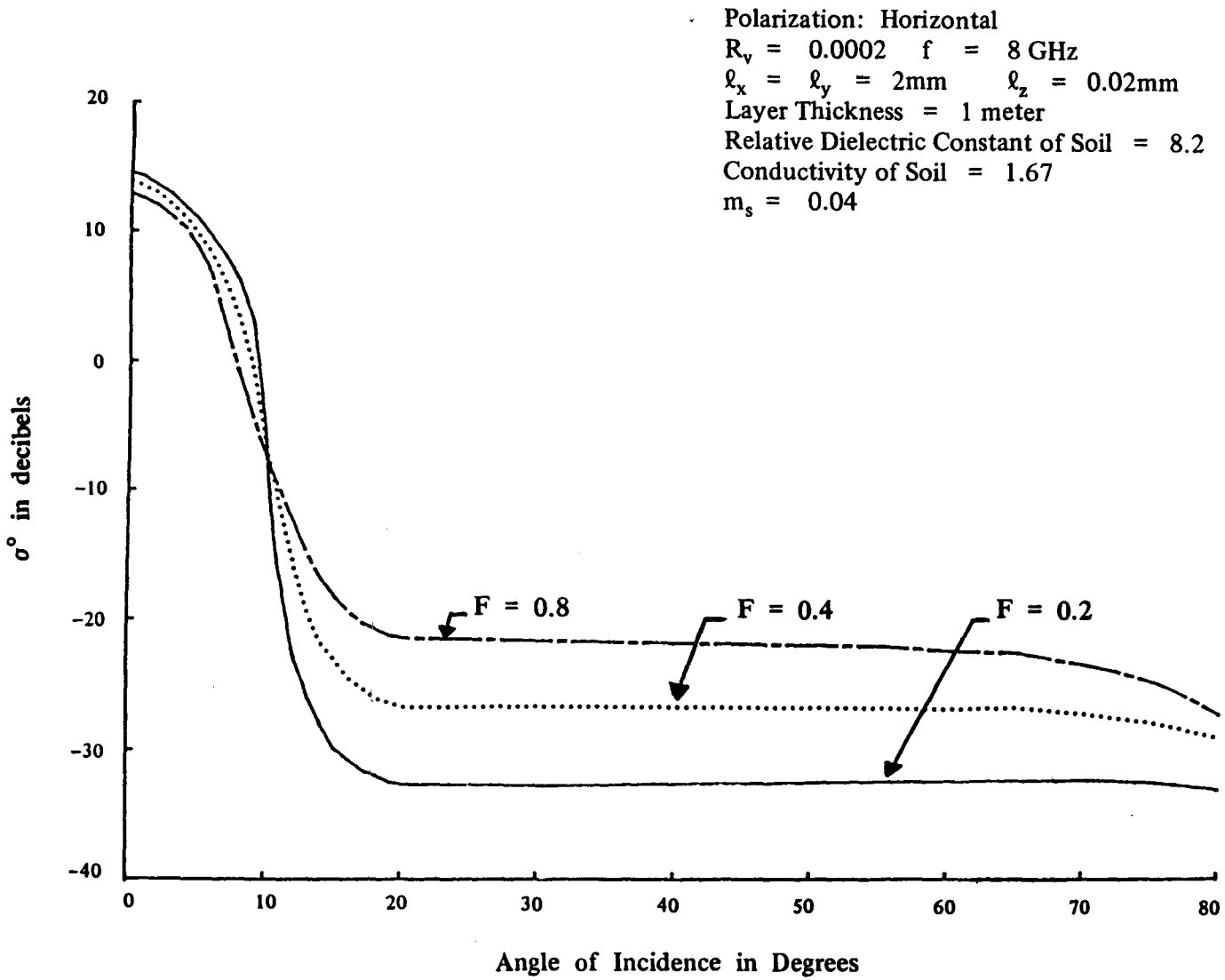

Figure 22. Study of σ° Variations with F.

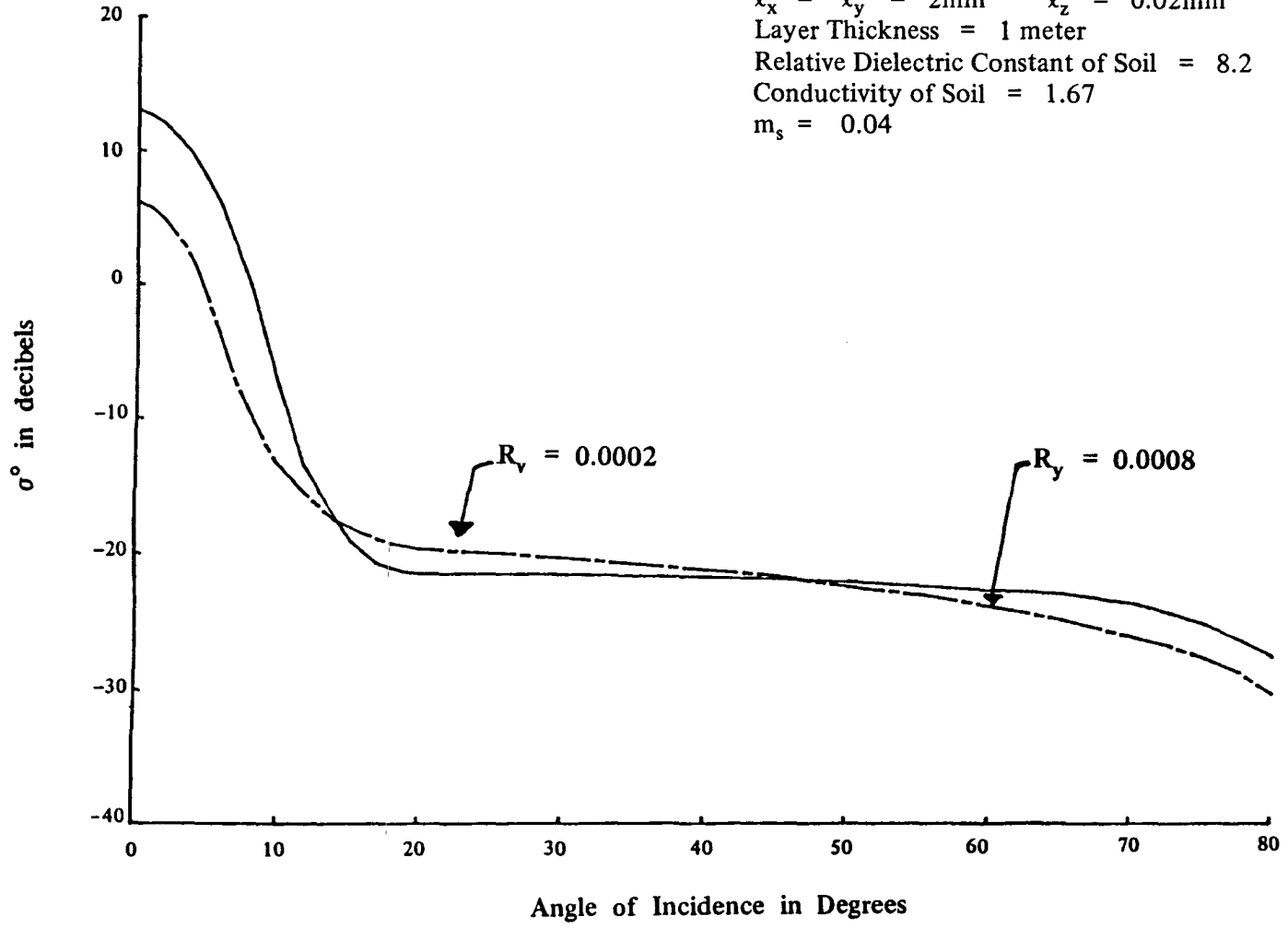

Figure 23. Study of σ° Variations with R_v.

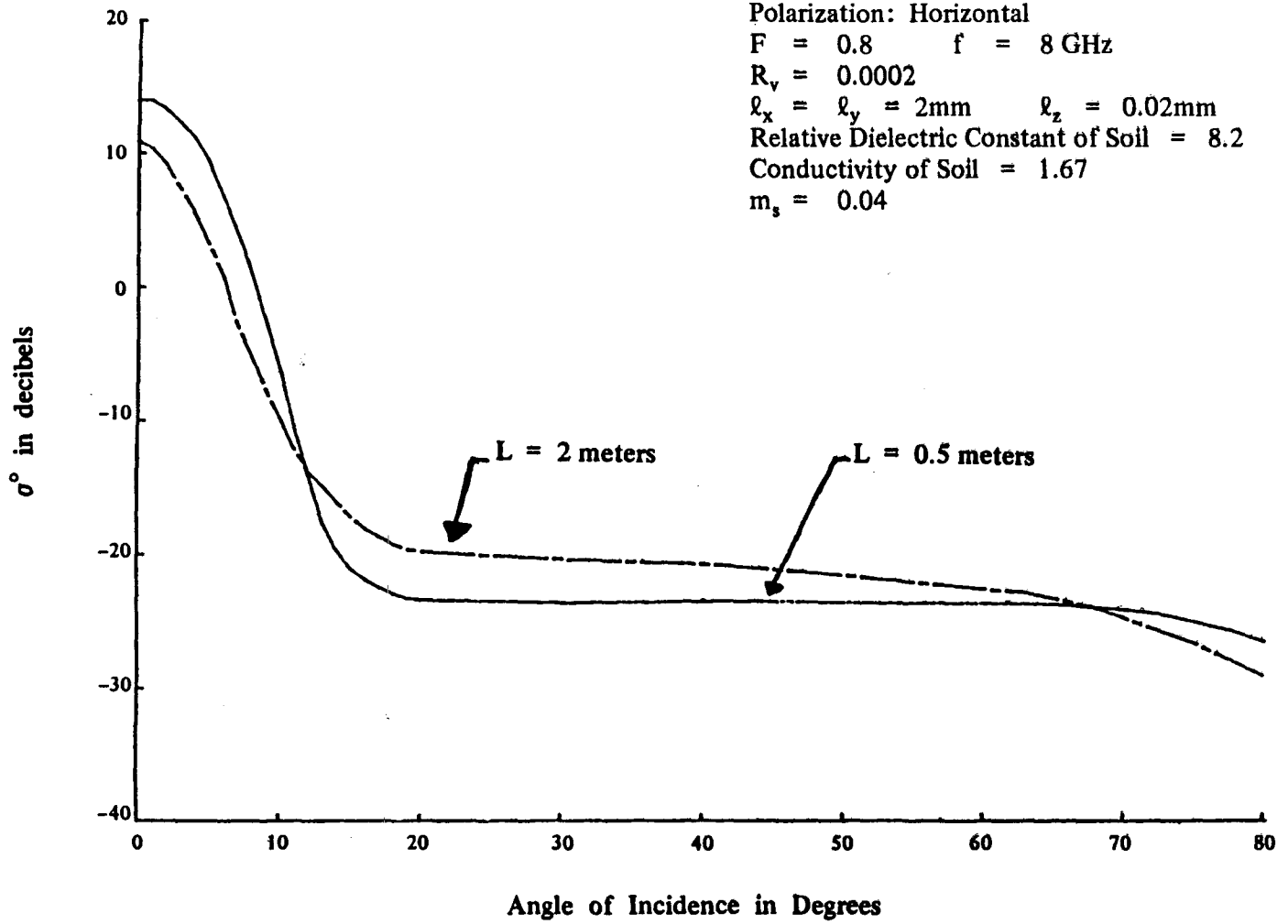

Figure 24. Study of σ° Variations with L.

Figure 25 shows a study of σ° variations with soil moisture. The soil moisture influences both the dielectric constant and the conductivity. The effect is shown of doubling the soil moisture underneath a 1-meter layer of vegetation. Thus, doubling the soil moisture content increases the level of σ° slightly over all angles of incidence.

In figure 26, a study is presented of σ° variations with frequency for two angles of incidence. We see only a slight frequency dependence at $\theta_i = 10^\circ$, because the rough surface scattering is independent of frequency except for the attenuation portion. At $\theta_i = 30^\circ$ where volume scattering is playing a more important role,we see a very significant frequency dependence.

In figure 27, σ° variations with the parameter m_s are shown. This parameter represents the ratio of the standard deviation of the rough surface undulations to the correlation distance. The most specular surface ($m_s = 0.04$) yields the highest value of σ° at $\theta_i = 0^\circ$. However, for this surface, σ° falls off very fast with increasing incidence angle so that at $\theta_i = 20^\circ$, the rough surface effect has disappeared. When m_s is allowed to increase, the value of σ° at $\theta_i = 0^\circ$ decreases. Also, as m_s increases, the rough surface influences σ° over a larger range of incidence angles.

In figure 28, σ° variations with ℓ_x are shown. Notice first that a change in ℓ_x yields virtually no influence upon σ° for angles of incidence less than 10°. For angles of incidence greater than 10°, the curve associated with the larger value of ℓ_x is higher until a crossover point is reached around $\theta_i = 48^\circ$. For angles of incidence greater than 48°, the curve associated with the larger value of ℓ_x falls off much faster than the curve associated with the smaller value of ℓ_x. Increasing the value of ℓ_x will then move the curve upward for angles of incidence less than about 50°, but will lower the curve for angles of incidence greater than about 50°.

In figure 29, σ° variations with ℓ_y are shown. Once again, notice that a change in ℓ_y has virtually no influence on σ° for angles less than 10°. For angles of incidence greater than or equal to 20°, an increase in ℓ_y results in an increase in σ°. Therefore, increasing ℓ_y simply increases the level of the curve for angles equal to and greater than 20°.

In figure 30, σ° variations with ℓ_z are shown. For angles of incidence less than 10°, changes in ℓ_z have no influence on σ° owing to the dominance of the rough surface. For angles of incidence greater than 20°, increasing the value of ℓ_z simply increases the overall level of the curve without changing the shape. It can be seen that the σ° curve is sensitive to slight changes in ℓ_z. A change in ℓ_z of only a fraction of a millimeter produces a significant change in σ°. This sensitivity may make any attempt to determine ℓ_z in a rigorous experimental manner very difficult.

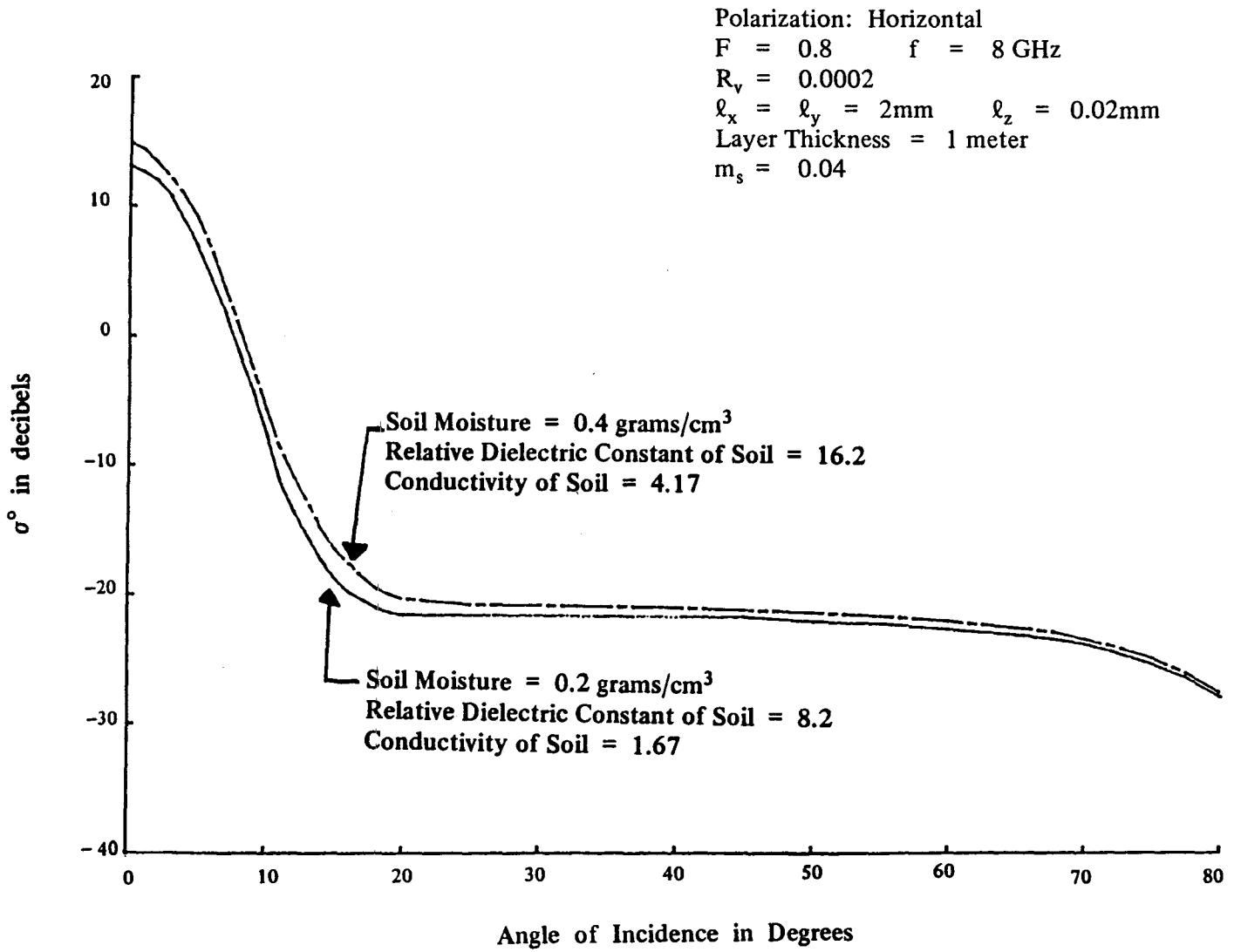

Figure 25. Study of σ° Variations with Soil Moisture.

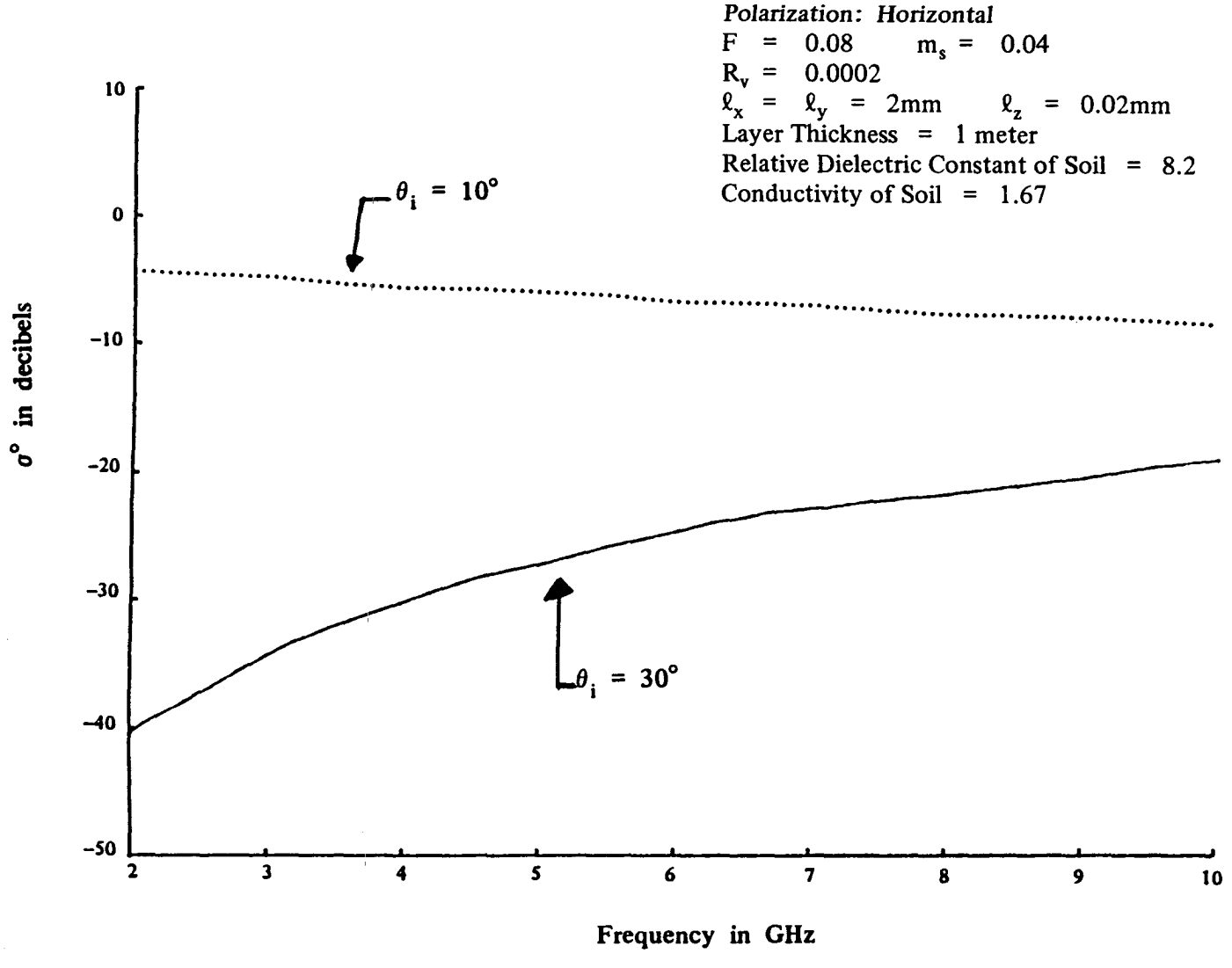

Figure 26. Study of σ° Variations with Frequency.

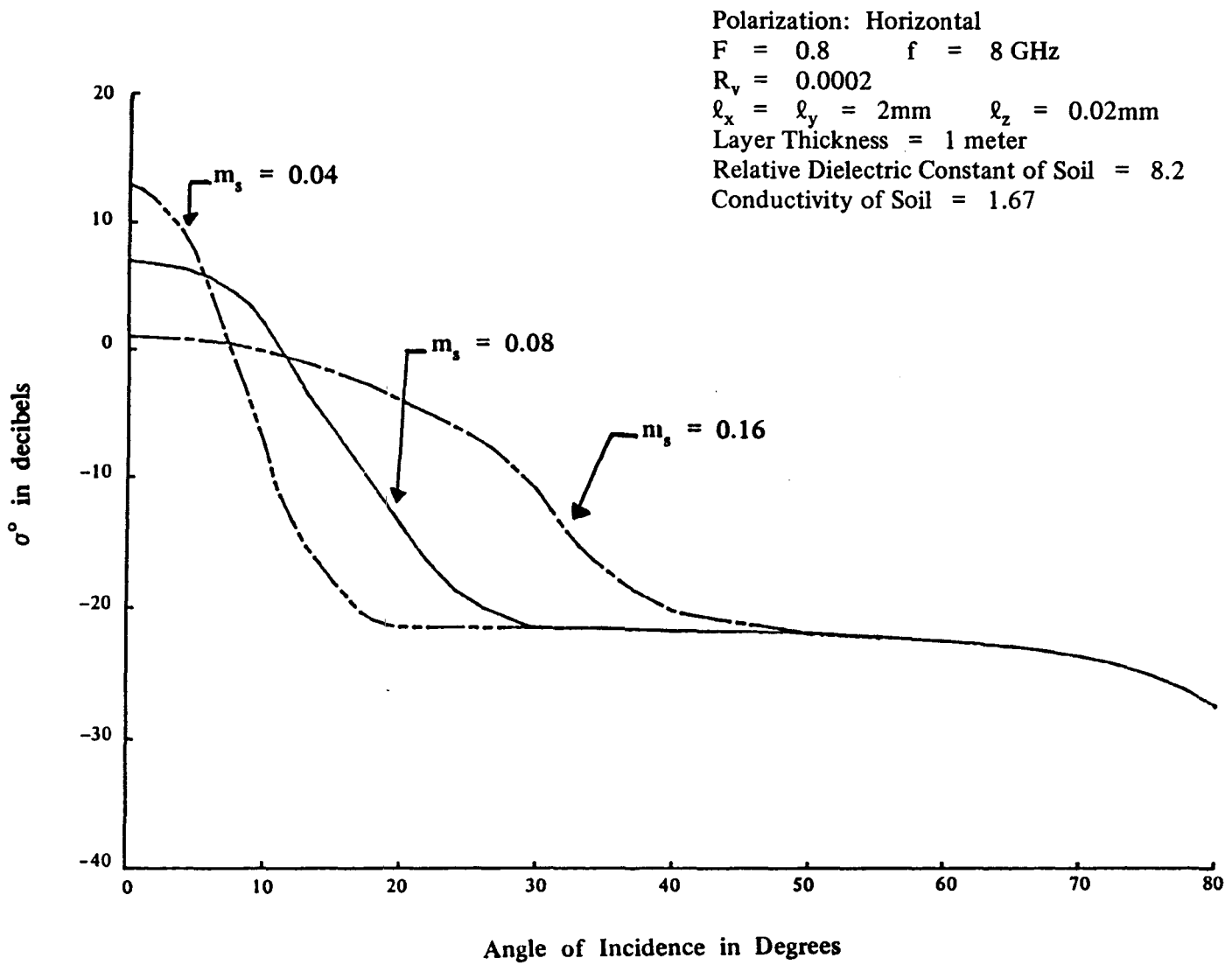

Figure 27. Study of σ° Variations with m_s.

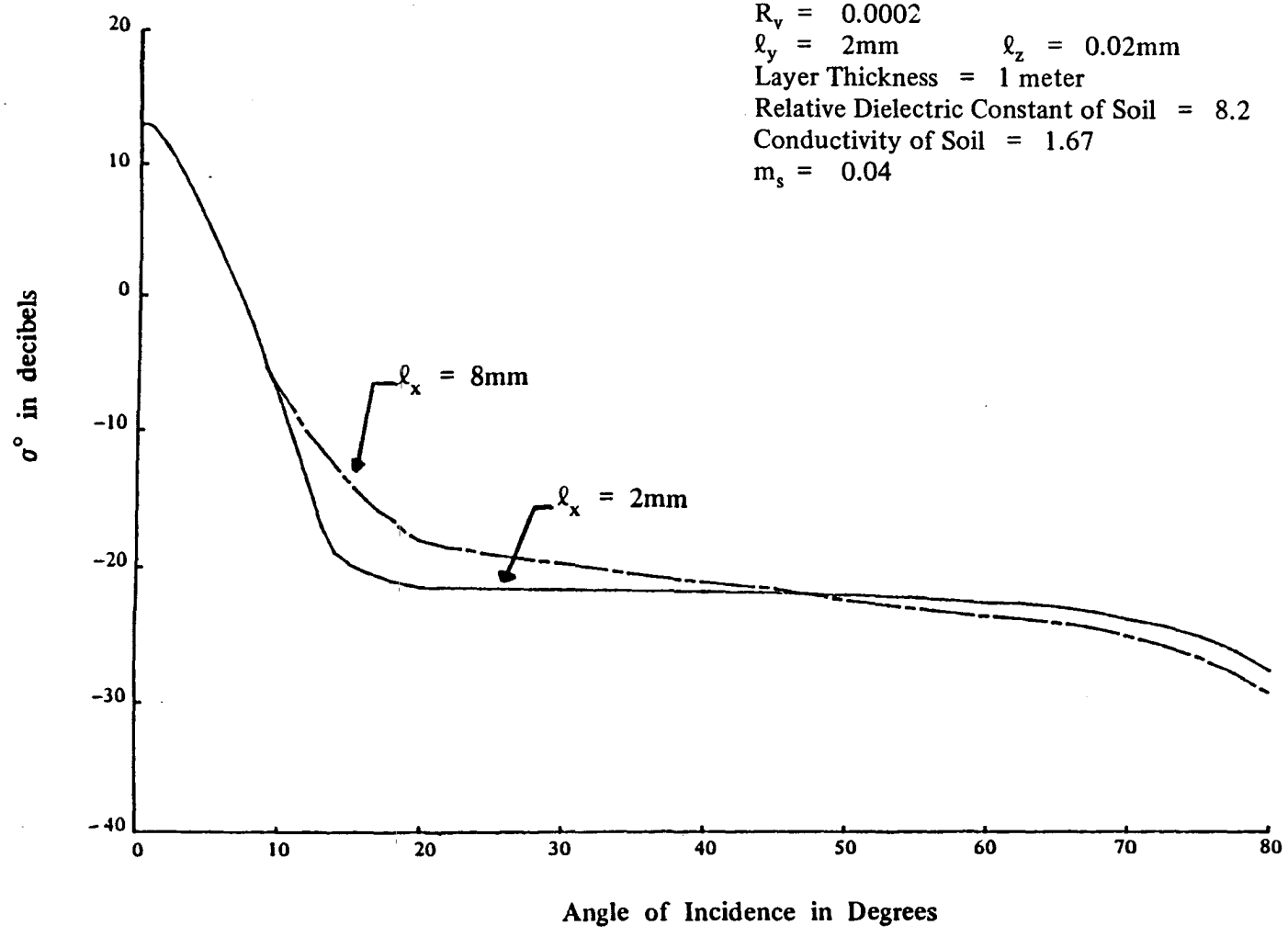

Figure 28. Study of σ° Variations with ℓ_x.

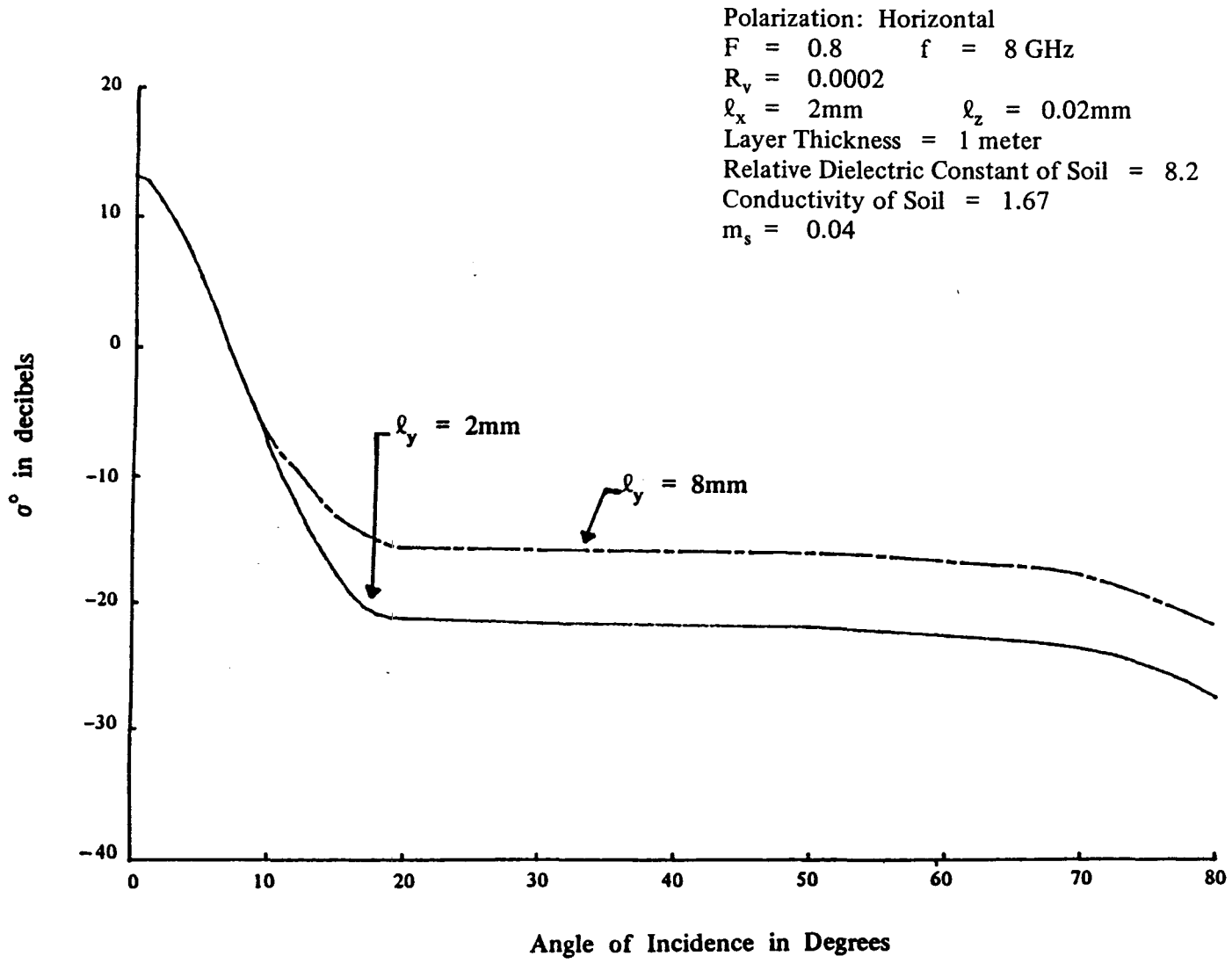

Figure 29. Study of σ° Variations with ℓ_y.

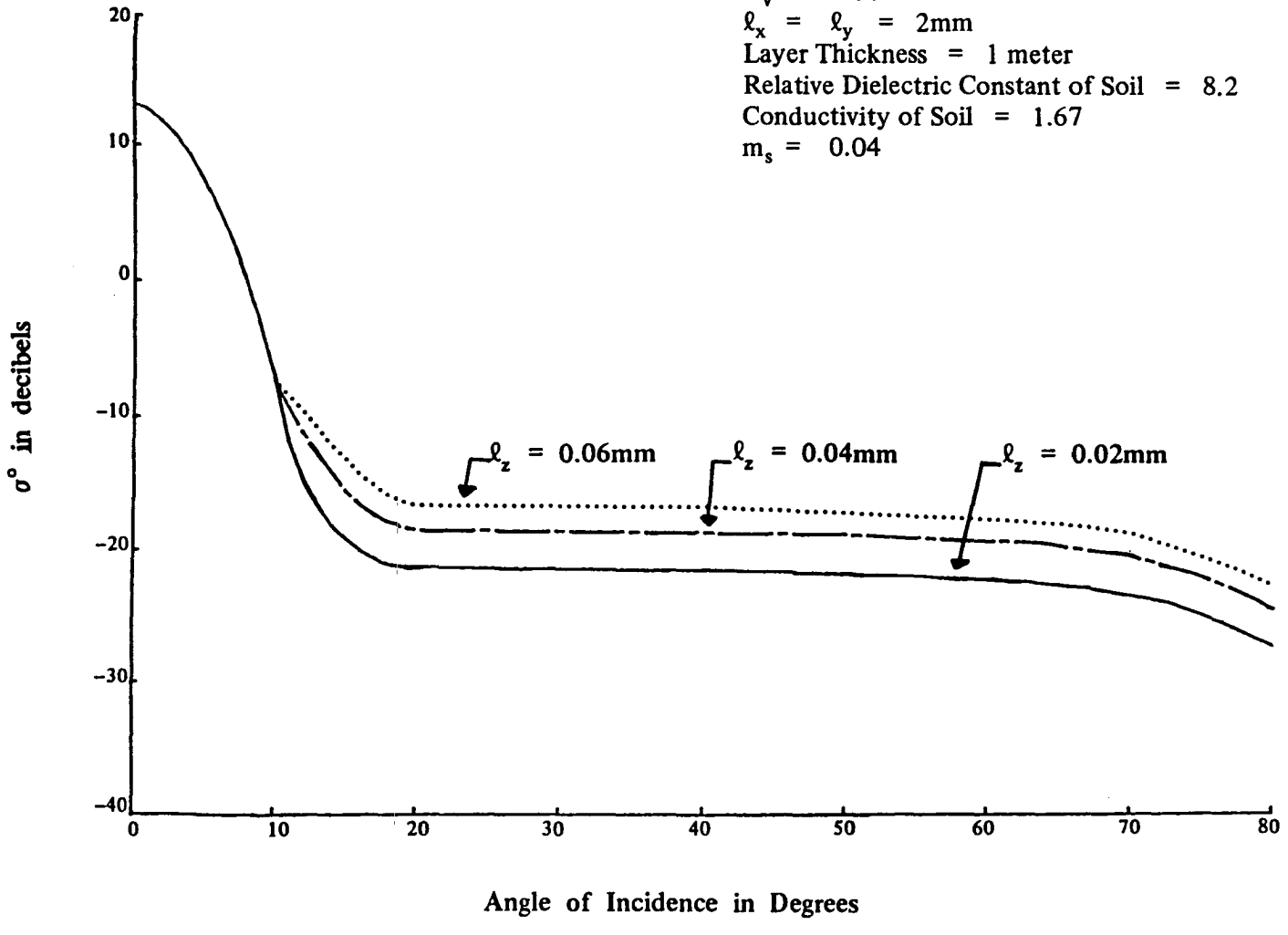

Figure 30. Study of σ° Variations with ℓ_z.

This section concludes with a brief discussion on the limitations and difficulties encountered in developing the theory presented in this report. It appears valid to simulate a region of vegetation with a continuous random medium, although it is not certain as to how well the first-order renormalization technique does in solving the problem. It is not clear how much multiple scattering is being considered, and it is not even clear as to how much multiple scattering must be considered. A free space dyadic Green's function was used in solving the Dyson's equation; however, what should have been used was a Green's function applicable to a layered problem. Such Green's functions are very complicated to develop and work with. Also, it is not clear how much the final result will change if a more complicated Green's function is used.

An equation for the radar backscatter coefficient σ° was developed by first obtaining plane wave solutions to the Dyson's equation. Expressions were found for the z component of the effective propagation constant for both horizontal and vertical polarizations. The mean wave was then used to calculate the scattered wave, which in turn was used to compute σ°. The final result for σ° indicated the necessity to develop a permittivity model that would relate some of the permittivity parameters in the scattering model to the physical parameters of the vegetation. This was accomplished with only limited success since a rather elementary permittivity model was used. The final result for σ° still contained five input parameters that were unknown. The five parameters are ℓ_x, ℓ_y, ℓ_z, R_V, and m_s.

Further work in this area should attempt to determine correlation functions and distances, as well as R_V and m_s to relate clearly theory and experiment. An anisotropic correlation function was used; however, this did not result in a depolarization term. The existance of depolarization is clearly evident from the experimental data. The reason for this depolarization is, as yet, unknown. A depolarization term could be obtained by computing the scattered field to a second-order approximation. It could also be obtained by initially allowing for an anisotropic random medium. At this time, it is unclear which approach is correct.

CONCLUSIONS

1. For certain types of vegetation, such as corn, the irregular vegetation soil boundary dominates the backscattering results for angles of incidence between 0° and 20°. Any remote sensing of surface phenomena beneath vegetation should be done in this angular range.

2. The effect of the rough surface boundary between the vegetation and soil increases with decreases in frequency, vegetation moisture content, vegetation volume, and layer thickness.

3. Increasing the soil moisture content increases the level of the σ° curve slightly.

4. Using different correlation distances in x and y does not completely explain the effect of look direction on scattering from a row crop.

5. The σ° curve versus incidence angle curve is sensitive to very slight changes in the correlation distance in z.

6. The predictability of the σ° curve is dependent on meteorological phenomena, such as rain.

7. The correlation distances and the vegetation volume ratio do not stay constant throughout the entire growth cycle of the corn crop. However, once the crop matured, these parameters remained fairly constant.

8. Because different correlation distances were required to match the experimental data for horizontal and vertical polarizations, a more correct model for the vegetation may be an anisotropic random media model.

9. The predictability of the σ° versus incidence angle curve depends upon a very detailed knowledge of the dielectric fluctuations of the vegetation and the surface roughness properties of the soil below. However, such knowledge for particular vegetation features does not exist at the present time. This detailed understanding should be obtained if theoretical models are to have ultimate usefulness in predicting scattering from vegetation features.

APPENDIX A. Definition of Terms Involved in Computing

$$<A_y A_y^*>,\quad <A_x A_x^*>,\quad <A_z A_z^*>,\quad <A_x A_z^*>,\quad <A_x A_y^*>$$

Repeating equation (67) produces

$$<A_y A_y^*> = \frac{4\ell_x \ell_y \ell_z A_I(\omega^2 \mu_o^2 \eta_2^2 + k_o^4 \eta_1^2) k_a^2 k_a^{*2} M_o M_o^*}{(1 + 4k_o^2 \ell_x^2 \sin^2\theta_i)}$$

$$\cdot \sum_{n=1}^{16} \frac{A_n}{(c_n + d_n)} \left\{ \frac{1 - \ell_z d_n + \ell_z(c_n + d_n)e^{-L(c_n + 1/\ell_z)} - (1 + \ell_z c_n)e^{-L(c_n + d_n)}}{(1 + \ell_z c_n)(1 - \ell_z d_n)} \right.$$

$$\left. + \frac{1 - \ell_z c_n + \ell_z(c_n + d_n)e^{-L(d_n + 1/\ell_z)} - e^{-L(c_n + d_n)}(1 + d_n \ell_z)}{(1 + \ell_z d_n)(1 - \ell_z c_n)} \right\}$$

The values for A_n, c_n, and d_n are defined below:

A_1	=	$\tilde{a}_1 \tilde{a}_1^* T_2 T_2^*$	c_1	=	D_1	d_1	=	D_1^*
A_2	=	$\tilde{a}_1 T_2 \tilde{a}_1^* V_2^*$	c_2	=	D_1	d_2	=	D_2^*
A_3	=	$\tilde{a}_1 T_2 T_2^*$	c_3	=	D_1	d_3	=	$-D_2^*$
A_4	=	$\tilde{a}_1 T_2 V_2^*$	c_4	=	D_1	d_4	=	$-D_1^*$
A_5	=	$\tilde{a}_1 V_2 a_1^* T_2^*$	c_5	=	D_2	d_5	=	D_1^*
A_6	=	$\tilde{a}_1 \tilde{a}_1^* V_2 V_2^*$	c_6	=	D_2	d_6	=	D_2^*
A_7	=	$\tilde{a}_1 V_2 T_2^*$	c_7	=	D_2	d_7	=	$-D_2^*$

$$A_8 = \tilde{a}_1 V_2 V_2^* \qquad c_8 = D_2 \qquad d_8 = -D_1^*$$

$$A_9 = \tilde{a}_1^* T_2 T_2^* \qquad c_9 = -D_2 \qquad d_9 = D_1^*$$

$$A_{10} = \tilde{a}_1^* T_2 V_2^* \qquad c_{10} = -D_2 \qquad d_{10} = D_2^*$$

$$A_{11} = T_2 T_2^* \qquad c_{11} = -D_2 \qquad d_{11} = -D_2^*$$

$$A_{12} = T_2 V_2^* \qquad c_{12} = -D_2 \qquad d_{12} = -D_1^*$$

$$A_{13} = V_2 \tilde{a}_1^* T_2^* \qquad c_{13} = -D_1 \qquad d_{13} = D_1^*$$

$$A_{14} = \tilde{a}_1^* V_2 V_2^* \qquad c_{14} = -D_1 \qquad d_{14} = D_2^*$$

$$A_{15} = V_2 T_2^* \qquad c_{15} = -D_1 \qquad d_{15} = -D_2^*$$

$$A_{16} = V_2 V_2^* \qquad c_{16} = -D_1 \qquad d_{16} = -D_1^*$$

A basic expression for $< A_x A_x^* >$ can be written as follows:

$$< A_x A_x^* > = \frac{4\ell_x \ell_y \ell_z A_I (\omega^2 \mu_o^2 \eta_2^2 + k_o^4 \eta_1^2)}{(1 + 4k_o^2 \ell_x^2 \sin^2 \theta_i)}$$

$$\sum_{n=1}^{16} \frac{\Lambda_n}{(\beta_n + \gamma_n)} \left\{ \frac{1 - \ell_z \gamma_n + \ell_z (\beta_n + \gamma_n) e^{-L(\beta_n + 1/\ell_z)} - (1 + \ell_z \beta_n) e^{-L(\beta_n + \gamma_n)}}{(1 + \ell_z \beta_n)(1 - \ell_z \gamma_n)} \right.$$

$$\left. + \frac{1 - \ell_z \beta_n + \ell_z (\beta_n + \gamma_n) e^{-L(\beta_n + \gamma_n)} (1 + \gamma_n \ell_z)}{(1 + \ell_z \gamma_n)(1 - \ell_z \beta_n)} \right\}$$

Before giving the values for Λ_n, β_n, and γ_n, the following parameters are defined:

$$D_1' = p_2 + jq_2 - jk_z'$$

$$D_2' = -(p_2 + jq_2 + jk_z')$$

$$h_1 = b_6 [T_1(k_a^2 - k_o^2 \sin^2\theta_i) - T_3 k_o k_z' \sin\theta_i]$$

$$h_2 = b_6 [V_1(k_a^2 - k_o^2 \sin^2\theta_i) - V_3 k_o k_z' \sin\theta_i]$$

$$h_3 = b_5 [T_1(k_a^2 - k_o^2 \sin^2\theta_i) + T_3 k_o k_z' \sin\theta_i]$$

$$h_4 = b_5 [V_1(k_a^2 - k_o^2 \sin^2\theta_i) + V_3 k_o k_z' \sin\theta_i]$$

The values of Λ_n, β_n, and γ_n will now be written in terms of the above parameters:

$\Lambda_1 = h_1 h_1^*$		$\beta_1 = D_1'$		$\gamma_1 = D_1'^*$	
$\Lambda_2 = h_1 h_2^*$		$\beta_2 = D_1'$		$\gamma_2 = D_2'^*$	
$\Lambda_3 = h_1 h_3^*$		$\beta_3 = D_1'$		$\gamma_3 = D_2'^*$	
$\Lambda_4 = h_1 h_4^*$		$\beta_4 = D_1'$		$\gamma_4 = D_1'^*$	
$\Lambda_5 = h_2 h_1^*$		$\beta_5 = D_2'$		$\gamma_5 = D_1'^*$	
$\Lambda_6 = h_2 h_2^*$		$\beta_6 = D_2'$		$\gamma_6 = D_2'^*$	
$\Lambda_7 = h_2 h_3^*$		$\beta_7 = D_2'$		$\gamma_7 = -D_2'^*$	

$$\Lambda_8 = h_2 h_4^* \qquad \beta_8 = D_2' \qquad \gamma_8 = -D_1'^*$$

$$\Lambda_9 = h_3 h_1^* \qquad \beta_9 = -D_2' \qquad \gamma_9 = D_1'^*$$

$$\Lambda_{10} = h_3 h_2^* \qquad \beta_{10} = -D_2' \qquad \gamma_{10} = D_2'^*$$

$$\Lambda_{11} = h_3 h_3^* \qquad \beta_{11} = -D_2' \qquad \gamma_{11} = -D_2'^*$$

$$\Lambda_{12} = h_3 h_4^* \qquad \beta_{12} = -D_2' \qquad \gamma_{12} = -D_1'^*$$

$$\Lambda_{13} = h_4 h_1^* \qquad \beta_{13} = -D_1' \qquad \gamma_{13} = D_1'^*$$

$$\Lambda_{14} = h_4 h_2^* \qquad \beta_{14} = -D_1' \qquad \gamma_{14} = D_2'^*$$

$$\Lambda_{15} = h_4 h_3^* \qquad \beta_{15} = -D_1' \qquad \gamma_{15} = -D_2'^*$$

$$\Lambda_{16} = h_4 h_4^* \qquad \beta_{16} = -D_1' \qquad \gamma_{16} = -D_1'^*$$

The basic equation for $\langle A_x A_y^* \rangle$ can be written as

$$\langle A_x A_y^* \rangle = \frac{-4\ell_x \ell_y \ell_z A_I (\omega^2 \mu_o^2 \eta_2^2 + k_o^4 \eta_1^2)\, k_a^{*2}\, M_o^*}{(1 + 4k_o^2 \ell_x^2 \sin^2\theta_i)}$$

$$\cdot \sum_{n=1}^{16} \frac{P_n}{(\nu_n + \rho_n)} \left\{ \frac{1 - \ell_z\rho_n + \ell_z(\nu_n + \rho_n)e^{-L(\nu_n + 1/\ell_z)} - (1 + \ell_z\nu_n)e^{-L(\nu_n + \rho_n)}}{(1 + \ell_z\nu_n)\ (1 - \ell_z\rho_n)} \right.$$

$$\left. + \frac{1 - \ell_z\nu_n + \ell_z(\nu_n + \rho_n)e^{-L(\rho_n + 1/\ell_z)} - e^{-L(\nu_n + \rho_n)}\ (1 + \rho_n\ell_z)}{(1 + \ell_z\rho_n)\ (1 - \ell_z\nu_n)} \right\}$$

The values of P_n, ρ_n, and ν_n can be defined in terms of previous parameters.

P_1	=	$h_1 \hat{a}_1^* T_2^*$	ν_1	=	D_1'	ρ_1	=	D_1^*
P_2	=	$h_1 \hat{a}_1^* V_2^*$	ν_2	=	D_1'	ρ_2	=	D_2^*
P_3	=	$h_1 T_2^*$	ν_3	=	D_1'	ρ_3	=	$-D_2^*$
P_4	=	$h_1 V_2^*$	ν_4	=	D_1'	ρ_4	=	$-D_1^*$
P_5	=	$h_2 \hat{a}_1^* T_2^*$	ν_5	=	D_2'	ρ_5	=	D_1^*
P_6	=	$h_2 \hat{a}_1^* V_2^*$	ν_6	=	D_2'	ρ_6	=	D_2^*
P_7	=	$h_2 T_2^*$	ν_7	=	D_2'	ρ_7	=	$-D_2^*$
P_8	=	$h_2 V_2^*$	ν_8	=	D_2'	ρ_8	=	$-D_1^*$
P_9	=	$h_3 \hat{a}_1^* T_2^*$	ν_9	=	$-D_2'$	ρ_9	=	D_1^*
P_{10}	=	$h_3 \hat{a}_1^* V_2^*$	ν_{10}	=	$-D_2'$	ρ_{10}	=	D_2^*
P_{11}	=	$h_3 T_2^*$	ν_{11}	=	$-D_2'$	ρ_{11}	=	$-D_2^*$
P_{12}	=	$h_3 V_2^*$	ν_{12}	=	$-D_2'$	ρ_{12}	=	$-D_1^*$
P_{13}	=	$h_4 \hat{a}_1^* T_2^*$	ν_{13}	=	$-D_1'$	ρ_{13}	=	D_1^*
P_{14}	=	$h_4 \hat{a}_1^* V_2^*$	ν_{14}	=	$-D_1'$	ρ_{14}	=	D_2^*

$$P_{15} = h_4 T_2^* \qquad \nu_{15} = -D_1' \qquad \rho_{15} = -D_2^*$$

$$P_{16} = h_4 V_2^* \qquad \nu_{16} = -D_1' \qquad \rho_{16} = -D_1^*$$

Expressions for $<A_z A_z^*>$, and $<A_x A_z^*>$ can be obtained in terms of previous results.

$$<A_z A_z^*> = \frac{k_o^2 \sin^2\theta_i}{k_{1z} k_{1z}^*} <A_x A_x^*>$$

$$<A_x A_z^*> = \frac{k_o \sin\theta_i}{k_{1z}^*} <A_x A_x^*>$$

APPENDIX B.

Computer Programs for Calculating the Backscattering Coefficients

```
      PROGRAM MODEL(INPUT,OUTPUT,TAPE5=INPUT,TAPE6=OUTPUT)
C     THIS PROGRAM CALCULATES THE RADAR BACKSCATTER COEFFICIENT
C     FROM A RANDOM MEDIA POSSESSING AN ANISOTROPIC CORRELATION
C     FUNCTION.  THE EFFECTIVE PROPAGATION CONSTANTS FOR THE
C     MEAN WAVE ARE CALCULATED FOR AN ARBITRARILY
C     POLARIZED INCIDENT PLANE WAVE
      COMPLEX QJ,QKA,QKK,QC,QF11(31),QMI11(31,31),QF12(31),QMI12(31,31),
     1QF13(31),QMI13(31,31),QF22(31),QMI22(31,31),QF23(31),QMI23(31,31),
     2QF33(31),QMI33(31,31),QI112(31),QI113(31),QI122(31),QI123(31),
     3QI132(31),QI133(31),QI222(31),QI223(31),QI232(31),QI233(31),
     4QI332(31),QI333(31),QI11(31),QI12(31),QI13(31),QI22(31),QI23(31),
     5QI33(31),QGI11,QGI12,QGI13,QGI22,QGI23,QGI33,QG112,QG122,QG132,
     6QG222,QG232,QG113,QG123,QG133,QG223,QG233,QG333,QG332,QES4,
     7QI11A(2),QI12A(2),QI13A(2),QM11,QM12,QM13,QM22,QSG,QES3,Q
     8M23,QM33,QEWW,QE11,QE12,QE13,QE22,QE23,QE33,QKV1,QKV2,QVN,QA3H,
     9QKV,QKH,QA1,QA3,QT21,QT22,QT2,QT131,QT132,QT133,QT134,QT13,QT3,
     1QT1,QAY1,QAX2,QAZ2,QKZP,Q11,Q22,Q,QAZ,QCX2,QCX1,QD(8),QKZPC,QSM,
     2QK(3),QAL(8),QB(4),QG(4),QERX,QERZ,QES1,QES2,QS11,QS12,QS13,QS,
     3QS14,QS8,QED,QK3C3,QK3,QA11,QA12,QA21,QA22,QT2N,QT2D,QV2N,QV2,
     4QAA1,QAL1,QE11,QB12,QB21A,QB21,QB22,QT1A,QT1N,QT1D,QV1N,QV1,
     5QT3A,QT33,QT3C,QT3D,QV3,QK3Z,QA1HN,QA1HD,QA1H,QA2HA,QA2HB,QA2H,
     6QA3HA,QA3H,QA4H,QA5H,QA6H,QA7H,QB1,QB2,QB3,QB4,QM1,QM2,QM,QD1,
     7QD1C,QD2,QD2C,QA(16),QBC(16),QLD(16),QNYY1,QNYY2,QNYY,QAYY,QB5,
     8QB6,QD1P,QH11,QH12,QH1,QH21,QH22,QH2,QH3,QH4,QAXX,QAZZ,QAXZ,QD2P,
     9QAXY1,QAXY2,QAXY,QSO1,QSO2,QSO3,QSO4,QSO5,QSS1,QSO6,QS1,QS2,QSA
      COMPLEX QI22A(2),QI23A(2),QI33A(2),QNJ1,QNJ2,QNJ3,QNJ4,
     1QNJ5,QNJ6,QNJ7,QJJ1,QJJ2
      COMMON DT,DK,A,B,C,D,XLZ,XLY,XLX,XKO,W,UO,EO,PI,SIGA,AER,BO,AO,SN,
     1XL
      MC=1
    7 CONTINUE
      READ(5,101)PM,RLV,XLX,XLY,XLZ
  101 FORMAT(5F10.8)
      READ(5,102)F
  102 FORMAT(F15.3)
      READ(5,109)XL,EC,SG
  109 FORMAT(3F10.8)
      READ(5,110)XMS
  110 FORMAT(F10.8)
      PI=3.1415926536
      EO=8.854*10.**(-12)
      U=4.*10.**(-7)
      UO=PI*U
      W=2.*PI*F
      QJ=(0.0,1.0)
      XLAMC=3.*10.**(10)/F
      QEWW=5.+75./(1.+QJ*1.85/XLAMC)
      ELP=0.5*PM*REAL(QEWW)
      ELPP=PM*AIMAG(QEWW)/3.
      SIGL=-W*EO*ELPP
      AER=ELP*RLV+(1.-RLV)
      SIGA=SIGL*RLV
      ETA11=RLV*(ELP-AER)**2+(1.-RLV)*(1.-AER)**2
      ETA1=SQRT(ETA11)
      ETA22=RLV*(SIGL-SIGA)**2+(1.-RLV)*SIGA**2
      ETA2=SQRT(ETA22)
      WRITE(6,106)PM
```

```
  100 FORMAT(1H ,45HFRACTION OF WATER BY WEIGHT IN THE VEGETATION=,
     1F6.3)
      WRITE(6,10)PLV
   10 FORMAT(1H ,45HVOLUME OF VEGETATION DIVIDED BY TOTAL VOLUME=,
     1F10.7)
      WRITE(6,11)F
   11 FORMAT(1H ,18HFREQUENCY=,E15.6)
      WRITE(6,13)XMS
   13 FORMAT(1H ,114HRATIO OF THE STANDARD DEVIATION OF THE ROUGH SURFAC
     1E FLUCTUATIONS TO THE CORRELATION DISTANCE OF THE FLUCTUATIONS=,
     2F10.5)
      WRITE(6,105)XLX,XLY,XLZ
  105 FORMAT(1H ,4HXLX=,F13.8,5X,4HXLY=,F13.8,5X,4HXLZ=,F13.8)
      WRITE(6,708)XL
  708 FORMAT(1H ,27HLAYER THICKNESS IN METERS =,F10.6)
      WRITE(6,709)EC
  709 FORMAT(1H ,33HDIELECTRIC CONSTANT OF THE SOIL =,F10.6)
      WRITE(6,710)SS
  710 FORMAT(1H ,28HCONDUCTIVITY OF THE SOIL =,F10.7)
      EA=AEP*EC
      XR1=SQRT(1.+(SIG4/(W*EA))**2)
      WRITE(6,711)AEP
  711 FORMAT(1H ,32HTHE AVERAGE DIELECTRIC CONSTANT=,F10.6)
      WRITE(6,712)ETA1
  712 FORMAT(1H ,37HSTD. DEV. OF DIELECTRIC FLUCTUATIONS=,F10.7)
      WRITE(6,713)ETA2
  713 FORMAT(1H ,39HSTD. DEV. OF CONDUCTIVITY FLUCTUATIONS=,F10.7)
      BO=W*SQRT(UO*EA*(XR1+1.)/2.)
      AO=W*SQRT(UO*EA*(XR1-1.)/2.)
      WRITE(6,714)AO
  714 FORMAT(1H ,3HAO=,E15.7)
      CC=3.*10.**(8)
      XLAM=CC/F
      XKO=W*SQRT(UO*EO)
      QKA=BO-QJ*AO
      THETA=0.0
  801 TH=PI*THETA/180.
      SN=SIN(TH)
      CS=COS(TH)
      ETA=UO*3.*10.**8
      QKK=QJ*PI*((ETA*ETA2)**2-(XKO*ETA1)**2)/(QKA*QKA)
      QC=4.*QKK*XLX*XLY*XLZ
      M=1
      A=0.0
      B=90/2.
  808 C=0.0
      D=2.*PI
      NT=30
      NK=30
      ENK=NK
      ENT=NT
      DK=(B-A)/ENK
      DT=(D-C)/ENT
      NKK=NK+1
      NM=NT+1
      CALL SNOPT(NM,NKK,QMI11,QMI12,QMI13,QMI22,QMI23,QMI33)
      I=1
```

```
      202 QF11(I)=QMI11(I,1)+QMI11(I,NM)
          QF12(I)=QMI12(I,1)+QMI12(I,NM)
          QF13(I)=QMI13(I,1)+QMI13(I,NM)
          QF22(I)=QMI22(I,1)+QMI22(I,NM)
          QF23(I)=QMI23(I,1)+QMI23(I,NM)
          QF33(I)=QMI33(I,1)+QMI33(I,NM)
          QI112(I)=(0.0,0.0)
          QI113(I)=(0.0,0.0)
          QI122(I)=(0.0,0.0)
          QI123(I)=(0.0,0.0)
          QI132(I)=(0.0,0.0)
          QI133(I)=(0.0,0.0)
          QI222(I)=(0.0,0.0)
          QI223(I)=(0.0,0.0)
          QI232(I)=(0.0,0.0)
          QI233(I)=(0.0,0.0)
          QI332(I)=(0.0,0.0)
          QI333(I)=(0.0,0.0)
          DO 203 J=2,NT,2
          QI112(I)=QI112(I)+QMI11(I,J)
          QI122(I)=QI122(I)+QMI12(I,J)
          QI132(I)=QI132(I)+QMI13(I,J)
          QI222(I)=QI222(I)+QMI22(I,J)
          QI232(I)=QI232(I)+QMI23(I,J)
      203 QI332(I)=QI332(I)+QMI33(I,J)
          NTT=NT-1
          DO 204 J=3,NTT,2
          QI113(I)=QI113(I)+QMI11(I,J)
          QI123(I)=QI123(I)+QMI12(I,J)
          QI133(I)=QI133(I)+QMI13(I,J)
          QI223(I)=QI223(I)+QMI22(I,J)
          QI233(I)=QI233(I)+QMI23(I,J)
      204 QI333(I)=QI333(I)+QMI33(I,J)
          QI11(I)=(DT/3.)*(QF11(I)+4.*QI112(I)+2.*QI113(I))
          QI12(I)=(DT/3.)*(QF12(I)+4.*QI122(I)+2.*QI123(I))
          QI13(I)=(DT/3.)*(QF13(I)+4.*QI132(I)+2.*QI133(I))
          QI22(I)=(DT/3.)*(QF22(I)+4.*QI222(I)+2.*QI223(I))
          QI23(I)=(DT/3.)*(QF23(I)+4.*QI232(I)+2.*QI233(I))
          QI33(I)=(DT/3.)*(QF33(I)+4.*QI332(I)+2.*QI333(I))
          IF(I-NKK)205,206,206
      205 I=I+1
          GO TO 202
      206 QGI11=QI11(1)+QI11(NKK)
          QGI12=QI12(1)+QI12(NKK)
          QGI13=QI13(1)+QI13(NKK)
          QGI22=QI22(1)+QI22(NKK)
          QGI23=QI23(1)+QI23(NKK)
          QGI33=QI33(1)+QI33(NKK)
          QG112=(0.0,0.0)
          QG122=(0.0,0.0)
          QG132=(0.0,0.0)
          QG222=(0.0,0.0)
          QG232=(0.0,0.0)
          QG332=(0.0,0.0)
          QG113=(0.0,0.0)
          QG123=(0.0,0.0)
          QG133=(0.0,0.0)
```

```
      QG223=(0.0,0.0)
      QG233=(0.0,0.0)
      QG333=(0.0,0.0)
      DO 207 I=2,NK,2
      QG112=QG112+QI11(I)
      QG122=QG122+QI12(I)
      QG132=QG132+QI13(I)
      QG222=QG222+QI22(I)
      QG232=QG232+QI23(I)
  207 QG332=QG332+QI33(I)
      NN=NK-1
      DO 208 I=3,NN,2
      QG113=QG113+QI11(I)
      QG123=QG123+QI12(I)
      QG133=QG133+QI13(I)
      QG223=QG223+QI22(I)
      QG233=QG233+QI23(I)
  208 QG333=QG333+QI33(I)
      QI11A(M)=(DK/3.)*(QGI11+4.*QG112+2.*QG113)
      QI12A(M)=(DK/3.)*(QGI12+4.*QG122+2.*QG123)
      QI13A(M)=(DK/3.)*(QGI13+4.*QG132+2.*QG133)
      QI22A(M)=(DK/3.)*(QGI22+4.*QG222+2.*QG223)
      QI23A(M)=(DK/3.)*(QGI23+4.*QG232+2.*QG233)
      QI33A(M)=(DK/3.)*(QGI33+4.*QG332+2.*QG333)
      IF(M-1)304,305,307
  305 M=M+1
      A=S0/2.
      B=S0
      GO TO 308
  307 QM11=QC*(QI11A(1)+QI11A(2))
      QM12=QC*(QI12A(1)+QI12A(2))
      QM13=QC*(QI13A(1)+QI13A(2))
      QM22=QC*(QI22A(1)+QI22A(2))
      QM23=QC*(QI23A(1)+QI23A(2))
      QM33=QC*(QI33A(1)+QI33A(2))
      QE11=(QKA/YKO)**2-QM11/((2.*PI)**3)
      QE12=-QM12/((2.*PI)**3)
      QE13=-QM13/((2.*PI)**3)
      QE22=(QKA/XKO)**2-QM22/((2.*PI)**3)
      QE23=-QM23/((2.*PI)**3)
      QE33=(QKA/YKO)**2-QM33/((2.*PI)**3)
C     CALCULATE THE EFFECTIVE PROPAGATION CONSTANTS FOR
C     HORIZONTAL AND VERTICALLY POLARIZED WAVES
      X22=REAL(QM22)
      Y22=AIMAG(QM22)
      PN=W*UO*SIGA/(XKO**2)+Y22/((2.*PI)**3)
      PB=ATR-SN*SN-X22/((2.*PI)**3)
      PH3=ATAN2(PN,PB)
      R3=SQRT(PN**2+PB**2)
      QKH=-XKO*SQRT(R3)*CEXP(-QJ*PH3/2.)
      XH=REAL(QKH)
      YH=AIMAG(QKH)
      P1=XH
      Q1=-YH
      QKV1=QE11*SN*SN-QE11*QE33+QE13**2
      QKV2=(QE13*SN)**2-QE33*QKV1
      X4=REAL(QKV2)
```

```
      Y4=AIMAG(QKV2)
      R4=SQRT(X4**2+Y4**2)
      PH4=ATAN2(Y4,X4)
      QVN=QE13*SN+SQRT(R4)*CEXP(QJ*PH4/2.)
      QKV=-XK0*(QVN/QE33)
      XV=REAL(QKV)
      YV=AIMAG(QKV)
      R2=YV
      R2=-YV
      XE11=REAL(QE11)
      YE11=AIMAG(QE11)
      XE12=REAL(QE12)
      YE12=AIMAG(QE12)
      XE13=REAL(QE13)
      YE13=AIMAG(QE13)
      XE22=REAL(QE22)
      YE22=AIMAG(QE22)
      XE23=REAL(QE23)
      YE23=AIMAG(QE23)
      XE33=REAL(QE33)
      YE33=AIMAG(QE33)
C   THE FOLLOWING CARDS CALCULATE THE RADAR
C   BACKSCATTER COEFFICIENT FOR A HALF SPACE BASED ON THE MEAN
C   WAVE DETERMINED ABOVE
      QA1=(0.0,0.0)
      A2=1.0
      QA3=(0.0,0.0)
      QT21=2.*A2*XK0*CS
      QT22=XK0*CS-QKH
      QT2=QT21/QT22
      QT131=QKV*SN+XK0*QE13
      QT132=XK0*(SN*SN-QE33)
      QT13=QT131/QT132
      QT131=2.*QA1*CS+QA3*SN
      QT132=QA1*SN*SN/CS
      QT133=XK0*SN*QT13-QKV
      QT134=XK0*CS+XK0*SN*SN/CS
      QT1=XK0*(QT131+QT132)/(QT133+QT134)
      QT3=QT1*QT13
      AX1=0.0
      QAY1=QT2
      AZ1=0.0
      QAY2=QT1
      AY2=0.0
      QAZ2=QT3
      XKX=XK0*SN
      XKZ=XK0*CS
      R11=W*U0*SIGA
      R12=W*W*U0*E0*AFF-(XK0*SN)**2
      R2=SQRT(R11**2+R12**2)
      PH2=ATAN2(R11,R12)
      QKZP=SQRT(R2)*CEXP(-QJ*PH2/2.)
      Q11=QKZP*(QKZP+XKZ)
      Q22=XKX*(KX*(1.+QKZP/XKZ)
      Q=-QJ*(Q11+Q22)
      QAZ=AZ1+QAZ2
      QCY1=QKZP*AX1+AZ1*XK0*SN
```

```
                  QQY2=QKZP*QAY2+QAZ2*YKQ*SN
                  QD(1)=P1+QJ*(Q1+QKZP)
                  QKZPC=CONJG(QKZP)
                  QK(1)=P1-QJ*(Q1+QKZPC)
290               QD(2)=P1+QJ*(Q1+QKZP)
                  QK(2)=P2-QJ*(Q2+QKZPC)
                  QD(3)=P2+QJ*(Q2+QKZP)
                  QK(3)=P1-QJ*(Q1+QKZPC)
                  QD(4)=P2+QJ*(Q2+QKZP)
295               QK(4)=P2-QJ*(Q2+QKZPC)
                  QAL(1)=QCX1*CONJG(QCX1)
                  QAL(2)=QCX1*CONJG(QCX2)
                  QAL(3)=QCX2*CONJG(QCX1)
                  QAL(4)=QCX2*CONJG(QCX2)
300               QD(5)=P1+QJ*(Q1+QKZP)
                  QK(5)=P1-QJ*(Q1+QKZPC)
                  QD(6)=P1+QJ*(Q1+QKZP)
                  QK(6)=P2-QJ*(Q2+QKZPC)
                  QD(7)=P2+QJ*(Q2+QKZP)
305               QK(7)=P1-QJ*(Q1+QKZPC)
                  QD(8)=P2+QJ*(Q2+QKZP)
                  QK(8)=P2-QJ*(Q2+QKZPC)
                  QAL(5)=QCX1*CONJG(QAY1)
                  QAL(6)=QCX1*AY2
310               QAL(7)=QCX2*CONJG(QAY1)
                  QAL(8)=QCY2*AY2
                  QB(1)=QAY1*CONJG(QAY1)
                  QB(2)=QAY1*AY2
                  QB(3)=AY2*CONJG(QAY1)
315               QB(4)=AY2*AY2
                  QG(1)=QAY1*CONJG(QCX1)
                  QG(2)=QAY1*CONJG(QCX2)
                  QG(3)=AY2*CONJG(QCX1)
                  QG(4)=AY2*CONJG(QCX2)
320               QERX=QA1
                  ERY=A2
                  QERZ=QA3
                  QES1=(0.0,0.0)
                  QES2=(0.0,0.0)
325               DO 510 I=1,4
                  QS11=2.+XLZ*(QK(I)+QD(I))
                  QS12=(1.+XLZ*QD(I))*(1.+XLZ*QK(I))
                  QS13=QAL(I)/(QK(I)+QD(I))
                  QS=QS13*QS11/QS12
330               QES1=QES1+QS
                  QS14=QB(I)/(QK(I)+QD(I))
                  QS3=QS14*QS11/QS12
              510 QES2=QES2+QS3
                  QES3=(0.0,0.0)
335               QES4=(0.0,0.0)
                  DO 511 I=5,8
                  QS11=2.+XLZ*(QK(I)+QD(I))
                  QS12=(1.+XLZ*QD(I))*(1.+XLZ*QK(I))
                  QS13=QAL(I)/(QK(I)+QD(I))
340               QS=QS13*QS11/QS12
                  QES3=QES3+QS
                  QS14=QG(I-4)/(QK(I)+QD(I))
```

```
                      QSG=QS14*QS11/QS12
                  511 QES4=QES4+QSG
      345             QS=QERX*CONJG(QERX)
                      QSB=Q*CONJG(Q)
                      QJJ1=QS*QES1/QSB
                      R1=REAL(QJJ1)
                      QS=QERX*ERY*QES3
      350             QED=QJ*Q*(XKZ+QKZPC)
                      QJJ2=QS/QED
                      R2=2.*REAL(QJJ2)
                      QS=QERX*XKO*SN*QES1*CONJG(QEPZ)
                      QED=XKZ*QSB
      355             QJJ2=QS/QED
                      R3=2.*REAL(QJJ2)
                      QS=ERY*ERY*QES2
                      QED=(XKZ+QKZP)*(XKZ+QKZPC)
                      QJJ2=QS/QED
      360             R4=REAL(QJJ2)
                      QS=QJ*ERY*XKO*SN*QES4*CONJG(QEPZ)
                      QED=(XKZ*(XKZ+QKZP)*CONJG(Q)
                      QJJ2=QS/QED
                      R5=2.*REAL(QJJ2)
      365             QS=QERZ*CONJG(QERZ)*QES1*(XKO*SN)**2
                      QED=QSB*XKZ**2
                      QJJ2=QS/QED
                      R6=REAL(QJJ2)
                      R=R1+R2+R3+R4+R5+R6
      370             ER1=XLY*XLY*XL7*((W*U0*ETA2)**2+(XKO*XKO*ETA1)**2)
                      ERD=PI*PI*(1.+(2.*XKO*XLX*SN)**2)
                      ER=((XKO*CS)**2)*ER1*R/ERD
                      SIG=4.*PI*ER
                      DBSIG=10.*ALOG10(SIG)
      375       C  THE FOLLOWING CARDS CALCULATE THE BACKSCATTER COEFFICIENT
                C  FOR A PLANE LAYER
                      PI=3.1415926536
                      E0=8.854*10.**(-12)
                      U=4.*10.**(-7)
      380             U0=PI*U
                      W=2.*PI*F
                      ER=EG*E0
                      BB=SQRT(1.+(SG/(W*E3))**2)
                      B3=W*SQRT(E3*U0*(BB+1.)/2.)
      385             A3=W*SQRT(E3*U0*(BB-1.)/2.)
                      RH1=B3**2-A3**2-(XKO*SN)**2
                      RH2=2.*B3*A3
                      R3=SQRT(RH1**2+RH2**2)
                      PH3=ATAN2(RH2,RH1)
      390             QK3C=SQRT(R3)*CEXP(-QJ*PH3/2.)
                      QK3=B3-QJ*A3
                      IF(THETA)3J+,311,312
                  311 EH=(Q1**2-P1**2)/(W*W*U0)
                      EV=(Q2**2-P2**2)/(W*W*U0)
      395         312 QA11=(QJ*QK3C3-P1-QJ*Q1)*CEXP(-XL*(P1+QJ*Q1))
                      QA12=(QJ*QK3C3+P1+QJ*Q1)*CEXP(XL*(P1+QJ*Q1))
                      QA21=QJ*XKO*CS+P1+QJ*Q1
                      QA22=QJ*XKO*CS-P1-QJ*Q1
                      QT2N=2.*QJ*XKO*QA12*A2*CS
```

```
      QT2D=QA21*QA12-QA11*QA22
      QT2=QT2N/QT2D
      QV2N=-2.*QJ*XKO*A2*QA11*CS
      QV2=QV2N/QT2D
      QAA1=(QJ*(1.-E3/EV)*(XKO*SN)**2)/QK3C3
      QAL1=QJ*QK3C3+QAA1
      QB11=(P2+QJ*Q2-QAL1)*CEXP(-XL*(P2+QJ*Q2))
      QB21=P2+QJ*Q2+QB21A
      QB12=-(P2+QJ*Q2+QAL1)*CEXP(XL*(P2+QJ*Q2))
      QB21A=QJ*XKO*(CS+SN*SN*(1.-E0/EV)/CS)
      QB22=-P2-QJ*Q2+QB21A
      QT1A=SN*(1.-E0/EV)*(QA3+QA1*SN/CS)
      QT1N=QJ*XKO*QB12*(2.*QA1*CS+QT1A)
      QT1D=QB12*QB21-QB22*QB11
      QT1=QT1N/QT1D
      QV1N=-QJ*XKO*QB11*(2.*QA1*CS+QT1A)
      QV1=QV1N/QT1D
      QT3A=QT1*CEXP(-XL*(P2+QJ*Q2))+QV1*CEXP(XL*(P2+QJ*Q2))
      QT3B=E3*XKO*SN*QT3A/QK3C3
      QT3C=E0*(QA3-SN*(QT1+QV1-QA1)/CS)*CEXP(XL*(P2+QJ*Q2))
      QT3D=EV*(CEXP(-XL*(P2+QJ*Q2))-CEXP(XL*(P2+QJ*Q2)))
      QT3=(QT3B-QT3C)/QT3D
      QV3=E0*(QA3-SN*(QT1+QV1-QA1)/CS)/EV-QT3
      XKX=XKO*SN
      XKY=0.0
      RH31=B3**2-A3**2-XKX**2-XKY**2
      RH32=2.*B3*A3
      RH3=SQRT(RH31**2+RH32**2)
      PH3=ATAN2(RH32,RH31)
      QK3Z=SQRT(RH3)*CEXP(-QJ*PH3/2.)
      XK1Z=SQRT(XKO**2-XKX**2-XKY**2)
      QA1HN=(QKZP-QK3Z)*CEXP(-2.*QJ*QKZP*XL)
      QA1HD=QKZP+QK3Z
      QA1H=QA1HN/QA1HD
      QA2HA=(QK3Z**2+XKY**2)*QKZP**2
      QA2HB=QK3Z*(QKZP**2+XKX**2)*QKZP
      QA2H=(QA2HB-QA2HA)*CEXP(-2.*QJ*QKZP*XL)
      QA2H=QA2H/(QA2HB+QA2HA)
      QA3HA=QK3Z*XKY*CEXP(-QJ*QKZP*XL)
      QA3H=QA3HA/(QA2HB+QA2HA)
      QA5H=XK1Z*(QKZP**2+XKX**2)*QKZP*(1.-QA2H)
      QA4H=(XK1Z**2+XKY**2)*QKZP**2
      QA6H=XK1Z*(QKZP**2+XKX**2)*QKZP*QA3H
      QA7H=XK1Z*(QKZP**2+XKY**2)/(2.*QJ*QKA**2)
      QA9H=QA5H+QA4H*(QA2H+1.)
      QB11=QKZP**3+QKZP*XKY**2
      QE1=2.*XK1Z*QB11*QA3H/QA9H
      QE2=-XK1Z*XKX*(QA2H+1.)/QA9H
      QE3=QA7H*(QA2H+1.)/QA9H
      QE4=QA6H/(2.*QJ*QA9H*QKZP*QKA*QKA)
      QM1=QKZP*(1.-QA1H)
      QM2=XK1Z*(1.+QA1H)
      QM=-1./(QJ*QKA*QKA*(QM1+QM2))
      QD1=P1+QJ*(Q1-QKZP)
      QD1C=CONJG(QD1)
      QD2=-(P1+QJ*(Q1+QKZP))
      QD2C=CONJG(QD2)
```

```
                QNJ1=QA1H*QT2
                QA(1)=QNJ1*CONJG(QNJ1)
                QCC(1)=QD1
                QLD(1)=QD1C
                QNJ2=QA1H*QV2
                QA(2)=QNJ1*CONJG(QNJ2)
                QCC(2)=QD1
                QLD(2)=QD2C
                QA(3)=QT2*QA1H*CONJG(QT2)
                QCC(3)=QD1
                QLD(3)=-QD2C
                QA(4)=QA1H*QT2*CONJG(QV2)
                QCC(4)=QD1
                QLD(4)=-QD1C
                QA(5)=QA1H*QV2*CONJG(QNJ1)
                QCC(5)=QD2
                QLD(5)=QD1C
                QA(6)=QA1H*QV2*CONJG(QNJ2)
                QCC(6)=QD2
                QLD(6)=CONJG(QJ2)
                QA(7)=QA1H*QV2*CONJG(QT2)
                QCC(7)=QD2
                QLD(7)=-QD2C
                QA(8)=QA1H*QV2*CONJG(QV2)
                QCC(8)=QD2
                QLD(8)=-QD1C
                QA(9)=QT2*CONJG(QNJ1)
                QCC(9)=-QD2
                QLD(9)=QD1C
                QA(10)=QT2*CONJG(QNJ2)
                QCC(10)=-QD2
                QLD(10)=QD2C
                QA(11)=QT2*CONJG(QT2)
                QCC(11)=-QD2
                QLD(11)=-QD2C
                QA(12)=QT2*CONJG(QV2)
                QCC(12)=-QD2
                QLD(12)=-QD1C
                QA(13)=QV2*CONJG(QNJ1)
                QCC(13)=-QD1
                QLD(13)=QD1C
                QA(14)=QV2*CONJG(QNJ2)
                QCC(14)=-QD1
                QLD(14)=QD2C
                QA(15)=QV2*CONJG(QT2)
                QCC(15)=-QD1
                QLD(15)=-QD2C
                QA(16)=QV2*CONJG(QV2)
                QCC(16)=-QD1
                QLD(16)=-QD1C
                IN=16
                CALL SUM(IN,QA,QCC,QLD,QSM)
                AL11=(W*UO*ETA2)**2+(XKO*XKO*ETA1)**2
                ALO=1.+4.*(XKO*XLX*SN)**2
                QNYY1=QKA*QKA*QM*CONJG(QM)
                QNYY2=4.*XLX*XLY*XLZ*AL11*QNYY1
                QNYY=QNYY2*CONJG(QKA)*CONJG(QKA)
```

```
                QAYY=QNYY*OSM/ALD
515             QQ5=Q33+Q84
                QEe=Q83-Q84
                QD1P=Q2+QJ*Q2-QJ*QKZP
                QD2P=-(P2+QJ*Q2+QJ*QKZP)
                QH11=QT1*(QKA**2-(XKO*SN)**2)
520             QH12=QT3*XKO*SN*QKZP
                QH1=QB6*(QH11-QH12)
                QH21=QV1*(QKA**2-(XKO*SN)**2)
                QH22=QV3*XKO*QKZP*SN
                QH2=Q36*(QH21-QH22)
525             QH3=Q8E*(QH11+QH12)
                QH4=Q85*(QH21+QH22)
                QA(1)=QH1*CONJG(QH1)
                QCC(1)=QD1P
                QLD(1)=CONJG(QD1P)
530             QA(2)=QH1*CONJG(QH2)
                QCC(2)=QD1P
                QLD(2)=CONJG(QD2P)
                QA(3)=QH1*CONJG(QH3)
                QCC(3)=QD1P
535             QLD(3)=-CONJG(QD2P)
                QA(4)=QH1*CONJG(QH4)
                QCC(4)=QD1P
                QLD(4)=-CONJG(QD1P)
                QA(5)=QH2*CONJG(QH1)
540             QCC(5)=QD2P
                QLD(5)=CONJG(QD1P)
                QA(6)=QH2*CONJG(QH2)
                QCC(6)=QD2P
                QLD(6)=CONJG(QD2P)
545             QA(7)=QH2*CONJG(QH3)
                QCC(7)=QD2P
                QLD(7)=-CONJG(QD2P)
                QA(8)=QH2*CONJG(QH4)
                QCC(8)=QD2P
550             QLD(8)=-CONJG(QD1P)
                QA(9)=QH3*CONJG(QH1)
                QCC(9)=-QD2P
                QLD(9)=CONJG(QD1P)
                QA(10)=QH3*CONJG(QH2)
555             QCC(10)=-QD2P
                QLD(10)=CONJG(QD2P)
                QA(11)=QH3*CONJG(QH3)
                QCC(11)=-QD2P
                QLD(11)=-CONJG(QD2P)
560             QA(12)=QH3*CONJG(QH4)
                QCC(12)=-QD2P
                QLD(12)=-CONJG(QD1P)
                QA(13)=QH4*CONJG(QH1)
                QCC(13)=-QD1P
565             QLD(13)=CONJG(QD1P)
                QA(14)=QH4*CONJG(QH2)
                QCC(14)=-QD1P
                QLD(14)=CONJG(QD2P)
                QA(15)=QH4*CONJG(QH3)
570             QCC(15)=-QD1P
```

```
                  QLO(15)=-CONJG(QD2P)
                  QA(16)=QH4*CONJG(QH4)
                  QCC(16)=-QD1P
                  QLO(16)=-CONJG(QV1P)
575               CALL SUM(IN,QA,QCC,QLO,QSM)
                  AX1=4.*XLX*XLY*XLZ*AL11/ALO
                  QAXX=AX1*QSM
                  QAZZ=(QAXX*(XKO*SN)**2)/(XK17**2)
                  QAYZ=XKO*SN*QAXX/XK17
580               QNJ3=QA1H*QT2
                  QA(1)=QH1*CONJG(QNJ3)
                  QCC(1)=QD1P
                  QLO(1)=CONJG(QD1)
                  QNJ4=QA1H*QV2
585               QA(2)=QH1*CONJG(QNJ4)
                  QCC(2)=QD1P
                  QLO(2)=CONJG(QD2)
                  QA(3)=QH1*CONJG(QT2)
                  QCC(3)=QD1P
590               QLO(3)=-CONJG(QD2)
                  QA(4)=QH1*CONJG(QV2)
                  QCC(4)=QD1P
                  QLO(4)=-CONJG(QD1)
                  QA(5)=QH2*CONJG(QNJ3)
595               QCC(5)=QD2P
                  QLO(5)=CONJG(QD1)
                  QA(6)=QH2*CONJG(QNJ4)
                  QCC(6)=QD2P
                  QLO(6)=CONJG(QD2)
600               QA(7)=QH2*CONJG(QT2)
                  QCC(7)=QD2P
                  QLO(7)=-CONJG(QD2)
                  QA(8)=QH2*CONJG(QV2)
                  QCC(8)=QD2P
605               QLO(8)=-CONJG(QD1)
                  QA(9)=QH3*CONJG(QNJ3)
                  QCC(9)=-QD2P
                  QLO(9)=CONJG(QL1)
                  QA(10)=QH3*CONJG(QNJ4)
610               QCC(10)=-QD2P
                  QLO(10)=CONJG(QD2)
                  QA(11)=QH3*CONJG(QT2)
                  QCC(11)=-QD2P
                  QLO(11)=-CONJG(QL2)
615               QA(12)=QH3*CONJG(QV2)
                  QCC(12)=-QL2P
                  QLO(12)=-CONJG(QD1)
                  QA(13)=QH4*CONJG(QNJ3)
                  QCC(13)=-QD1P
620               QLO(13)=CONJG(QD1)
                  QA(14)=QH4*CONJG(QNJ4)
                  QCC(14)=-QL1P
                  QLO(14)=CONJG(QD2)
                  QA(15)=QH4*CONJG(QT2)
625               QCC(15)=-QD1P
                  QLO(15)=-CONJG(QL2)
                  QA(16)=QH4*CONJG(QV2)
```

```
                QCC(15)=-QD1P
                QLD(16)=-CONJG(QD1)
630             CALL SUM(IN,QA,QCC,QLD,QSM)
                QAXY1=CONJG(QKA)*CONJG(QKA)*CONJG(QM)
                QAXY2=-4.*XLX*XLY*XL7*AL11*QAXY1/ALD
                QAXY=QAXY2*QSM
                QS01=QERX*CONJG(QERX)*QAXX
635             QNJ5=QERX*ERY*QAXY
                QSC2=2.*REAL(QNJ5)
                QNJ6=QERA*QAXZ*CONJG(QERZ)
                QS03=2.*REAL(QNJ6)
                QS04=ERY*ERY*QAYY
640             QNJ7=ERY*QERZ*QAXY/XK1Z
                QS05=2.*XKO*SN*REAL(QNJ7)
                QSS1=QA1*CONJG(QA1)+A2**2+QA3*CONJG(QA3)
                QS06=QERZ*CONJG(QERZ)*QAZZ
                QS1=QS01+QS02+QS03
645             QS2=QS04+QS05+QS06
                QSA=((XKO*CS)**2)*(QS1+QS2)/(PI*QSS1)
                SIGO=REAL(QSA)
                DBSIGO=10.*ALOG10(SIGO)
            C  THE FOLLOWING CARDS CALCULATE THE BACKSCATTER COEFFICIENT
650         C  FOR A VEGETATION LAYER WITH A ROUGH VEGETATION SOIL BOUNDARY
                Y1=2.*P1*Q1
                X1=Q1**2-P1**2+(XKO*SN)**2
                PHE=ATAN2(Y1,X1)
                RHOE=SQRT(Y1**2+X1**2)
655             ALE=(SQRT(RHOE))*SIN(PHE/2.)
                BE=(SQRT(RHOE))*COS(PHE/2.)
                A=XKO*BE/(BE**2+ALE**2)
                B=XKO*ALE/(BE**2+ALE**2)
                G1=2.*A*B*SN**2
660             G2=1.-(A**2-B**2)*SN**2
                GAM=0.5*ATAN2(G1,G2)
                RHO=(G1**2+G2**2)**0.25
                D1=RHO*(BE*COS(GAM)-ALE*SIN(GAM))
                D2=SQRT((XKO*SN)**2+D1**2)
665             SECS=D2/D1
                SINS=XKO*SN/D2
                COSS=D1/D2
                TANS=SINS/COSS
                R1=SQRT(R3**2-(BE*SINS)**2)
670             R2=BE*COSS
                RO=(R2-R1)/(R2+R1)
                R3=(RO/(2.*XMS))**2
                ZZ1=(TANS/(2.*XMS))**2
                ZZ2=4.*ALE*XL*SECS
675             GTO=1.-2.*EE*COSS/P1
                GT1=(1.+GTO**2)*SINS*SINS
                GT2=2.*(1.-GTO*COSS*COSS)
                GT=1.-SINS*SINS*(GT2-GT1)
                R4=R3*GT/COSS**4
680             IF(ZZ1-500.)801,802,802
            802 R5=0.0
                GO TO 803
            801 R5=R4*EXP(-ZZ1)*EXP(-ZZ2)
            803 AYY=REAL(QAYY)
```

```
685                 SIGHH=R5+(AYY*(XKO*DS)**2)/PI
                    DBHH=10.*ALOG10(SIGHH)
                    WRITE(6,601)THETA
                601 FORMAT(1H ,6HTHETA=,F5.2)
                    DD1=1./P1
690                 WRITE(6,715)P1,DD1
                715 FORMAT(1H ,3HP1=,E15.7,10X,3HD1=,E15.7)
                    WRITE(6,602)D3SIG
                602 FORMAT(1H ,10X,22HHALF SPACE SIGMA ZERO=,F15.8)
                    WRITE(6,603) D3SIGO
695                 603 FORMAT(1H ,10X,17HLAYER SIGMA ZERO=,F15.8)
                    WRITE(6,604)DBHH
                    604 FORMAT(1H ,10X,39HLAYER WITH ROUGH SURFACE SIGMA ZERO HH=,F15.8//)
                    IF(THETA-PC.)303,304,304
                303 THETA=THETA+10.
700                 GO TO 401
                304 IF(MQ-4)605,606,606
                    605 MQ=MQ+1
                    GO TO 7
                606 STOP
705                 END
```

95

SYMBOLIC REFERENCE MAP (OPT=1)

ENTRY POINTS
4136 MODEL

VARIABLES	SN	TYPE	RELOCATION				
2	A	REAL	/ /	17	AER	REAL	/ /
12213	ALD	REAL		12262	ALE	REAL	
12212	ALA1	REAL		21	AO	REAL	/ /
12151	AX1	REAL		12245	AYY	REAL	
12153	AY2	REAL		12152	AZ1	REAL	
12150	A2	REAL		12177	A3	REAL	
*	B	REAL	/ /	12175	BB	REAL	
12223	BE	REAL		20	BO	REAL	/ /
12176	B3	REAL		4	C	REAL	/ /
12071	CC	REAL		12234	COOS	REAL	
12075	CS	REAL		5	D	REAL	/ /
12247	DBHH	REAL		12173	D3SIG	REAL	
12215	D3SIGO	REAL		12250	DD1	REAL	
1	DK	REAL	/ /	0	DT	REAL	/ /
12230	E1	REAL		12231	E2	REAL	
12067	EA	REAL		12053	EC	REAL	
12202	EH	REAL		12060	ELP	REAL	
12061	ELPP	REAL		14	EO	REAL	/ /
12171	ER	REAL		12170	ERO	REAL	
12162	ERV	REAL		12167	EP1	REAL	
12076	ETA	REAL		12064	ETA1	REAL	
12063	ETA11	REAL		12066	ETA2	REAL	
12065	ETA22	REAL		12203	EV	REAL	
12174	E3	REAL		12052	F	REAL	
12102	FNK	REAL		12103	FNT	REAL	

VARIABLES	SN	TYPE	RELOCATION
12226	GAM	REAL	
12241	GTO	REAL	
12243	GT2	REAL	
12225	G2	REAL	
12211	IN	INTEGER	
12077	M	INTEGER	
12101	NK	INTEGER	
12105	NM	INTEGER	
12100	NT	INTEGER	
12115	PO	REAL	
12161	PH2	REAL	
12127	PH4	REAL	
12060	PM	REAL	
12122	P1	REAL	
11515	Q	COMPLEX	
11603	QAA1	COMPLEX	
11605	QAL1	COMPLEX	
11772	QAXY	COMPLEX	
11776	QAXY2	COMPLEX	
11503	QAY2	COMPLEX	
11501	QAY1	COMPLEX	
11765	QAZZ	COMPLEX	
11451	QA1	COMPLEX	
11651	QA1HD	COMPLEX	
11565	QA11	COMPLEX	
11661	QA2H	COMPLEX	
11657	QA2HB	COMPLEX	
11571	QA22	COMPLEX	
11665	QA3H	COMPLEX	
11667	QA4H	COMPLEX	
11673	QA5H	COMPLEX	
11643	QA9H	COMPLEX	
11677	QB1	COMPLEX	
11611	QB12	COMPLEX	
11615	QB21	COMPLEX	
11617	QB22	COMPLEX	
11706	QB4	COMPLEX	
11737	QBE	COMPLEX	
43761	QC	COMPLEX	ARRAY
11521	QCX2	COMPLEX	
11745	QD1	COMPLEX	
11741	QD1P	COMPLEX	
11727	QD2C	COMPLEX	
11535	QEP	COMPLEX	
11503	QEP2	COMPLEX	
11567	QES2	COMPLEX	
11776	QES4	COMPLEX	
11424	QE11	COMPLEX	
11425	QE12	COMPLEX	
11431	QE23	COMPLEX	
12051	QF11	COMPLEX	ARRAY
22051	QF13	COMPLEX	ARRAY
31051	QF23	COMPLEX	ARRAY
43711	QG	COMPLEX	ARRAY
11337	QGI12	COMPLEX	
11757	QGI22	COMPLEX	
11545	QGI32	COMPLEX	
12244	QT	REAL	
12242	QT1	REAL	
12224	Q1	REAL	
12106	I	INTEGER	
12107	J	INTEGER	
12047	MQ	INTEGER	
12104	NKK	INTEGER	
12111	NN	INTEGER	
12110	NTT	INTEGER	
12220	PHE	REAL	
12116	PH3	REAL	
15	PI	REAL	/ /
12114	PN	REAL	
12132	P2	REAL	
43721	QA	COMPLEX	ARRAY
43661	QAL	COMPLEX	ARRAY
11763	QAXX	COMPLEX	
11773	QAXY1	COMPLEX	
11767	QAXZ	COMPLEX	
11733	QAYY	COMPLEX	
11517	QAZ	COMPLEX	
11505	QAZ2	COMPLEX	
11653	QA1H	COMPLEX	
11647	QA1HN	COMPLEX	
11565	QA12	COMPLEX	
11655	QA2HA	COMPLEX	
11567	QA21	COMPLEX	
11453	QA3	COMPLEX	
11663	QA3HA	COMPLEX	
11671	QA5H	COMPLEX	
11675	QA7H	COMPLEX	
43701	QB	COMPLEX	ARRAY
11667	QB11	COMPLEX	
11701	QB2	COMPLEX	
11613	QB21A	COMPLEX	
11703	QB3	COMPLEX	
11735	QB5	COMPLEX	
11327	QC	COMPLEX	
11523	QCX1	COMPLEX	
43021	QD	COMPLEX	ARRAY
11717	QD1C	COMPLEX	
11721	QD2	COMPLEX	
11771	QD2P	COMPLEX	
11531	QEPX	COMPLEX	
11535	QFS1	COMPLEX	
11441	QES3	COMPLEX	
11417	QENN	COMPLEX	
11423	QE12	COMPLEX	
11427	QF22	COMPLEX	
11433	QE33	COMPLEX	
16161	QF12	COMPLEX	ARRAY
29751	QF23	COMPLEX	ARRAY
35551	QF33	COMPLEX	ARRAY
11331	QGI11	COMPLEX	
11335	QGI13	COMPLEX	
11341	QGI23	COMPLEX	
11345	QGI12	COMPLEX	

VARIABLES	SN	TYPE	RELOCATION				
11357	QG113	COMPLEX		11347	QG122	COMPLEX	
11361	QG123	COMPLEX		11351	QG132	COMPLEX	
11363	QG133	COMPLEX		11353	QG212	COMPLEX	
11365	QG213	COMPLEX		11355	QG222	COMPLEX	
11367	QG223	COMPLEX		11373	QG232	COMPLEX	
11371	QG233	COMPLEX		11747	QH1	COMPLEX	
11743	QH11	COMPLEX		11745	QH12	COMPLEX	
11755	QH2	COMPLEX		11751	QH21	COMPLEX	
11753	QH22	COMPLEX		11757	QH3	COMPLEX	
11761	QH4	COMPLEX		43021	QI11	COMPLEX	ARRAY
43005	QI11A	COMPLEX	ARRAY	41451	QI112	COMPLEX	ARRAY
41547	QI113	COMPLEX	ARRAY	43117	QI12	COMPLEX	ARRAY
43011	QI12A	COMPLEX	ARRAY	41645	QI122	COMPLEX	ARRAY
41743	QI123	COMPLEX	ARRAY	43215	QI13	COMPLEX	ARRAY
43015	QI13A	COMPLEX	ARRAY	42041	QI132	COMPLEX	ARRAY
42137	QI133	COMPLEX	ARRAY	43313	QI22	COMPLEX	ARRAY
44061	QI22A	COMPLEX	ARRAY	42235	QI222	COMPLEX	ARRAY
42333	QI223	COMPLEX	ARRAY	43411	QI23	COMPLEX	ARRAY
44065	QI23A	COMPLEX	ARRAY	42431	QI232	COMPLEX	ARRAY
42527	QI233	COMPLEX	ARRAY	43507	QI33	COMPLEX	ARRAY
44071	QI33A	COMPLEX	ARRAY	42625	QI332	COMPLEX	ARRAY
42723	QI333	COMPLEX	ARRAY	11521	QJ	COMPLEX	
12043	QJJ1	COMPLEX		12045	QJJ2	COMPLEX	
43641	QK	COMPLEX	ARRAY	11323	QKA	COMPLEX	
11447	QKH	COMPLEX		11325	QKK	COMPLEX	
11445	QKV	COMPLEX		11435	QKV1	COMPLEX	
11477	QKV2	COMPLEX		11507	QKZP	COMPLEX	
11525	QKZPC	COMPLEX		11561	QK3	COMPLEX	
11557	QK3C3	COMPLEX		11645	QK3Z	COMPLEX	
44021	QLD	COMPLEX	ARRAY	11713	QM	COMPLEX	
12347	QMI11	COMPLEX	ARRAY	16247	QMI12	COMPLEX	ARRAY
22147	QMI13	COMPLEX	ARRAY	26047	QMI22	COMPLEX	ARRAY
31747	QMI23	COMPLEX	ARRAY	35647	QMI33	COMPLEX	ARRAY
11707	QM1	COMPLEX		11377	QM11	COMPLEX	
11401	QM12	COMPLEX		11403	QM13	COMPLEX	
11711	QM2	COMPLEX		11405	QM22	COMPLEX	
11413	QM23	COMPLEX		11415	QM33	COMPLEX	
12025	QNJ1	COMPLEX		12027	QNJ2	COMPLEX	
12031	QNJ3	COMPLEX		12033	QNJ4	COMPLEX	
12035	QNJ5	COMPLEX		12037	QNJ6	COMPLEX	
12041	QNJ7	COMPLEX		11731	QNYY	COMPLEX	
11725	QNYY1	COMPLEX		11727	QNYY2	COMPLEX	
11547	QS	COMPLEX		12023	QSA	COMPLEX	
11553	QSB	COMPLEX		11407	QSG	COMPLEX	
11527	QSM	COMPLEX		12001	QSO1	COMPLEX	
12003	QSO2	COMPLEX		12005	QSO3	COMPLEX	
12007	QSO4	COMPLEX		12011	QSO5	COMPLEX	
12015	QSO6	COMPLEX		12013	QSS1	COMPLEX	
12017	QS1	COMPLEX		11541	QS11	COMPLEX	
11543	QS12	COMPLEX		11545	QS13	COMPLEX	
11551	QS14	COMPLEX		12021	QS2	COMPLEX	
11477	QT1	COMPLEX		11621	QT1A	COMPLEX	
11625	QT1D	COMPLEX		11623	QT1N	COMPLEX	
11473	QT13	COMPLEX		11463	QT131	COMPLEX	
11465	QT132	COMPLEX		11467	QT133	COMPLEX	
11471	QT134	COMPLEX		11461	QT2	COMPLEX	
11575	QT2D	COMPLEX		11573	QT2N	COMPLEX	

VARIABLES	SN	TYPE	RELOCATION					
11455	QT21	COMPLEX			11457	QT22	COMPLEX	
11475	QT2	COMPLEX			11633	QT3A	COMPLEX	
11635	QT33	COMPLEX			11637	QT3C	COMPLEX	
11641	QT3B	COMPLEX			11441	QVN	COMPLEX	
11651	QV1	COMPLEX			11627	QV1N	COMPLEX	
11661	QV2	COMPLEX			11677	QV2N	COMPLEX	
11647	QV3	COMPLEX			12123	Q1	REAL	
11511	Q21	COMPLEX			12133	Q2	REAL	
11514	Q22	COMPLEX			12166	R	REAL	
12227	RHO	REAL			12221	RHOE	REAL	
12201	RH1	REAL			12231	RH2	REAL	
12205	RH3	REAL			12205	RH31	REAL	
12206	RH32	REAL			12051	RLV	REAL	
12236	R0	REAL			12163	R1	REAL	
12150	R11	REAL			12157	R12	REAL	
12160	R2	REAL			12117	R3	REAL	
12126	R4	REAL			12164	R5	REAL	
12165	R6	REAL			12232	SEGS	REAL	
12054	SG	REAL			12172	SIG	REAL	
16	SIGA	REAL		/ /	12246	SIGHH	REAL	
12062	SIGL	REAL			12214	SIGO	REAL	
12237	SIGS	REAL			22	SN	REAL	/ /
12235	TAMS	REAL			12074	TH	REAL	
12073	THETA	REAL			12056	U	REAL	
13	UC	REAL		/ /	12	W	REAL	/ /
12070	XB1	REAL			12134	XE11	REAL	
12136	XE12	REAL			12140	XE13	REAL	
12142	XE22	REAL			12144	XE23	REAL	
12146	XE33	REAL			12120	XH	REAL	
11	XKO	REAL		/ /	12154	XKX	REAL	
12204	XKY	REAL			12155	XKZ	REAL	
12210	XM1Z	REAL			23	XL	REAL	/ /
12072	XLAM	REAL			12057	XLAMC	REAL	
10	XLX	REAL		/ /	7	XLY	REAL	/ /
6	XLZ	REAL		/ /	12055	XMS	REAL	
12130	XV	REAL			12217	X1	REAL	
12112	X22	REAL			12124	X4	REAL	
12135	YE11	REAL			12137	YE12	REAL	
12141	YE13	REAL			12143	YE22	REAL	
12145	YE23	REAL			12147	YE33	REAL	
12121	YH	REAL			12131	YV	REAL	
12216	Y1	REAL			12113	Y22	REAL	
12125	Y4	REAL			12237	ZZ1	REAL	
12240	ZZ2	REAL						

FILE NAMES	MODE						
5 INPUT		2054	OUTPUT	0	TAPE5	FMT	2054 TAPE6 FMT

EXTERNALS	TYPE	ARGS					
ALOG10	REAL	1	LIBRARY	ATAN2	REAL	2	LIBRARY
CEXP	COMPLEX	1	LIBRARY	COS	REAL	1	LIBRARY
EXP	REAL	1	LIBRARY	SIN	REAL	1	LIBRARY
SNORT		8		SQRT	REAL	1	LIBRARY
SUM		5					

INLINE FUNCTIONS TYPE ARGS
AIMAG REAL 1 INTRIN CONJG COMPLEX 1 INTRIN
REAL REAL 1 INTRIN

STATEMENT LABELS

4140	7			11043	10	FMT		11056	11	FMT	
11066	13	FMT		10773	101	FMT		11002	102	FMT	
11142	105	FMT		11036	106	FMT		11013	109	FMT	
11022	110	FMT		4567	202			0	203		
0	204			0	205	INACTIVE		4627	206		
0	207			0	208			0	303		INACTIVE
10723	304			0	305	INACTIVE		5036	307		
4352	308			0	311	INACTIVE		6270	312		
4312	401			0	510			0	511		
11226	601	FMT		11246	602	FMT		11257	603	FMT	
11270	604	FMT		0	605	INACTIVE		10727	606		
11124	708	FMT		11135	709	FMT		11147	710	FMT	
11160	711	FMT		11172	712	FMT		11204	713	FMT	
11217	714	FMT		11236	715	FMT		10666	801		
0	802	INACTIVE		10674	803						

LOOPS	LABEL	INDEX	FROM-TO	LENGTH	PROPERTIES
4456	203	J	133 139	273	OPT
4511	204	J	141 147	278	OPT
4710	207	I	175 181	276	OPT
4735	208	I	183 189	273	OPT
5620	510	I	325 332	623	OPT
5710	511	I	336 344	623	OPT

COMMON BLOCKS LENGTH
/ / 20

STATISTICS
PROGRAM LENGTH 377453 16357
BUFFER LENGTH 41308 4136
CM BLANK COMMON LENGTH 240 20
564008 CM USED

```
      SUBROUTINE SNOFT(NMN,NKK,QMI11,QMI12,QMI13,QMI22,QMI23,QMI33)
      COMPLEX JO,JQQD,QKA,QKEZ,QQQ1,QG,QQQ2,QH,QM1,QM12,QDD,
     1QMI12(31,31),QM13,QMI13(31,31),QM22,QMI22(31,31),QM23,QMI23(31,31)
     2,QM33,QMI33(31,31),QMI11(31,31)
      COMMON DT,DK,A,B,C,D,XLZ,X_Y,XLX,XKO,W,UO,EO,PI,SIGA,AER,BO,AO,SN,
     1XL
      DO 201 J=1,NMN
      DO 201 I=1,NKK
      WI=I-1
      WJ=J-1
      XK=A+WI*DK
      TT=C+WJ*DT
      R11=W*CO*SIGA
      R12=XKO*XK*AER-XK*XK
      R1=SQRT(R11**2+R12**2)
      IF(R12)501,502,503
  501 PH1=PI-ASIN(R11/R1)
      GO TO 504
  502 PH1=PI/2.
      GO TO 504
  503 PH1=ASIN(R11/R1)
  504 JO=(0.0,1.0)
      QQOJ=SQRT(R1)*CEXP(-OJ*PH1/2.)
      QKA=JO-OJ*AO
      R22=XKO*XKO*AER-(XKO*SN)**2
      R2=SQRT(R11**2+R22**2)
      PH2=ATAN2(R11,R22)
      QKEZ=-SQRT(R2)*CEXP(-OJ*PH2/2.)
      QQQ1=OJ*XLZ*(QKEZ+QQQO)
      QG=-1./(1.+QQQ1)
      QQQ2=OJ*XLZ*(QKEZ-QQQO)
      QH=1./(QQQ2-1.)
      SNN=SIN(TT)
      CNN=COS(TT)
      QM1=(QG+QH)*(QKA**2-(XK*CNN)**2)
      QMO1=1.+XLX*XLY*(XKO*SN+YK*CNN)**2
      QMO2=1.+(XLY*YK*SNN)**2
      QDD=YK/JQQD
      QMI11(I,J)=QJ*QM1/(QMO1*QMO2)
      QM12=-YK*YK*CNN*SNN*(QG+QH)
      QMI12(I,J)=QJ*QM12/(QMO1*QMO2)
      QM13=XK*CNN*QQQ2*(QH-QG)
      QMI13(I,J)=QJ*QM13/(QMO1*QMO2)
      QM22=(QKA**2-(YK*SNN)**2)*(QH+QG)
      QMI22(I,J)=QJ*QM22/(QMO1*QMO2)
      QM23=(XK*YK*(QG+QH)
      QMI23(I,J)=QJ*QM23/(QMO1*QMO2)
      QM33=(QKA**2-(XK*CNN)**2)*(QG+QH)
      QMI33(I,J)=QJ*QM33/(QMO1*QMO2)
      CONTINUE
      RETURN
      END
```

100

SYMBOLIC REFERENCE MAP (R=1)

ENTRY POINTS
3 SNORT

VARIABLES	SN	TYPE		RELOCATION					
2	A	REAL		/ /	17	AER	REAL		/ /
21	AO	REAL		/ /	3	B	REAL		/ /
20	BO	REAL		/ /	4	C	REAL		/ /
400	CNN	REAL			5	D	REAL		/ /
1	DK	REAL		/ /	0	DT	REAL		/ /
14	EO	REAL		/ /	363	I	INTEGER		
362	J	INTEGER			9	NKK	INTEGER		F.P.
0	NMM	INTEGER		F.P.	373	PH1	REAL		
376	PH2	REAL			15	PI	REAL		/ /
350	QDD	COMPLEX			336	QG	COMPLEX		
342	QH	COMPLEX			324	QJ	COMPLEX		
330	QKA	COMPLEX			332	QKEZ	COMPLEX		
401	QMD1	REAL			402	QMD2	REAL		
0	QMI11	COMPLEX	ARRAY	F.P.	0	QMI12	COMPLEX	ARRAY	F.P.
0	QMI13	COMPLEX	ARRAY	F.P.	0	QMI22	COMPLEX	ARRAY	F.P.
0	QMI23	COMPLEX	ARRAY	F.P.	0	QMI33	COMPLEX	ARRAY	F.P.
344	QM1	COMPLEX			346	QM12	COMPLEX		
352	QM13	COMPLEX			354	QM22	COMPLEX		
356	QM23	COMPLEX			360	QM33	COMPLEX		
326	QQDD	COMPLEX			334	QQQ1	COMPLEX		
340	QQQ2	COMPLEX			372	R1	REAL		
370	R11	REAL			371	R12	REAL		
375	R2	REAL			374	R22	REAL		
16	SIGA	REAL		/ /	22	SN	REAL		/ /
377	SNN	REAL			367	TT	REAL		
13	UO	REAL		/ /	12	W	REAL		/ /
364	WI	REAL			365	WJ	REAL		
366	XK	REAL			11	XKO	REAL		/ /
23	XL	REAL		/ /	10	XLX	REAL		/ /
7	XLY	REAL		/ /	6	XLZ	REAL		/ /

EXTERNALS	TYPE	ARGS			
ASIN	REAL	1	LIBRARY	ATAN2	REAL	2	LIBRARY
CEXP	COMPLEX	1	LIBRARY	COS	REAL	1	LIBRARY
SIN	REAL	1	LIBRARY	SQRT	REAL	1	LIBRARY

STATEMENT LABELS
0 201 0 501 INACTIVE 45 502
50 503 53 504

LOOPS	LABEL	INDEX	FROM-TO	LENGTH	PROPERTIES
16	201	* J	7 50	2678	EXT REFS NOT INNER
17	201	* I	8 50	2643	EXT REFS

COMMON BLOCKS	LENGTH
/ /	20

STATISTICS
PROGRAM LENGTH 4233 275
CM BLANK COMMON LENGTH 248 20

STATISTICS
>20003 CM USED

```
      1              SUBROUTINE SUM(IM,QA,QCC,QLD,QSM)
                     COMPLEX QA(16),QCC(16),QLD(16),QSM,Q1,Q2,Q3,Q4,Q5,QCHK,QCHKK,
                    1Qc,Q1N,Q1D,Q7,Q8,Q9,Q10,Q11,Q12N,Q12D,Q12,QS
                     COMMON DT,DK,A,B,C,D,XLZ,XLY,XLX,XKO,W,UO,EO,PI,SIGA,AER,BO,AO,SN,
      5              1XL
                     QSM=(0.0,0.0)
                     DO 520 II=1,IM
                     Q1=QA(II)/(QCC(II)+QLD(II))
                     Q2=1.-XLZ*QLD(II)
     10              Q3=XLZ*(QCC(II)+QLD(II))
                     QCHK=XL*(QCC(II)+1./XLZ)
                     ACHK=REAL(QCHK)
                     IF(ACHK-6Cc.)522,522,521
                 521 Q4=(0.0,0.0)
     15              GO TO 523
                 522 Q4=Q3*CEXP(-QCHK)
                 523 Q5=1.+XLZ*QCC(II)
                     Q6=Q3*CEXP(-XL*(QCC(II)+QLD(II)))
                     Q1N=Q2+Q4-Q5
     20              Q10=Q5*Q2
                     Q7=Q1N/Q1D
                     Q8=1.-XLZ*QCC(II)
                     QCHKK=XL*(1./XLZ+QLD(II))
                     ACHKK=REAL(QCHKK)
     25              IF(ACHKK-600.)525,525,524
                 524 Q9=(0.0,0.0)
                     GO TO 526
                 525 Q9=Q3*CEXP(-QCHKK)
                 526 Q10=1.+QLD(II)*XLZ
     30              Q11=Q10*CEXP(-XL*(QCC(II)+QLD(II)))
                     Q12N=Q8+Q9-Q11
                     Q12D=Q10*Q6
                     Q12=Q12N/Q12D
                     QS=Q1*(Q7+Q12)
     35              QSM=QSM+QS
                 520 CONTINUE
                     RETURN
                     END
```

SYMBOLIC REFERENCE MAP (OPT=1)

ENTRY POINTS
3 SUM

VARIABLES	SN	TYPE	RELOCATION					
2 A		REAL	/ /	254 ACHK		REAL		
265 ACHKK		REAL		17 AER		REAL	/ /	
21 AO		REAL	/ /	3 B		REAL	/ /	
20 BO		REAL	/ /	4 C		REAL	/ /	
5 D		REAL	/ /	1 DK		REAL	/ /	
0 DT		REAL	/ /	14 EO		REAL	/ /	
257 II		INTEGER		0 IM		INTEGER	F.P.	
15 PI		REAL	/ /	2 QA		COMPLEX	ARRAY	F.P.

VARIABLES	SN	TYPE	RELOCATION					
0	QCC	COMPLEX	ARRAY	F.P.	227	QCHK	COMPLEX	
231	QCHKK	COMPLEX			0	QLD	COMPLEX	ARRAY F.P.
261	QS	COMPLEX			0	QSM	COMPLEX	F.P.
215	Q1	COMPLEX			237	Q1D	COMPLEX	
235	Q1M	COMPLEX			247	Q10	COMPLEX	
251	Q11	COMPLEX			257	Q12	COMPLEX	
255	Q12D	COMPLEX			253	Q12N	COMPLEX	
217	Q2	COMPLEX			221	Q3	COMPLEX	
223	Q4	COMPLEX			225	Q5	COMPLEX	
233	Q6	COMPLEX			241	Q7	COMPLEX	
243	Q8	COMPLEX			245	Q9	COMPLEX	
16	SIGA	REAL	/ /		22	SN	REAL	/ /
13	U0	REAL	/ /		12	W	REAL	/ /
41	XK0	REAL	/ /		23	XL	REAL	/ /
10	XLX	REAL	/ /		7	XLY	REAL	/ /
6	XLZ	REAL	/ /					

EXTERNALS	TYPE	ARGS
CEXP	COMPLEX	1 LIBRARY

INLINE FUNCTIONS	TYPE	ARGS
REAL	REAL	1 INTRIN

STATEMENT LABELS

0	520	0	521	INACTIVE	52	522	
61	523	0	524	INACTIVE	132	525	
141	526						

LOOPS	LABEL	INDEX	FROM-TO	LENGTH	PROPERTIES
20	520	* I	7 35	1713	EXT REFS

COMMON BLOCKS	LENGTH
/ /	20

STATISTICS
PROGRAM LENGTH 3063 138
CM BLANK COMMON LENGTH 240 20
020000 CM USED

FRACTION OF WATER BY WEIGHT IN THE VEGETATION= .800
VOLUME OF VEGETATION DIVIDED BY TOTAL VOLUME= .0010000
FREQUENCY= .[illegible]E+10
RATIO OF THE STANDARD DEVIATION OF THE ROUGH SURFACE FLUCTUATIONS TO THE CORRELATION DISTANCE OF THE FLUCTUATIONS= .10000
XLX= .[illegible] XLY= .[illegible] XLZ= .[illegible]
LAYER THICKNESS IN METERS = [illegible]
DIELECTRIC CONSTANT OF THE SOIL = [illegible]
CONDUCTIVITY OF THE SOIL = [illegible]
THE AVERAGE DIELECTRIC CONSTANT= [illegible]
STD. DEV. OF DIELECTRIC FLUCTUATIONS= .[illegible]
STD. DEV. OF CONDUCTIVITY FLUCTUATIONS= .[illegible]
A0= .[illegible]
THETA= [illegible]
P1= .[illegible] Q1= .[illegible]
HALF SPACE SIGMA ZERO= -[illegible]
LAYER BOTTOM ZERO= -[illegible]
LAYER WITH ROUGH SURFACE SIGMA ZERO AND HH= -[illegible]

THETA=[illegible]
P1= .[illegible] Q1= .[illegible]
HALF SPACE SIGMA ZERO= -[illegible]

```
                LAYER WITH ROUGH SURFACE SIGMA ZERO HH=    -1.6583606

THETA=20.00
P1=    .8295379E+01          D1=    .1265493E+00
           HALF SPACE SIGMA ZERO=     -2.14150169
           LAYER SIGMA ZERO=     -2.16972928
           LAYER WITH ROUGH SURFACE SIGMA ZERO HH=     -2.16972928

THETA=30.00
P1=    .9163499E+01          D1=    .1091286E+00
           HALF SPACE SIGMA ZERO=     -2.60139696
           LAYER SIGMA ZERO=     -2.64857649
           LAYER WITH ROUGH SURFACE SIGMA ZERO HH=     -2.64857649

THETA=40.00
P1=    .1055435E+02          D1=    .9475832E-01
           HALF SPACE SIGMA ZERO=     -3.14455143
           LAYER SIGMA ZERO=     -3.11359811
           LAYER WITH ROUGH SURFACE SIGMA ZERO HH=     -3.11359811

THETA=50.00
P1=    .1276879E+02          D1=    .7831505E-01
           HALF SPACE SIGMA ZERO=     -3.63355751
           LAYER SIGMA ZERO=     -3.54758324
           LAYER WITH ROUGH SURFACE SIGMA ZERO HH=     -3.54758324

THETA=60.00
P1=    .1655454E+02          D1=    .6040637E-01
           HALF SPACE SIGMA ZERO=     -3.94924145
           LAYER SIGMA ZERO=     -3.94716745
           LAYER WITH ROUGH SURFACE SIGMA ZERO HH=     -3.94716745

THETA=70.00
P1=    .2371631E+02          D1=    .4216561E-01
           HALF SPACE SIGMA ZERO=     -5.04036386
           LAYER SIGMA ZERO=     -5.03837894
           LAYER WITH ROUGH SURFACE SIGMA ZERO HH=     -5.03837894

THETA=80.00
P1=    .3470571E+02          D1=    .2881370E-01
           HALF SPACE SIGMA ZERO=     -9.53713292
           LAYER SIGMA ZERO=     -9.53709514
           LAYER WITH ROUGH SURFACE SIGMA ZERO HH=     -9.53709514

FRACTION OF WATER BY WEIGHT IN THE VEGETATION=  .900
VOLUME OF VEGETATION DIVIDED BY TOTAL VOLUME=  .0010000
FREQUENCY=     .7650000E+10
RATIO OF THE STANDARD DEVIATION OF THE ROUGH SURFACE FLUCTUATIONS TO THE CORRELATION DISTANCE OF THE FLUCTUATIONS=     .03000
XLX=     .01000000      XLY=     .00400000      XLZ=     .00800000
LAYER THICKNESS IN METERS =  2.500000
DIELECTRIC CONSTANT OF THE SOIL =  7.500000
CONDUCTIVITY OF THE SOIL = 1.300000
THE AVERAGE DIELECTRIC CONSTANT=  1.025002
STD. DEV. OF DIELECTRIC FLUCTUATIONS=  .8218577
STD. DEV. OF CONDUCTIVITY FLUCTUATIONS=  .0349991
AO=    .5589796E+00
THETA= 0.00
```

P1= .6797672E+01 D1= .1471064E+00
HALF SPACE SIGMA ZERO= -1.09287153
LAYER SIGMA ZERO= -1.07259785
LAYER WITH ROUGH SURFACE SIGMA ZERO HH= -1.07259785

THETA=10.00
P1= .6929453E+01 D1= .1443115E+00
HALF SPACE SIGMA ZERO= -2.13624033
LAYER SIGMA ZERO= -2.06511277
LAYER WITH ROUGH SURFACE SIGMA ZERO HH= -2.06511277

THETA=20.00
P1= .7031446E+01 D1= .1365987E+00
HALF SPACE SIGMA ZERO= -4.14902047
LAYER SIGMA ZERO= -4.17178520
LAYER WITH ROUGH SURFACE SIGMA ZERO HH= -4.17178520

THETA=30.00
P1= .8032644E+01 D1= .1244936E+00
HALF SPACE SIGMA ZERO= -5.98710841
LAYER SIGMA ZERO= -5.97414737
LAYER WITH ROUGH SURFACE SIGMA ZERO HH= -5.97414737

THETA=40.00
P1= .9110429E+01 D1= .1097543E+00
HALF SPACE SIGMA ZERO= -7.34962684
LAYER SIGMA ZERO= -7.32183067
LAYER WITH ROUGH SURFACE SIGMA ZERO HH= -7.32183067

THETA=50.00
P1= .1077268E+02 D1= .9292571E-01
HALF SPACE SIGMA ZERO= -8.27761762
LAYER SIGMA ZERO= -8.28943467
LAYER WITH ROUGH SURFACE SIGMA ZERO HH= -8.28943467

THETA=60.00
P1= .1357193E+02 D1= .7368202E-01
HALF SPACE SIGMA ZERO= -8.98810703
LAYER SIGMA ZERO= -8.98850962
LAYER WITH ROUGH SURFACE SIGMA ZERO HH= -8.98850962

THETA=70.00
P1= .1692412E+02 D1= .5284201E-01
HALF SPACE SIGMA ZERO= -10.13759989
LAYER SIGMA ZERO= -10.13592344
LAYER WITH ROUGH SURFACE SIGMA ZERO HH= -10.13592344

THETA=80.00
P1= .2870640E+02 D1= .3545672E-01
HALF SPACE SIGMA ZERO= -14.30669351
LAYER SIGMA ZERO= -14.30665782
LAYER WITH ROUGH SURFACE SIGMA ZERO HH= -14.30665782

FRACTION OF WATER BY WEIGHT IN THE VEGETATION= .900
VOLUME OF VEGETATION DIVIDED BY TOTAL VOLUME= .0010000
FREQUENCY= .5250000E+10
RATIO OF THE STANDARD DEVIATION OF THE ROUGH SURFACE FLUCTUATIONS TO THE CORRELATION DISTANCE OF THE FLUCTUATIONS= .10000

LAYER THICKNESS IN METERS = 2.500000
DIELECTRIC CONSTANT OF THE SOIL = 7.000000
CONDUCTIVITY OF THE SOIL = 1.700000
THE AVERAGE DIELECTRIC CONSTANT= 1.002154
STD. DEV. OF DIELECTRIC FLUCTUATIONS= .0898589
STD. DEV. OF CONDUCTIVITY FLUCTUATIONS= .0541018
AO= .317982E+00
THETA= 0.00
P1= .368206E+01 Q1= .271567E+00
HALF SPACE SIGMA ZERO= -1.35917420
LAYER SIGMA ZERO= -1.00289426
LAYER WITH ROUGH SURFACE SIGMA ZERO HH= -1.00289426

THETA=10.00
P1= .375220BE+01 Q1= .266E097E+00
HALF SPACE SIGMA ZERO= -1.44297544
LAYER SIGMA ZERO= -1.25050475
LAYER WITH ROUGH SURFACE SIGMA ZERO HH= -1.25050475

THETA=20.00
P1= .397238?E+01 Q1= .251737BE+00
HALF SPACE SIGMA ZERO= -1.67492667
LAYER SIGMA ZERO= -1.46087852
LAYER WITH ROUGH SURFACE SIGMA ZERO HH= -1.46087862

THETA=30.00
P1= .437535?E+01 Q1= .223551?1E+00
HALF SPACE SIGMA ZERO= -1.93938343
LAYER SIGMA ZERO= -1.94811031
LAYER WITH ROUGH SURFACE SIGMA ZERO HH= -1.94811031

THETA=40.00
P1= .503119?E+01 Q1= .196?59?E+00
HALF SPACE SIGMA ZERO= -2.36054875
LAYER SIGMA ZERO= -2.22384987
LAYER WITH ROUGH SURFACE SIGMA ZERO HH= -2.22384987

THETA=50.00
P1= .6?837?4E+01 Q1= .1?42E?3?E+00
HALF SPACE SIGMA ZERO= -2.73990125
LAYER SIGMA ZERO= -2.91635312
LAYER WITH ROUGH SURFACE SIGMA ZERO HH= -2.91635312

THETA=60.00
P1= .?63446?E+01 Q1= .142?317E+00
HALF SPACE SIGMA ZERO= -3.40?2?69?
LAYER SIGMA ZERO= -3.?47?19?1
LAYER WITH ROUGH SURFACE SIGMA ZERO HH= -3.?47?1?41

THETA=70.00
P1= .1127?37E+02 Q1= .?47?2?2?5?-01
HALF SPACE SIGMA ZERO= -4.?19?14?7
LAYER SIGMA ZERO= -4.?47?2?3?1
LAYER WITH ROUGH SURFACE SIGMA ZERO HH= -4.?47?2?3?1

THETA=?0.00
P1= .1?0?2?2?E+02 Q1= .?75?7?0?-01

```
          HALF SPACE SIGMA ZERO=    -8.97623184
          LAYER SIGMA ZERO=     -8.98272473
          LAYER WITH ROUGH SURFACE SIGMA ZERO HH=     -8.98272473


FRACTION OF WATER BY WEIGHT IN THE VEGETATION=  .800
VOLUME OF VEGETATION DIVIDED BY TOTAL VOLUME=  .0010000
FREQUENCY=    .525000E+10
RATIO OF THE STANDARD DEVIATION OF THE ROUGH SURFACE FLUCTUATIONS TO THE CORRELATION DISTANCE OF THE FLUCTUATIONS=    .03000
XLX=    .01000000     XLY=    .03400000     XLZ=    .00800000
LAYER THICKNESS IN METERS =  2.500000
DIELECTRIC CONSTANT OF THE SOIL =  7.530000
CONDUCTIVITY OF THE SOIL = 1.3900000
THE AVERAGE DIELECTRIC CONSTANT=  1.029154
STD. DEV. OF DIELECTRIC FLUCTUATIONS=  .8898589
STD. DEV. OF CONDUCTIVITY FLUCTUATIONS=  .0541018
AO=   .3179828E+00
THETA= 0.00
P1=   .3347386E+01           Q1=    .2987406E+00
          HALF SPACE SIGMA ZERO=     -.98218625
          LAYER SIGMA ZERO=      -.68883693
          LAYER WITH ROUGH SURFACE SIGMA ZERO HH=      -.68883693


THETA=10.00
P1=   .3401339E+01           Q1=    .2940027E+00
          HALF SPACE SIGMA ZERO=     -1.50766106
          LAYER SIGMA ZERO=     -1.34911258
          LAYER WITH ROUGH SURFACE SIGMA ZERO HH=     -1.34911258


THETA=20.00
P1=   .3562417E+01           Q1=    .2802632E+00
          HALF SPACE SIGMA ZERO=     -2.82533200
          LAYER SIGMA ZERO=     -2.61360943
          LAYER WITH ROUGH SURFACE SIGMA ZERO HH=     -2.61368943


THETA=30.00
P1=   .3864594E+01           Q1=    .2586255E+00
          HALF SPACE SIGMA ZERO=     -4.19250385
          LAYER SIGMA ZERO=     -4.12386720
          LAYER WITH ROUGH SURFACE SIGMA ZERO HH=     -4.12386720


THETA=40.00
P1=   .4347065E+01           Q1=    .2312270E+00
          HALF SPACE SIGMA ZERO=     -5.36523194
          LAYER SIGMA ZERO=     -5.22486772
          LAYER WITH ROUGH SURFACE SIGMA ZERO HH=     -5.22486772


THETA=50.00
P1=   .5105719E+01           Q1=    .1997391E+00
          HALF SPACE SIGMA ZERO=     -6.34107157
          LAYER SIGMA ZERO=     -6.34567892
          LAYER WITH ROUGH SURFACE SIGMA ZERO HH=     -6.34567892


THETA=60.00
P1=   .6413024E+01           Q1=    .1577932E+00
          HALF SPACE SIGMA ZERO=     -7.27005507
          LAYER SIGMA ZERO=     -7.31006552
          LAYER WITH ROUGH SURFACE SIGMA ZERO HH=     -7.31006552
```

```
THETA=70.00
P1=    .2972890E+01            D1=    .1113494E+00
          HALF SPACE SIGMA ZERO=     -8.74498087
          LAYER SIGMA ZERO=     -8.75987527
          LAYER WITH ROUGH SURFACE SIGMA ZERO HH=     -8.75987527

THETA=90.00
P1=    .1383920E+02            D1=    .7227419E-01
          HALF SPACE SIGMA ZERO=    -12.85746341
          LAYER SIGMA ZERO=    -12.96307538
          LAYER WITH ROUGH SURFACE SIGMA ZERO HH=    -12.96307538
```

```
  MFA    ETL NOS/BE 1.2      RELEASE 447 06/03/80
09.21.01.ETRH01N  FROM
09.21.01.IP  00002344 WORDS - FILE INPUT  , DC 04
09.21.01.ETRH0.        UNCLASSIFIED
09.21.01.TASK(TNFT76767,PW*****,TKTS)REVENUE
09.21.02.FTN.
09.22.42.     26.422 CP SECONDS COMPILATION TIME
09.22.42.LGO.
09.22.54.  CM LWA+1 = 610158, LOADER USED  75300B
09.29.56.     STOP
09.29.56.   152.777 CP SECONDS EXECUTION TIME
09.29.56.CLTST(T=U)
09.29.56.
09.29.56.UNCLASSIFIED
09.29.58. CLIST COMPLETE.
09.29.58.EXIT(S)
09.29.58.OP  00010176 WORDS - FILE OUTPUT , DC 40
09.29.58.MS   10752  WORDS  (   43008 MAX USED)
09.29.58.CPA    161.325 SEC.         2.419  $ CP
09.29.58.IO       4.120 SEC.          .052  $ IO
09.29.58.CM    3607.171 KWS.         6.097  $ CM
09.29.58.SS MAINFRAME CHARGES       16.479 TOT.
09.29.58.           * * * * NOTE * * * *
09.29.58.CHARGES FOR CARDS READ/PUNCHED AND
09.29.58.LINES PRTD NOT INCLUDED. ADD $1.00 FOR
09.29.58.EACH TAPE/DISK MOUNTED.
09.29.58.PP        10.573 SEC.      DATE 09/08/80
09.29.58.
09.29.58.I CERTIFY THAT I HAVE REVIEWED THE
09.29.58.CONTENTS OF THIS ADP INFORMATION AND
09.29.58.THAT, TO THE BEST OF MY KNOWLEDGE, IT
09.29.58.CONTAINS NO SCI/COLLATERAL DATA.
09.29.58.
09.29.58.
09.29.58.                      --------------------
09.29.58.                      SIGNATURE/DATE
09.29.58.
09.29.58.EJ  END OF JOB, **
```

LIST OF SYMBOLS

$\underline{r}$	Position vector
$\epsilon(\underline{r})$	Permittivity of the random medium
$\sigma(\underline{r})$	Conductivity of the random medium
ϵ_a	Average relative dielectric constant of the random medium
σ_a	Average conductivity of the random medium
η_1	Standard deviation of the dielectric fluctuations
η_2	Standard deviation of the conductivity fluctuations
L	Mean thickness of the vegetation layer
k_3	Complex propagation constant in the soil
θ_i	Angle of incidence
k_o	Free space propagation constant
$\underline{\underline{\Gamma}}(\underline{r}, \underline{r}')$	Infinite space dyadic Green's function
$<\underline{E}(\underline{r})>$	Mean wave in the random medium
$G_o(\underline{r}, \underline{r}')$	Infinite space scalar Green's function
$\underline{E}_s(\underline{r})$	Scattered electric field in the random medium
$\delta(\underline{r}-\underline{r}')$	Three-dimensional Dirac delta function equal to $\delta(x-x')\,\delta(y-y')\,\delta(z-z')$
$\underline{\underline{I}}$	Unit dyadic
$\underline{a}_x, \underline{a}_y, \underline{a}_z$	Unit vectors in x, y, and z

k_x, k_y	Fourier transform variables
j	$\sqrt{-1}$
δ_{ij}	Kronecker Delta
k_{ex}, k_{ey}, k_{ez}	Components of the effective propagation constant
k_h	Value of k_{ez} for horizontal polarization
k_v	Value of k_{ez} for vertical polarization
$\underline{G}_s(\underline{k}_t, z)$	Two-dimensional Fourier transform of the scattered electric field in the random medium
$A_x(k_x, k_y)$, $A_y(k_x, k_y)$, $A_z(k_x, k_y)$	Fourier transform of the amplitudes of the scattered electric field in air
A_I	Illuminated surface area
ℓ_x, ℓ_y, ℓ_z	Correlation distances in x, y, and z, repectively
σ°_{HHv}	Backscatter coefficient for volume scattering and for the case of horizontal polarization transmit, horizontal polarization receive
σ°_{VVv}	Backscatter coefficient for volume scattering and for the case of vertical polarization transmit, vertical polarization receive
σ°_{HHs}	Backscatter coefficient for a randomly rough surface for the case of horizontal polarization transmit, horizontal polarization receive
σ°_{HH}	Final backscatter coefficient result that includes both volume scattering and rough surface scattering for the case of horizontal polarization transmit, horizontal polarization receive

σ°_{VV}	Final backscatter coefficient result that includes both volume scattering and rough surface scattering for the case of vertical polarization transmit, vertical polarization receive
F	Fraction of water by weight in the vegetation
R_V	Volume of vegetation divided by the total volume
m_s	Standard deviation of the rough surface fluctuations divided by the correlation distance
f	Frequency